



HAL
open science

Thermal and pH stabilities of i-DNA: confronting in vitro experiments with models and in-cell NMR data

Mingpan Cheng, Dehui Qiu, Liezel Tamon, Eva Ištvanková, Pavlína Víšková, Samir Amrane, Aurore Guédin, Jieli Chen, Laurent Lacroix, Huangxian Ju, et al.

► To cite this version:

Mingpan Cheng, Dehui Qiu, Liezel Tamon, Eva Ištvanková, Pavlína Víšková, et al.. Thermal and pH stabilities of i-DNA: confronting in vitro experiments with models and in-cell NMR data. *Angewandte Chemie International Edition*, 2021, 60, pp.10286-10294. 10.1002/anie.202016801 . hal-03149390

HAL Id: hal-03149390

<https://hal.science/hal-03149390>

Submitted on 23 Feb 2021

HAL is a multi-disciplinary open access archive for the deposit and dissemination of scientific research documents, whether they are published or not. The documents may come from teaching and research institutions in France or abroad, or from public or private research centers.

L'archive ouverte pluridisciplinaire **HAL**, est destinée au dépôt et à la diffusion de documents scientifiques de niveau recherche, publiés ou non, émanant des établissements d'enseignement et de recherche français ou étrangers, des laboratoires publics ou privés.

Thermal and pH stabilities of i-DNA: confronting *in vitro* experiments with models and in-cell NMR data

Mingpan Cheng,^{a,b} Dehui Qiu,^a Liezel Tamon,^c Eva Ištvančková,^d Pavlína Víšková,^d Samir Amrane,^b Aurore Guédin,^b Jieli Chen,^a Laurent Lacroix,^e Huangxian Ju,^a Lukáš Trantírek,^d Aleksandr B. Sahakyan,^c Jun Zhou,^{*,a} and Jean-Louis Mergny^{a,b,f}

[a] Dr. M. Cheng, D. Qiu, J. Chen, Prof. Dr. H. Ju, Prof. Dr. J. Zhou, Dr. J.L. Mergny
State Key Laboratory of Analytical Chemistry for Life Science, School of Chemistry & Chemical Engineering, Nanjing University, Nanjing 210023, China.
E-mail: jun.zhou@nju.edu.cn

[b] Dr. M. Cheng, Dr. S. Amrane, A. Guédin, Dr. J.L. Mergny
ARNA Laboratory, Université de Bordeaux, INSERM U 1212, CNRS UMR5320, IECB, Pessac 33607, France.

[c] L. Tamon, Prof. Dr. A.B. Sahakyan
MRC WIMM Centre for Computational Biology, MRC Weatherall Institute of Molecular Medicine, Radcliffe Department of Medicine, University of Oxford, Oxford OX3 9DS, UK.

[d] E. Ištvančková, P. Víšková, Prof. Dr. L. Trantírek
Central European Institute of Technology, Masaryk University, Brno 62500, Czech Republic.

[e] Dr. L. Lacroix
IBENS, Ecole Normale Supérieure, CNRS, INSERM, PSL Research University, Paris 75005, France.

[f] Dr. J.L. Mergny
Laboratoire d'Optique et Biosciences, Ecole Polytechnique, CNRS, INSERM, Institut Polytechnique de Paris, 91128 Palaiseau, France.

Supporting information for this article is given via a link at the end of the document.

Abstract: Recent studies indicate that i-DNA, a four-stranded cytosine-rich DNA also known as the i-motif, is actually formed *in vivo*; however, a systematic study on sequence effects on stability has been missing. Herein, an unprecedented number of different sequences (271) bearing four runs of 3-6 cytosines with different spacer lengths has been tested. While i-DNA stability is nearly independent on total spacer length, the central spacer plays a special role on stability. Stability also depends on the length of the C-tracts at both acidic and neutral pHs. This study provides a global picture on i-DNA stability thanks to the large size of the introduced data set; it reveals unexpected features and allows to conclude that determinants of i-DNA stability do not mirror those of G-quadruplexes. Our results illustrate the structural roles of loops and C-tracts on i-DNA stability, confirm its formation in cells, and allow establishing rules to predict its stability.

Introduction

i-DNA (also known as the i-motif) is a fascinating four-stranded structure discovered in the 1990s by M. Guéron and colleagues, and stemming from the interlocking of two equivalent parallel-stranded right-handed duplexes.^[1] Such cytosine-rich structure, which relies on the formation of hemi-protonated C:C⁺ base pairs (Figure 1A),^[2] can be formed with two or more independent strands, or be intramolecular, as depicted in Figure 1B.^[3] Different conformations are possible, but i-DNA is not as polymorphic as G-quadruplexes (G4s) as two diametrically distant strands must remain parallel to each other and adjacent strands are always running in opposite orientations (Figure 1C).^[3a,4] In addition, bi- or tetra-molecular complexes may coexist with intramolecular structures.^[5]

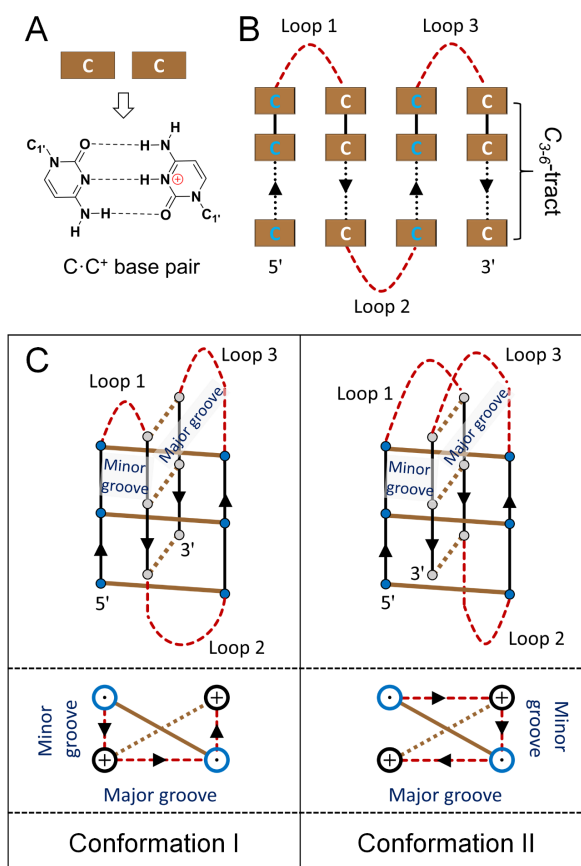


Figure 1. (A) Hemi-protonated C:C⁺ base pair. (B) Example of a sequence prone to form intramolecular i-DNA. (C) Possible loop arrangements in an i-DNA structure; Simplified diagram of two linking directions between strands: Central loop can across either major (left, conformation I) or minor (right, conformation II) groove.^[3a]

i-DNA has long remained in the shadow of G4s formed by complementary G-rich sequences, given its limited stability at physiological pH. Formation of each C·C⁺ base pair requires the protonation of one cytosine at its N3 position ($pK_a \approx 5$): as a consequence, the stability of this motif is optimal under mildly acidic conditions but remains questionable at neutral pH.^[6] i-DNA extreme pH dependency can actually become an asset to design sensitive pH-responsive devices^[7] and may be applicable to analytical chemistry,^[8] nanotechnology,^[7,9] and therapeutics.^[10] Regarding its biological relevance, two recent independent studies indicate that i-DNA is actually present within human cells.^[11,12] Similar to G4-prone sequences, i-DNA-prone motifs are widely distributed in genomes,^[13] and have been found to modulate telomerase activity,^[14] transcription of genes,^[15] and DNA biosynthesis.^[16]

Our understanding of i-DNA is still far from complete. Increasing cytosine tract lengths results in increased thermal stability; sequences with at least five cytosines per tract fold into i-DNA at room temperature and neutral pH.^[5a,5c,6] Additional interactions involving hydrogen bonding also stabilize i-DNA.^[17] Burrows and colleagues analyzed dC homo-oligonucleotides, and found that pure cytosine tracts may adopt stable i-motif conformations.^[18] These results somewhat mirror those found for G4 formation;^[19] as a consequence, the complementary strand of a G4-forming sequence is generally prone to i-DNA formation. Besides C-tracts, the nature of the loops (length and base composition) also plays a role in i-DNA formation.^[20] However, contradictory conclusions have been drawn upon how loop length influences i-DNA stability.^[18a,20b,20d,21] These results came from the investigations of a limited number of sequences; systematic studies based on large numbers of examples are needed to achieve an objective conclusion.

Herein, we systematically analyzed i-DNA stability on an unprecedented large selection of sequences (271 in total). This unique dataset unveiled important parameters governing the stability of i-DNA. Global trends were identified and more subtle effects were found using machine learning and other modeling approaches, allowing us to predict i-DNA stability from primary sequence with reasonable accuracy. i-DNA formation in cells with motifs stable *in vitro* at near neutral pH was confirmed by in-cell NMR.

Results

Sequences design and nomenclature

Sequences information and nomenclature are shown in **Table S1**. Each sequence bears four C-tracts, containing 3 to 6 cytosines (C_3 to C_6). These four C-tracts (which are generally of identical length) are separated by three spacer regions, which should allow the formation of an intramolecular structure.^[6] Sequences with four non-equal C-tracts have also been considered in a limited number of cases, as discussed later. The C_3 to C_6 range was chosen as i-DNA becomes unstable for shorter (C_2) C-tracts, and is prone to form competing structures (inter- or intra-molecular) when C-tract is longer than six.^[5a,5c,6] To reduce the number of spacer arrangements, most sequence groups contain two identical spacers, which are generally composed of thymines only. Each spacer involves one to six thymine nucleotides, and total spacer length is capped at twelve nucleotides in most cases. Note that the term “spacer”

corresponds here to the non-C nucleotides connecting C-tracts: as some cytosines may also participate to loops rather than to the i-motif stem, the operational *loop* length may therefore be longer than the *spacer* composed of thymines only.

The following nomenclature was chosen: unless otherwise stated, a “T” prefix means that the three spacers are composed of thymine bases only; the three consecutive numbers refer to three spacer length in the 5' to 3' direction; while the “-3”, “-4”, “-5” or “-6” suffix refers to four C-tracts of C_3 , C_4 , C_5 , and C_6 , respectively. To compare the effects of spacer arrangement on i-DNA stability, the notion of sequence *group* was introduced.^[22] The sequences in the same group are only differing in the way that spacers are arranged. A group is named after the first sequence in the group. For example, the *T112-3* group is composed of T112-3, T121-3, and T211-3. All three sequences have the same length, the same overall base content with short spacers composed of one or two thymines separating four runs of three cytosines. **Tables S1** and **S2** summarize the results obtained for 60 groups of three sequences with different spacer arrangements.

Evidence for i-DNA formation

First, i-DNA formation was checked under acidic (pH 5.0) or neutral (pH 7.0) conditions. Thermal difference spectra (TDS) are provided in **Figure S1** and clearly showed that they fold into an i-motif at pH 5.0 (two major peaks around 239 and 294 nm).^[23] In addition, i-DNA formation for 12 selected sequences was also proved by the presence of imino proton peaks from C·C⁺ at 15 to 16 ppm in ¹H NMR spectra (**Figure S2**).^[3a,3d]

The molecularities of the 49 sequences with a C_5 -tract in **Table S2** were checked at both pH 5.0 and 7.0 by native PAGE (**Figures S3** and **S4**). All sequences tested mainly fold into intramolecular species, in agreement with previous studies.^[5a,5c] The conclusions drawn from these work therefore apply to intramolecular i-DNAs, which are more likely to be physiologically relevant at the genome level. Once intramolecular i-DNA formation was established, we wished to examine its stability.

In contrast to TDS recorded at pH 5.0, the situation was more diverse at neutral pH. We divided the 60 groups into four classes, based on the number of sequences in the same group that fold into an i-DNA structure at neutral pH (**Figure 2**, dashed lines):

- I. None of the three sequences in a given group fold into an i-DNA at neutral pH. This category includes all groups with C_3 -tract (**Figures 2A**, **2B** and **S1A**), *T336-4* group (**Figure S1B**) and *T336-5* group (**Figure S1C**);
- II. Only one of three sequences within the same group folds into an i-DNA. This category includes *T121-4* (**Figure 2B**), *T161-4* (**Figure S1B**), *T262-4* (**Figure S1B**) as well as *T353-5* groups (**Figure S1C**);
- III. Two of the three sequences in the same group fold into an i-DNA. This category includes *T225-4* (**Figure 2C**), *T335-4* (**Figure S1B**), and *T225-5* groups (**Figure S1C**);
- IV. All three sequences in the same group fold into an i-DNA (**Figures 2D** and **S1B-C**).

An interesting trend emerges from this classification. In types II and III categories (for which some, but not all, group members form an i-DNA at pH 7.0), the sequence with a longer central spacer folds into an i-DNA while one or the two other group members do not form, or only partially form, an i-DNA structure.

This suggests that sequences with a longer central spacer are relatively more stable at neutral pH.

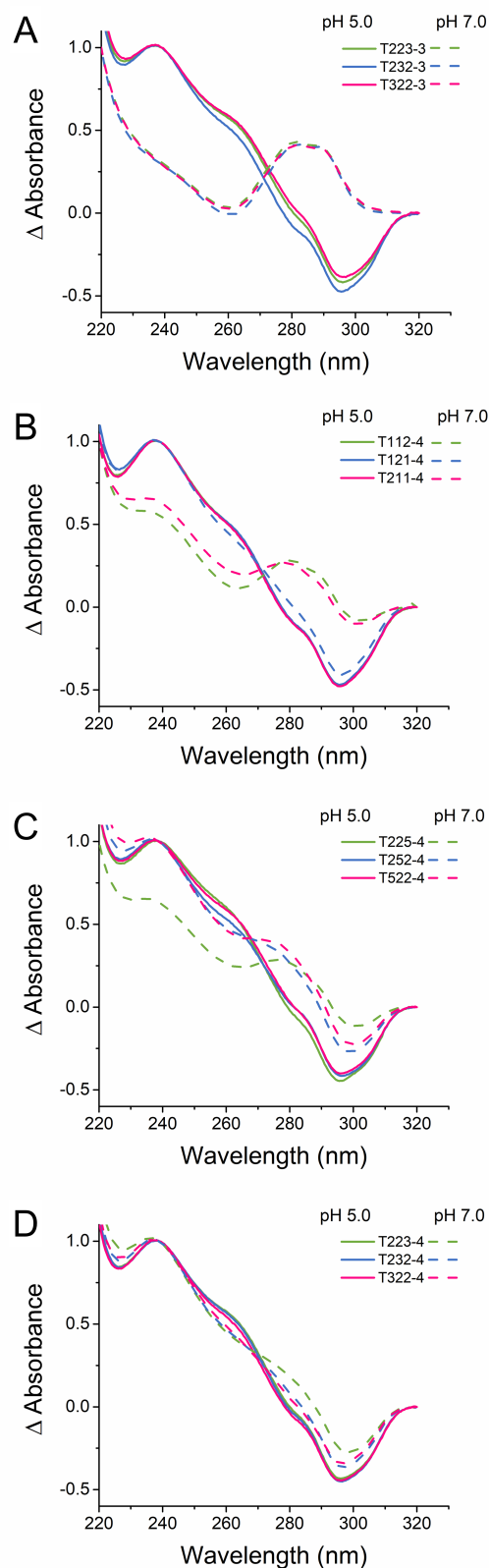


Figure 2. Normalized TDS of selected groups at pH 5.0 (solid lines) and 7.0 (dashed lines). (A) Zero, (B) one, (C) two, (D) all three sequences in a group fold into i-DNA completely at neutral pH.

i-DNAs with a long central spacer exhibit higher pH and thermal stabilities

To confirm the differences in stability inferred from TDS at pH 7.0, we performed CD and UV measurements (Figures S5-S14). pH transition mid-point (pH_T) was depicted in Figures S9 and S14 for pH-dependent CD and UV absorbance spectra, respectively; the consistency between pH_T obtained by ellipticity and absorbance was checked (Figure S15, pH_T values are provided in Tables S1-S2).

A consistent trend emerged from the comparison of pH_T values: in most groups, the sequence with a longer central spacer has a higher pH_T than other sequences. For example, in the T112-3 group, pH_T of T121-3 (6.30) is higher than the ones of T112-3 (6.11) and T211-3 (6.12) (Figure S5B). A precise count of groups obeying this “long central spacer is better” rule is presented in Table 1. Based on CD and UV spectra, 48 or 46 of the 60 groups (80% and 77%) follow this tendency, respectively.

Table 1. Enumeration of groups obeys the “long central spacer is better” rule.^[a]

Counts	i-DNAs in the same group				Total (percentage)
	C ₃ tract	C ₄ tract	C ₅ tract	C ₆ tract	
pH_T^{CD}	11/15	13/15	12/15	12/15	48/60 (80%)
pH_T^{UV}	10/15	13/15	12/15	11/15	46/60 (77%)
$T_{1/2}^{pH\ 5.0}$	15/15	15/15	15/15	15/15	60/60 (100%)
$T_{1/2}^{pH\ 7.0}$	--	--	12/15	12/15	24/30 (80%)

^[a] Counts based on results presented in Tables S1-S2, Figures S9 and S14. The thermal stability of sequences with C₃- and C₄-tracts at pH 7.0 was not evaluated.

Then thermal denaturation of i-DNAs at pH 5.0 and pH 7.0 was tracked by UV-absorbance at 295 nm (Figures S16-S18).^[24] At neutral pH, only sequences with longer C-tracts such as C₅ and C₆ were considered, as sequences with shorter C-tracts do not fold or exhibit low stabilities ($T_m < 12$ °C) preventing accurate determinations. Folding and unfolding processes follow relatively fast kinetics under mildly acidic conditions, as expected for intramolecular folding. However, this is no longer the case at near-neutral pH, where a hysteresis phenomenon occurs, leading to large differences in apparent mid-transition point (T_m) upon heating and cooling processes.^[5a,6] For some sequences, such as T444-6, T336-6, T363-6 and T633-6, this difference in melting/cooling T_m s can reach 19 °C (Figure S17). As a first approximation, T_m at pH 7.0 is assumed to be equal to the average of half-transition values for heating and cooling curves.^[25]

The analysis of T_m values further confirmed the “long central spacer is better” rule: for most groups, the sequence with a longer central spacer has a higher T_m than the other sequences in the same group (Figure S18). For example, in the T114-5 group at pH 5.0, the T_m of the sequence T141-5 (74.2 °C) is higher than the one of T114-5 (69.5 °C) or T411-5 (70.6 °C). At pH 7.0, a similar result is found, although all T_m s are much lower: the T_m of sequence T141-5 is 17.0 °C only, but still higher than the ones of T114-5 (13.6 °C) and T411-5 (14.8 °C) (Table S2). The counts of groups obeying this rule are summarized in Table 1: 24/30 and 60/60 follow this trend at pH 7.0 and 5.0, respectively.

Analyses of effects of spacer permutation are presented in Figures 3A-F. Sequences are divided into two categories: *i*) sequences with two relatively long (L) and one relatively short (S)

RESEARCH ARTICLE

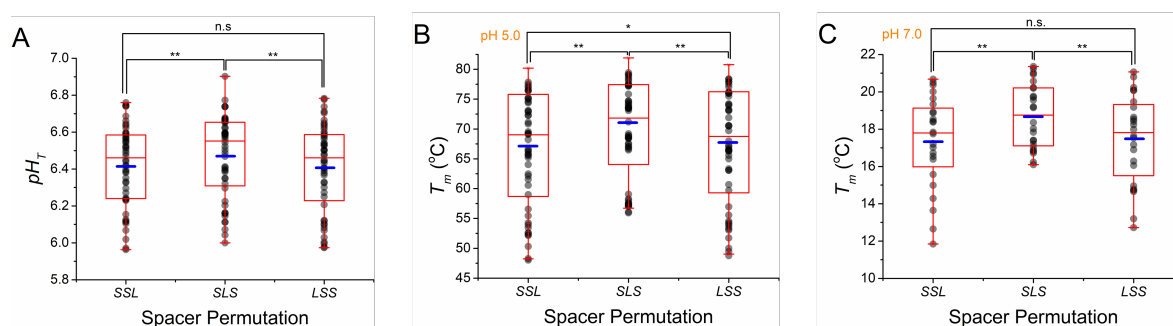
spacers and *ii*) sequences with two short and one long spacers. Average and median values of pH_T and T_m of sequences with a relatively longer central spacer, including *SLS* (Figures 3A-C), *LLS* and *SLL* (Figures 3D-F) are obviously higher than that of the corresponding sequences with a shorter central spacer (*SSL* and *LSS*, *LSL*). Considering that three sequences in the same group are generated by spacer permutations, any two sequences of them are treated as a paired sample. Then hypotheses of pair-sample *t*-test are performed between every two spacer combinations. Except for 3 comparisons (*LLS* versus *LSL* and *LSS* versus *SLL* shown in Figure 3F, and *LLS* versus *LSL* in Figure 3D), all 9 other *t*-tests support the conclusion that pH_T and T_m of the sequences with a longer central spacer are significantly higher ($p < 0.05$; *SLS* versus *SSL* or *LSS* in Figures 3A-C; *LLS* or *SLL* versus *LSL* in Figures 3D-E). In addition, except for one comparison (*SSL* versus *LSS* in Figure 3B), all 5 other *t*-tests show that the differences of pH_T and T_m values between two

sequences from the same group that have the identical central spacer are not significant ($p > 0.05$).

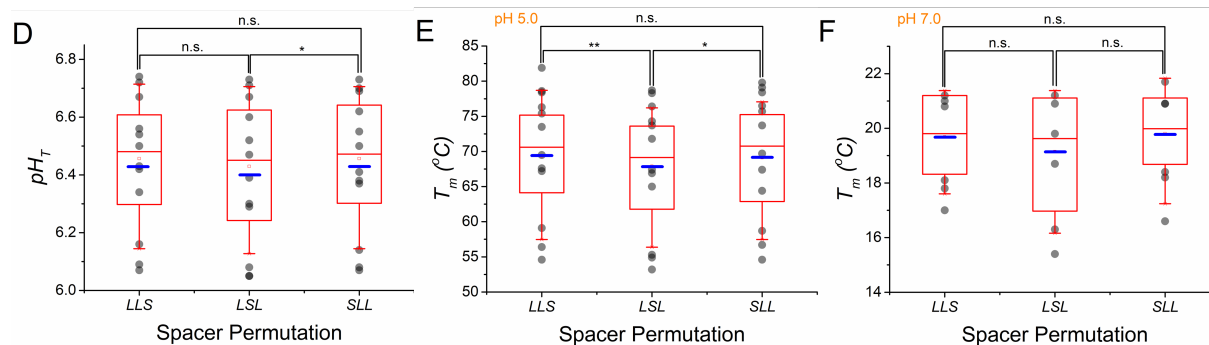
This “stability-spacer length-symmetry” may come from the linking pattern of three loops in intramolecular i-DNAs proposed previously^[3a] and depicted in Figure 1C. Three loops stretch and pass through either minor-major-minor grooves (conformation I) or major-minor-major grooves (conformation II). Given the results obtained here, assuming spacer length would allow both possibilities, conformation II generally appears less stable than conformation I.

Thermal stabilities of 12 sequences in 4 groups (*T112-5*, *T225-5*, *T112-6* and *T225-6*) at pH 5.0 and 7.0 were also evaluated by DSC (Figure S19), and T_m values and hysteresis are summarized in Table S4. These results are consistent with those obtained by UV experiments. The “long central spacer is better” was also observed for 7 of 8 group datasets.

I) Sequences with one long and two short spacers



II) Sequences with two long and one short spacers



III) Total spacer length

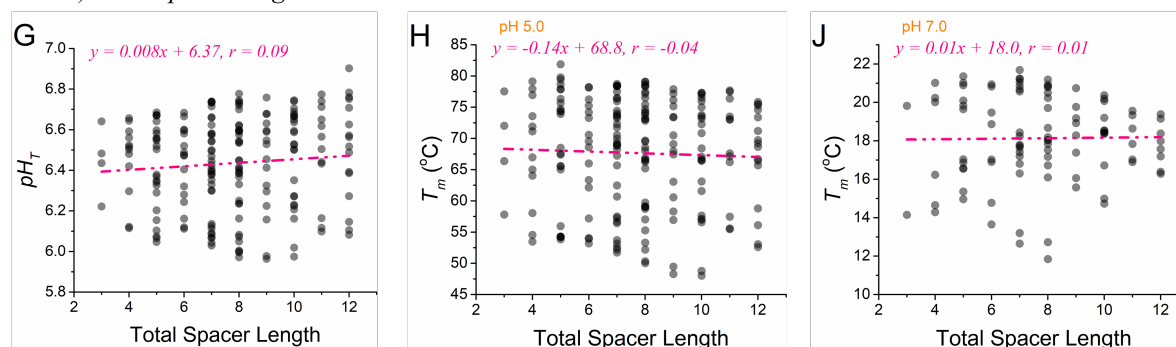


Figure 3. Effects of total spacer length and individual spacer permutation on pH_T and T_m . (A&D) pH_T versus spacer permutation; T_m s at (B&E) pH 5.0 or at (C&F) pH 7.0 versus spacer permutation. Sequences come from Table S2. Blue and red lines in the red box are the average and median values for each spacer combination, respectively. Hypotheses of pair-sample *t*-test are performed between every two spacer combinations: not significant (n.s.); $p > 0.05$; *, $p < 0.05$; **, $p < 0.0005$. pH_T (G), T_m s at (H) pH 5.0 and (J) pH 7.0 as a function of total spacer length. The dashed line corresponds to a linear fit (equation shown above).

Stability depends on C-tract but not total spacer length

pH_T and T_m (at pH 7.0, only the sequences with C_5 and C_6 -tracts are used) of 196 sequences are presented in **Table S2** and plotted as a function of total spacer length in **Figures 3G-J**. Values of pH_T or T_m are widely distributed for each spacer length from 3 to 12, and little or no correlation was found between T_m and total spacer length, indicating that it has a limited effect on the i-DNA stability at both acidic and neutral pHs. This may be the reason why previously reported studies about the effects of loop length on i-DNA are contradictory or negligible.^[5a,5c,18a,20b,20d]

Quantitative analyses of the relationships between pH_T or T_m vs C-tract length were previously missing.^[5a,5c,6] The assessment

of C-tract role on i-DNA stability is depicted in **Figure 4**. Stability increases with C-tracts length: averaged pH_T s with C_3 , C_4 , C_5 and C_6 -tracts are 6.11, 6.39, 6.56 and 6.68, respectively (**Figure 4A**). A similar relationship was found between T_m and C-tract length under both acidic and neutral conditions (**Figures 4B and C**). The increase in pH_T is monotonous but not linear: the average difference between C_4 and C_3 , C_5 and C_4 or C_6 and C_5 is 0.28, 0.17 or 0.12, respectively. Of note, sequences with C-tracts longer than six are prone to intermolecular i-DNA formation, and the corresponding pH_T increase with C-tract length becomes small.^[5a,5c]

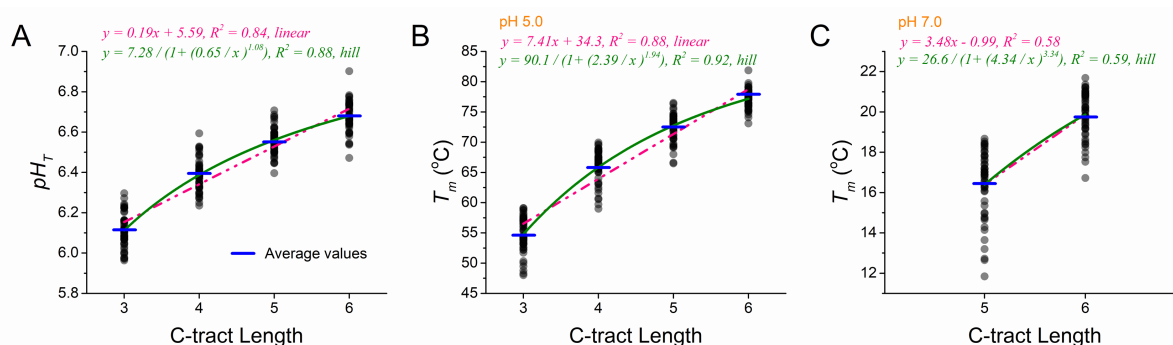


Figure 4. (A) pH_T , T_m s at (B) pH 5.0 and (C) pH 7.0 as a function of C-tract length. Averages of pH_T and T_m are indicated in blue short lines. Sequences in **Table S2** are used.

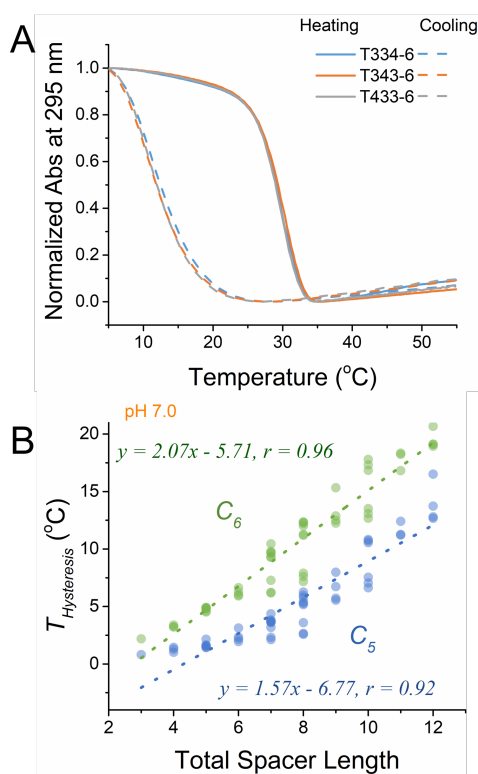


Figure 5. (A) Hysteresis for the T334-6 group in the UV-melting (solid line) and annealing (dashed line) processes at pH 7.0. Curves of other sequences are provided in **Figure S17**. (B) Hysteresis as a function of total spacer length ($T_{Hysteresis} = T_{Heating} - T_{Cooling}$).

Unfolding/folding rates depend on C-tract and loop lengths

As noted before, a hysteresis phenomenon is observed at near-neutral pH: the apparent melting transition is shifted towards higher temperatures than the value deduced from cooling profiles (**Figures 5A and S17**). The analysis of melting (heating) profiles alone would only lead to an overestimation of i-DNA thermal stability at neutral pH. Previous observations allowed to conclude that the average of $T_{Heating}$ and $T_{Cooling}$ provides a reasonable estimate of the thermodynamic T_m at equilibrium, using an infinitely slow temperature gradient; hysteresis being larger when fast temperature changes are implemented, as expected (not shown). What was not reported before is the strong dependency of the hysteresis phenomenon on total loop length, found both for C_5 and C_6 sequences (**Figure 5B**): in other words, sequences with longer T-loops fold and unfold slower than motifs with shorter ones. The hysteresis, induced by longer sequence length and higher pH value, is also observed in the DSC experiments (**Figure S19 and Table S4**). For this reason, the analysis of heating curves only would provide a wrong picture of i-DNA stability and lead to the inaccurate conclusion that stability increases with loop length. Restricting the analysis to cooling profiles would actually lead to the opposite, and also inaccurate, conclusion.

Expanding the “long central spacer is better” rule

All sequences studied above belong to a relatively narrow sequence space, in which (i) loops are entirely composed of thymines, (ii) total loop length is 12 or lower, (iii) two loops are of identical size and (iv) no individual loop involves more than 6 nucleotides. To validate our conclusions for a wider variety of motifs, we analyzed i-DNA stability for sequences that escape one or more of the conditions listed above (sequences listed in **Table**

RESEARCH ARTICLE

S1). i-DNA formation was confirmed by TDS (**Figure S20**). pH_T and T_m were also evaluated (**Figure S21**, data given in **Table S3**). For example, stability of sequences containing a longer central loop was analyzed, from 7 to 15 nucleotides, and results are summarized in **Figure S22**. These results allow us to conclude that i-DNA motif is still possible with a relatively long central loop (T_m is moderately affected while the drop in pH_T is more significant). In addition, this bell curve indicates that an optimal central loop length is 2-7 nucleotides for both T_m and pH_T .

Then *t*-tests show that the differences in pH_T and T_m values (**Table S3** and **Figures S23-S24**) between two sequences produced by swapping positions of two relatively short loops (SLM versus MLS, where S, M and L refer to the relatively short, middle, long loop length for the two sequences in a group, respectively) are not significant ($p > 0.05$) (**Figure S25**). This “stability-loop length-symmetry” is similar to the one disclosed above (**Figure 3**).

Replacement of one or two thymine residues in loops by adenine of three sequences from T115-5 groups produces 24

sequences in 7 groups (**Table S1**). pH_T and T_m were measured (**Figures S26, S27**) and given in **Table S3** and **Figure S28**. Sequences with longer central loops from 6 of 7 groups and all 7 groups have higher pH_T and T_m , respectively.

We further expanded the sequence space, including additional terminal nucleotides, spacer variants and odd numbers of C·C⁺ base pairs. We designed sequence variants based on T252-5. The results showed that the presence of a thymine, adenine or guanine at one (5' or 3') or both ends do not strongly affect the thermodynamic stability but influence the hysteresis of i-DNAs (**Figures S29-S31**, results summarized in **Table S5**). Interestingly, long adenine or guanine spacers result in the destabilization of i-DNA. Substitution of a single thymine by adenine or guanine in the second spacer increases the thermal stability, whereas the opposite effect is found in the first and third spacers. Significantly, the “long central spacer is better” rule can be extended to i-DNAs with odd numbers of C·C⁺ base pairs.

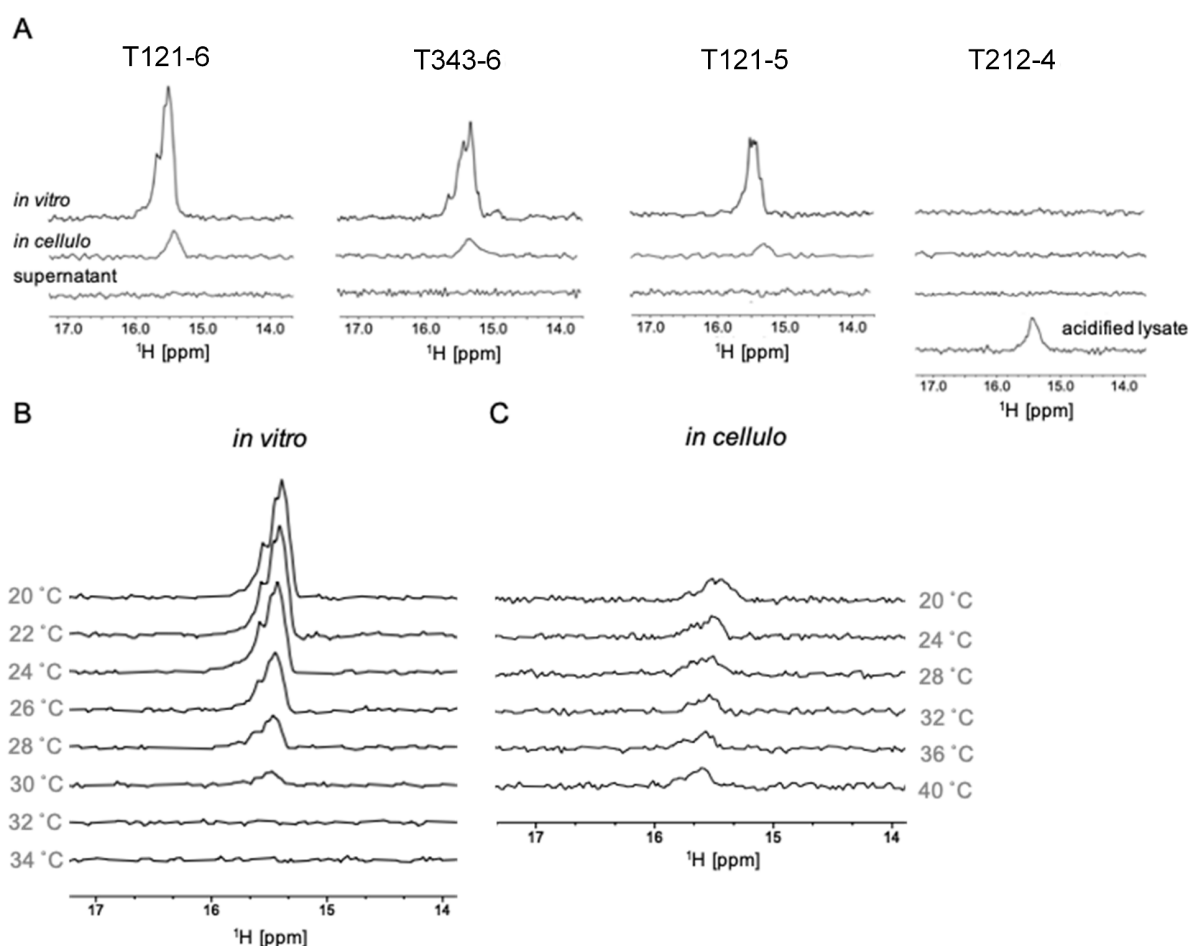


Figure 6. *in vitro* and in-cell NMR. **(A)** ¹H NMR spectra acquired at 20 °C *in vitro*, *in cellulo* (living HeLa cells), and in supernatant (medium) collected from in-cell NMR sample post in-cell NMR spectra acquisition, respectively. Absence of signals in the “supernatant” spectra evidences that the signals observed in in-cell NMR spectra originates from DNA localized in cells. Presence of i-DNA specific signals in the NMR spectrum of T212-4 acquired in acidified (pH < 6.5) lysate prepared from respective in-cell NMR sample (lysatation control) confirmed that T212-4 was present, yet unfolded, in the intracellular space of living cells. **(B, C)** ¹H NMR spectra of T121-6 acquired at various temperatures under **(B)** *in vitro* and **(C)** in living cells. The prerequisite flow cytometry plots and confocal images are shown in **Figure S32**.

Relative i-DNA stabilities in the intracellular environment parallel those found *in vitro*

To assess whether the rules we uncovered for the *in vitro* stability of i-DNA are applicable *in vivo*, we performed in-cell NMR experiments for four selected constructs (T212-4, T121-5, T121-6, and T343-6) differing by the virtue of their T_m and pH_T (Table S2). In-cell NMR spectra were acquired on a suspension of living HeLa cells transfected separately with individual constructs at 20 °C (Figure 6A). As evidenced from confocal microscopy images, all transfected constructs were localized in the nuclei (Figure S33). Observation of signals in region of the in-cell NMR spectra specific for imino protons involved in C·C* base pairs (15–16 ppm) corroborated i-DNA formation for T121-5, T121-6, and T343-6, while absence of signals indicated no i-DNA formation for T212-4 (Figure 6A). Notably, the order of relative intensities of the imino signals in the in-cell NMR spectra (T121-6 > T343-6 > T121-5 >> T212-4) essentially paralleled that obtained *in vitro*. Altogether, these data suggest that the rules derived on the basis of *in vitro* data are reasonably accurate to predict the behavior of i-DNAs in cells.

The absolute i-DNA stabilities in cells may differ from those observed *in vitro*.^[12] The intensities of imino signals in in-cell NMR spectra are perturbed by increasing temperature to lower extent than those in the corresponding *in vitro* NMR spectra: while the absence of imino signals in *in vitro* NMR spectrum acquired at 32 °C, the detectable in the corresponding in-cell NMR spectrum measured at 36 °C (and even 40 °C), demonstrating i-DNAs may be more stable in cells (Figures 6B and C).^[12]

Predicting i-DNA stability

Models for i-DNA stability were generated using three distinct approaches G4Hunter-based,^[26] machine learning based,^[27] and through a development of an analytical equation^[28] via an increasingly popular symbolic regression that has recently been shown to correctly discover physical laws as tested on known phenomena.^[29] The specifics of the approaches are detailed in the Supporting Information. We used the C/T-only restricted space for the i-DNAs, for which this work contributes an extensive set of systematic experimental data, therefore our models for T_m s (pH 5.0) or pH_T s can be used only to draw conclusions for C/T-based i-DNA structures (for instance, we do not take into account effect that may arise from competing Watson-Crick base-pairing while having G nucleobases in the loops) with similar restricted relation of the three spacer lengths (mostly with the two having the same length). The results and discussion of the G4Hunter-based and analytical equation based methods are described in Supporting Information (Figure S34). We focus on the machine learning based approach here only.

Gradient boosting machines (GBM) as machine learning framework (Supporting Information), resulted in models that capture the T_m and pH_T measurements with great performance (data from the 20% left-out validation dataset, Figure 7). The restricted feature set, necessary to comprehensively describe the C/T-based i-DNA candidates, compensated the relatively small (for machine learning standards) dataset used in this initiative, hence arriving to a good model performance in the validation trials. The optimal GBM architecture for T_m was found to have 0.01 learning rate, interaction depth of 4, subsampling ratio of 0.6, minimum child weight of 5, and contained 1000 trees as individual learners. This resulted in a model with 1.210 RMSE (root mean squared error) and 0.990 Pearson's R while predicting the T_m

values from the validation dataset. In contrast, the model developed for pH_T measurements had 0.01 learning rate, interaction depth of 6, subsampling ratio of 0.6, minimum child weight of 10, and contained 1500 trees as individual learners. The pH_T model had 0.053 RMSE and 0.973 Pearson's R, as applied on the validation dataset.

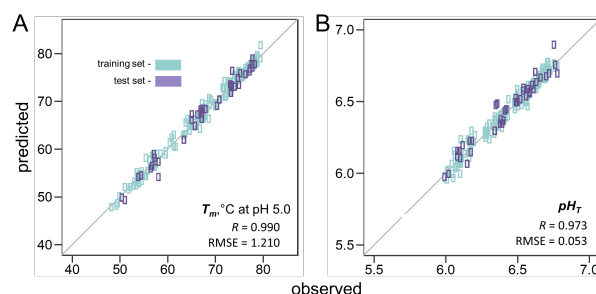


Figure 7. Correlation plots between the experimental stability measures (T_m at pH 5.0 and pH_T) and the i-DNA stability predicted via machine learning models obtained using gradient boosting machines. Plots are brought for both T_m (A) and pH_T (B) dependencies. The Pearson's correlation coefficients (R) and root mean squared errors (RMSE) are brought on the individual plots.

Discussion

Our work on i-DNA sequence requirements is of unprecedented magnitude, with 271 sequences tested. Even if impressive, this dataset does not allow to explore the full sequence space of i-DNA-prone sequences. Despite these restrictions, and because we tested a few sequences escaping this sequence space, our data already provides key information on i-DNA stability.

pH_T or T_m are useful to monitor i-DNA stability. As we found inappropriate to discard one of these parameters, both were used here, and it is difficult to conclude that one is superior to the other. If biological applications are contemplated, T_m and pH_T under physiological conditions would be recommended, although the accurate determination of intracellular (intranuclear) pH may prove harder than expected (see below). For both pH_T and T_m , one should remember that these transitions may not be at thermodynamic equilibrium and exhibit a hysteresis: the profiles obtained by varying a parameter (temperature or pH) in one direction are not superimposable when doing the reverse experiment.^[5b] Hysteresis is determined for each melting/annealing experiment described in this paper, and T_m average between cooling and heating was taken as a proxy for thermodynamic stability, as previously found for other i-DNA structures.^[24] For pH_T determination, each sample was allowed to anneal at a given pH for a long period (> 12 hours), allowing thermodynamic equilibrium.

We determined how well correlated these values are. The analyses of pH_T versus T_m (Figures 8A-B), and T_m at pH 7.0 versus 5.0 (Figure 8C) revealed good but not perfect positive correlations between these figures (Pearson's R between 0.79 and 0.95). This indicates that a higher pH_T generally translates into a higher T_m , both at pH 5.0 and 7.0, and that a higher T_m at pH 5.0 means a higher thermal stability at pH 7.0.

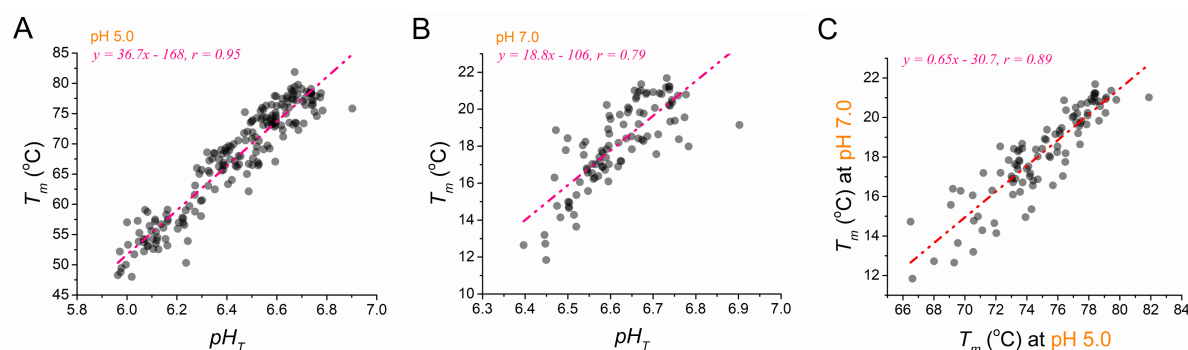


Figure 8. pH_T as function of T_m at (A) pH 5.0 or (B) pH 7.0. (C) T_m at pH 7.0 as a function of T_m at pH 5.0. Linear fits are presented as a red dashed line. Sequences in Table S2 were used.

i-DNA sequence constraints do not mirror G4 requirements.

A quick glance at our experimental results reveals several trends for i-DNA sequence requirements: (i) Stability increases with the length of the cytosine tract (Figure 4). (ii) The nature of the spacer regions does not play a critical role on stability. Correlation coefficients of pH_T and T_m versus total spacer length are close to zero, indicating that total *spacer* length, assumed to reflect total *loop* length, does not affect the i-DNA stability at both acidic and neutral pH. (iii) The “long central spacer is better” rule seems to hold for both G4^[22] and i-DNA. For G4s, sequences with long loop in the central position not only exhibit a relative high thermal stability, but are also more prone to form non-parallel conformations. As a consequence of this shared property, a duplex bearing a C-rich and a G-rich strand may be more prone to dismutation into G4 + i-DNA if a relatively long central spacer is present.

Overall, these observations confirm that i-DNA requirements do not perfectly match those of G4s. Increasing the number of quartets does lead to an increase in quadruplex stability. In addition, loop effects were more pronounced for G4 forming sequences, with large differences in T_m (and topology).^[22] In other words, the complementary strand of a very stable G4-forming sequence is not necessarily forming a very stable i-DNA. This indicates that the prediction tool we designed for G4 prediction, G4-Hunter^[26,30] is not optimized for i-DNA formation and should be recalibrated for this motif.

Gradient boosting machines (GBM). We built a *de novo* machine learning model to predict the experimental T_m and pH_T , for the limited sub-universe of C/T-based i-DNAs. The models used only four features - equally sized C-tract and three spacer lengths. Feature importance analysis from the GBM machine learning approach revealed that the most important feature in defining the stability of the i-motifs both in terms of T_m and pH_T is the C-tract length. For T_m prediction, the length of the 3rd spacer (T_3) is slightly more important than that of the other two. For pH_T prediction, this is unclear because the importance ranking of the 3 spacers differs whether total sequence length is included or not as a feature (data not shown). Unsurprisingly, Eureqa results (check Supporting Information) agree with GBM's in that C-tract length is far more important in predicting both T_m and pH_T of this sub-universe of i-DNAs, as already visible from the plots shown in Figure 4. The sequences tested here only cover a limited sequence space, and more data should be collected to apply these prediction tools to mixed motifs containing spacers of any

sequence or C-runs of unequal length. A “theory of every i” has yet to emerge!

Implications for biology. The NMR results suggesting the rules derived on the basis of *in vitro* data are reasonable approximation for i-DNA behavior in cells. i-DNA relative instability may be an asset for regulation of pH homeostasis, as modest and transient changes in intracellular pH should lead to important variations in i-DNA stability. For example, the physiological intracellular pH has been reported to vary between 7.0 and 7.4, depending on tissues and phase of the cell cycle.^[31] Invasive tumor cells tend to acidify their extracellular environment while keeping their pH_i more alkaline.^[32] It is therefore important to correlate *in vitro* and *in cellulo* observations. In-cell NMR measurements suggest that i-DNA stability may be slightly higher than what is found *in vitro*. The water activity, dielectric constant, local concentration of free ions, pH, may affect the stability of the structure of interest, as well as the presence of cellular competitors or natural ligands. This is a problem of general importance for biochemists, to make sure that the conclusions reached in the test tube reflect what is happening in the cell. We hope that further *in cellulo* - *in vitro* comparisons will provide decisive answers.

Conclusion

By performing an exhaustive experimental analysis of i-DNA formation on a dataset of unprecedented magnitude, we were able to provide a global picture of i-DNA formation *in vitro*, and propose tools to predict its stability as a function of primary sequence. The most stable candidates were confirmed to adopt an i-DNA conformation in cells. This work will be invaluable not only for those interested in the biological functions of this structure, but also when considering nano- or biotech applications with these pH-sensitive devices.

Acknowledgements

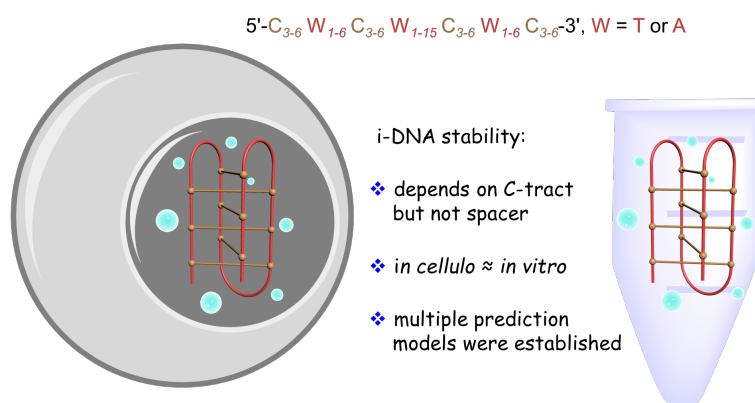
This work was supported in part by National Natural Science Foundation of China (21977045), Fundamental Research Funds for the Central Universities (02051430210), and funding from NJU (020514912216). J.L.M. acknowledges ERDF (CZ.02.1.01/0.0/0.0/15_003/0000477) and dedicates this manuscript to the memory of Jean-Louis Leroy, one of the i-DNA

pioneers in Ecole Polytechnique. M.C. acknowledges the China Postdoctoral Science Foundation (2019M661793), Lukáš T. acknowledges the Czech Science Foundation (19-26041X), the Ministry of Education, Youth and Sports of the Czech Republic (CIISB research infrastructure project LM2015043; CEITEC 2020, LQ1601). Liezel T. is grateful to the Jardine Foundation and A.B.S. thanks Medical Research Council (UK).

Keywords: DNA • i-motif • thermal stability • pH transition • intracellular stability

- [1] K. Gehring, J. L. Leroy, M. Guéron, *Nature* **1993**, 363, 561-565.
- [2] A. L. Lieblein, M. Kramer, A. Dreuw, B. Fürtig, H. Schwalbe, *Angew. Chem. Int. Ed.* **2012**, 51, 4067-4070; *Angew. Chem.* **2012**, 124, 4143-4146.
- [3] a) J. L. Leroy, M. Guéron, J. L. Mergny, C. Hélène, *Nucleic Acids Res.* **1994**, 22, 1600-1606; b) S. Nonin-Lecomte, J. L. Leroy, *J. Mol. Biol.* **2001**, 309, 491-506; c) A. T. Phan, M. Guéron, J. L. Leroy, *J. Mol. Biol.* **2000**, 299, 123-144; d) X. Han, J. L. Leroy, M. Guéron, *J. Mol. Biol.* **1998**, 278, 949-965; e) K. Snoussi, S. Nonin-Lecomte, J. L. Leroy, *J. Mol. Biol.* **2001**, 309, 139-153.
- [4] a) A. L. Lieblein, J. Buck, K. Schlepckow, B. Fürtig, H. Schwalbe, *Angew. Chem. Int. Ed.* **2012**, 51, 250-253; *Angew. Chem.* **2012**, 124, 255-259; b) A. L. Lieblein, B. Fürtig, H. Schwalbe, *ChemBioChem* **2013**, 14, 1226-1230.
- [5] a) E. P. Wright, J. L. Huppert, Z. A. E. Waller, *Nucleic Acids Res.* **2017**, 45, 2951-2959; b) R. A. Rogers, A. M. Fleming, C. J. Burrows, *Biophys. J.* **2018**, 114, 1804-1815; c) P. Školáková, D. Renčiuk, J. Palacký, D. Krafčík, Z. Dvořáková, I. Kejnovská, K. Bednářová, M. Vorlíčková, *Nucleic Acids Res.* **2019**, 47, 2177-2189.
- [6] J. L. Mergny, L. Lacroix, X. Han, J. L. Leroy, C. Hélène, *J. Am. Chem. Soc.* **1995**, 117, 8887-8898.
- [7] J. L. Mergny, D. Sen, *Chem. Rev.* **2019**, 119, 6290-6325.
- [8] J. J. Alba, A. Sadurni, R. Gargallo, *Crit. Rev. Anal. Chem.* **2016**, 46, 443-454.
- [9] K. Leung, K. Chakraborty, A. Saminathan, Y. Krishnan, *Nat. Nanotechnol.* **2018**, 14, 176-183.
- [10] M. Debnath, K. Fatma, J. Dash, *Angew. Chem. Int. Ed.* **2019**, 58, 2942-2957; *Angew. Chem.* **2019**, 131, 2968-2983.
- [11] M. Zeraati, D. B. Langley, P. Schofield, A. L. Moye, R. Rouet, W. E. Hughes, T. M. Bryan, M. E. Dinger, D. Christ, *Nat. Chem.* **2018**, 10, 631-637.
- [12] S. Dzatko, M. Krafcikova, R. Hansel-Hertsch, T. Fessler, R. Fiala, T. Loja, D. Krafcik, J.-L. Mergny, S. Foldynova-Trantirkova, L. Trantirek, *Angew. Chem. Int. Ed.* **2018**, 57, 2165-2169; *Angew. Chem.* **2018**, 130, 2187-2191.
- [13] E. Belmonte-Reche, J. C. Morales, *NAR Genom. Bioinform.* **2020**, 2, lqz005.
- [14] X. Li, Y. Peng, J. Ren, X. Qu, *Proc. Natl. Acad. Sci. U. S. A.* **2006**, 103, 19658-19663.
- [15] a) K. Niu, X. Zhang, H. Deng, F. Wu, Y. Ren, H. Xiang, S. Zheng, L. Liu, L. Huang, B. Zeng, S. Li, Q. Xia, Q. Song, S. R. Palli, Q. Feng, *Nucleic Acids Res.* **2018**, 46, 1710-1723; b) H. J. Kang, S. Kendrick, S. M. Hecht, L. H. Hurley, *J. Am. Chem. Soc.* **2014**, 136, 4172-4185.
- [16] S. Takahashi, J. A. Brazier, N. Sugimoto, *Proc. Natl. Acad. Sci. U. S. A.* **2017**, 114, 9605-9610.
- [17] a) B. Mir, I. Serrano, D. Buitrago, M. Orozco, N. Escaja, C. González, *J. Am. Chem. Soc.* **2017**, 139, 13985-13988; b) I. V. Nesterova, E. E. Nesterov, *J. Am. Chem. Soc.* **2014**, 136, 8843-8846.
- [18] a) A. M. Fleming, K. M. Stewart, G. M. Eyring, T. E. Ball, C. J. Burrows, *Org. Biomol. Chem.* **2018**, 16, 4537-4546; b) A. M. Fleming, Y. Ding, R. A. Rogers, J. Zhu, J. Zhu, A. D. Burton, C. B. Carlisle, C. J. Burrows, *J. Am. Chem. Soc.* **2017**, 139, 4682-4689.
- [19] A. Sengar, B. Heddi, A. T. Phan, *Biochemistry* **2014**, 53, 7718-7723.
- [20] a) S. Benabou, M. Garavis, S. Lyonnais, R. Eritja, C. González, R. Gargallo, *Phys. Chem. Chem. Phys.* **2016**, 18, 7997-8004; b) S. M. Reilly, R. K. Morgan, T. A. Brooks, R. M. Wadkins, *Biochemistry* **2015**, 54, 1364-1370; c) I. V. Nesterova, J. R. Briscoe, E. E. Nesterov, *J. Am. Chem. Soc.* **2015**, 137, 11234-11237; d) S. P. Gurung, C. Schwarz, J. P. Hall, C. J. Cardin, J. A. Brazier, *Chem. Commun.* **2015**, 51, 5630-5632; e) T. Fujii, N. Sugimoto, *Phys. Chem. Chem. Phys.* **2015**, 17, 16719-16722; f) M. McKim, A. Buxton, C. Johnson, A. Metz, R. D. Sheardy, *J. Phys. Chem. B* **2016**, 120, 7652-7661.
- [21] S. Kendrick, Y. Akiyama, S. M. Hecht, L. H. Hurley, *J. Am. Chem. Soc.* **2009**, 131, 17667-17676.
- [22] M. Cheng, Y. Cheng, J. Hao, G. Jia, J. Zhou, J. L. Mergny, C. Li, *Nucleic Acids Res.* **2018**, 46, 9264-9275.
- [23] J. L. Mergny, J. Li, L. Lacroix, S. Amrane, J. B. Chaires, *Nucleic Acids Res.* **2005**, 33, e138.
- [24] J. L. Mergny, L. Lacroix, *Nucleic Acids Res.* **1998**, 26, 4797-4803.
- [25] J. L. Mergny, L. Lacroix, *Oligonucleotides* **2003**, 13, 515-537.
- [26] A. Bedrat, L. Lacroix, J. L. Mergny, *Nucleic Acids Res.* **2016**, 44, 1746-1759.
- [27] A. B. Sahakyan, V. S. Chambers, G. Marsico, T. Santner, M. Di Antonio, S. Balasubramanian, *Sci. Rep.* **2017**, 7, 14535.
- [28] M. Schmidt, H. Lipson, *Science* **2009**, 324, 81-85.
- [29] S. M. Udrescu, M. Tegmark, *Sci. Adv.* **2020**, 6, eaay2631.
- [30] a) V. Brazda, J. Kolomaznik, J. Lysek, M. Bartas, M. Fojta, J. Stastny, J. L. Mergny, *Bioinformatics* **2019**, 35, 3493-3495; b) L. Lacroix, *Bioinformatics* **2019**, 35, 2311-2312.
- [31] J. R. Casey, S. Grinstein, J. Orlowski, *Nat. Rev. Mol. Cell Biol.* **2010**, 11, 50-61.
- [32] a) E. Persi, M. Duran-Frigola, M. Damaghi, W. R. Roush, P. Aloy, J. L. Cleveland, R. J. Gillies, E. Ruppín, *Nat. Commun.* **2018**, 9, 2997; b) B. A. Webb, M. Chimentì, M. P. Jacobson, D. L. Barber, *Nat. Rev. Cancer* **2011**, 11, 671-677.

Entry for the Table of Contents



Supporting Information
©Wiley-VCH 2019
69451 Weinheim, Germany

Thermal and pH stabilities of i-DNA: confronting *in vitro* experiments with models and in-cell NMR data

Mingpan Cheng, Dehui Qiu, Liezel Tamon, Eva Ištvánková, Pavlína Víšková, Samir Amrane, Aurore Guédin, Jielin Chen, Laurent Lacroix, Huangxian Ju, Lukáš Trantírek, Aleksandr B. Sahakyan, Jun Zhou,* and Jean-Louis Mergny

Abstract: Recent studies indicate that i-DNA, a four-stranded cytosine-rich DNA also known as the i-motif, is actually formed *in vivo*; however, a systematic study on sequence effects on stability has been missing. Herein, an unprecedented number of different sequences (271) bearing four runs of 3-6 cytosines with different spacer lengths has been tested. While i-DNA stability is nearly independent on total spacer length, the central spacer plays a special role stability. Stability also depends on the length of the C-tracts at both acidic and neutral pHs. This study provides a global picture on i-DNA stability thanks to the large size of the introduced data set; it reveals unexpected features and allows to conclude that determinants of i-DNA stability do not mirror those of G-quadruplexes. Our results illustrate the structural roles of loops and C-tracts on i-DNA stability, confirm its formation in cells, and allow establishing rules to predict its stability.

DOI: 10.1002/anie.2016XXXXX

SUPPORTING INFORMATION

Table of Contents

Experimental Procedures.....	S03
Results and Discussion	
Table S1 271 sequences information and BLAST results.....	S06
Table S2 pH transition midpoint and thermal stability of 196 pyrimidine sequences containing thymidine spacers and C-tract of variable lengths.....	S14
Table S3 pH transition and thermal stability at pH 5.0 of extended sequences with four C_5 -tracts.....	S18
Table S4 Thermal stability measured by DSC-melting and annealing experiments.....	S19
Table S5 Thermal stability of sequences with flanking sequences, different spacer contents and odd number of C-C ⁺ base pairs (Figures S33-34) and description of the results.....	S20
Figure S1 Thermal difference spectra (TDS).....	S21
Figure S2 ¹ H 1D NMR spectra.....	S24
Figures S3-S4 Non-denaturing PAGEs.....	S25
Figures S5-9 pH-dependent normalized ellipticities at 288 nm for sequences.....	S27
Figures S10-14 pH-dependent normalized absorbances at 295 nm for sequences.....	S38
Figure S15 Comparison of pH_T obtained by pH-dependent CD and UV absorbance spectra.....	S45
Figure S16 UV-melting curves at pH 5.0.....	S46
Figure S17 UV-melting and annealing curves at pH 7.0.....	S49
Figure S18 Melting temperature (T_m) at pH 5.0 and 7.0.....	S53
Figure S19 DSC-melting and annealing profiles of selected sequences.....	S54
Figure S20 TDS of 40 extended sequences with C_5 -tract.....	S55
Figure S21 pH-dependent ellipticities and UV-melting curves at pH 5.0 of sequences with C_5 -tract and longer central loop.....	S56
Figure S22 Effect of central spacer length on pH_T and T_m of T1N1-5 sequences.....	S57
Figure S23 pH-dependent CD spectra of sequences with two short loops of different length.....	S58
Figure S24 UV-melting curves at pH 5.0 of sequences with two short loops in different length.....	S59
Figure S25 Hypothesis of pair-sample t -test between SLM and MLS loop permutations.....	S60
Figure S26 pH-dependent ellipticities of sequences with C_5 -tract and one or two adenines in loop.....	S61
Figure S27 UV-melting curves at pH 5.0 of sequences with C_5 -tract and one or two adenines in loop.....	S62
Figure S28 Spacer permutation in sequences with different spacer compositions.....	S63
Figure S29 TDS at pH 5.0 and pH 7.0 of sequences with flanking sequences, different spacer contents and odd number of C-C ⁺ base pairs.....	S64
Figure S30 UV-melting/annealing at pH 5.0 of sequences with flanking sequences, different spacer contents and odd number of C-C ⁺ base pairs.....	S65
Figure S31 UV-melting/annealing at pH 7.0 of sequences with flanking sequences, different spacer contents and odd number of C-C ⁺ base pairs.....	S66
Figures S32-33 Cells viability, level of DNA transfection, and intracellular localization of transfected DNAs for in-cell NMR experiments.....	S67
Figure S34 Correlation plots between the experimental stability measures and the i-DNA stability scores obtained via optimized models analogous to G4Hunter.....	S68
Supplementary references	S69

SUPPORTING INFORMATION

Experimental Procedures

Nomenclature of sequences

271 i-DNA forming sequences were investigated, divided into four types based on C-tract length: each oligonucleotide contained four runs of 3, 4, 5, or 6 cytosines; see sequences information provided in **Tables S1** and **S2**. Each sequence generally contains four identical C-tracts (exceptions listed in **Table S5**), which are separated by three spacers. Note that we will generally prefer the word “spacer” over “loop” as the identity of the bases participating in the loop does not always matches the spacer sequence: some cytosines thought to be involved in the i-DNA stem may rather participate in the loops, especially when spacers are short. For most sequences (**212 out of 271**), these spacer regions were consisting of thymidines only, ranging from 1 to 6 nucleotides. The nomenclature is shown in **Table S2**: a “T” prefix means that the three spacers are composed of thymine bases only; the three consecutive numbers refer to lengths of the three spacers in the 5' to 3' direction; while the “-3”, “-4”, “-5” or “-6” suffix refers to sequences with four identical C₃, C₄, C₅, and C₆ tracts, respectively. In order to compare the effects of spacer arrangement on i-DNA stability, the notion of sequence group was introduced^[1]. The sequences in the same group are only differing in the way spacers are permuted. A group is named after the first sequence in the group. For example, the T112-3 group is composed of three sequences T112-3, T121-3, and T211-3. All three sequences have the same length, the same overall base content with short spacers composed of one or two thymines separating four runs of three cytosines.

Preparation of oligonucleotides and reagents

Chemicals were purchased from Sigma-Aldrich (Shanghai, China) and oligonucleotides purified by ultra-PAGE were ordered from Sangon Biotech (Shanghai, China) and dissolved in distilled and deionized water (18.2 MΩ·cm). Concentration of sample stock was determined by ultraviolet (UV) absorbance at 260 nm using the molar extinction coefficients provided by manufacturer. Samples were then stored at 4 °C and used without further purification. Unless otherwise stated, Britton-Robinson buffers (B-R) contain four components: H₃BO₃/H₃PO₄/CH₃COOH/NaOH; they were chosen in this work considering their wide buffering range and small temperature coefficient, which is important for i-DNA studies^[2]. pH was adjusted after the addition of 140 mM KCl at room temperature. Prior to all following experiments, all oligonucleotides samples were prepared in 20 mM B-R buffer containing 140 mM KCl at the chosen pH, denatured at 95 °C for 3 min, slowly cooled down during 2 hours to room temperature, and then incubated at 4 °C overnight to ensure complete equilibration of folding and unfolding processes.

Absorbance and circular dichroism (CD) measurements

Thermal difference spectra (TDS)^[3]. 5.0 μM oligonucleotide samples were prepared in 20 mM B-R buffer containing 140 mM KCl (pH 5.0 or 7.0). Ultraviolet (UV)-Visible absorbance spectra (220-320 nm, Cary100, Agilent) were recorded at low temperature (5 °C for both pH 5.0 and 7.0) first and then at high temperature (95 and 65 °C for pH 5.0 and 7.0, respectively). Prior to the measurements, samples were incubated at the corresponding temperature for at least 5.0 min. During each scan, high speed dry air was used to flush the cuvette holder in order to prevent condensation. TDS spectra were calculated by subtraction of the spectrum recorded at low temperature from the one at high temperature (after autozero at 320 nm), and normalized using the differential absorbance at 239 nm to compare the curve shapes.

pH-dependent transition experiments. Experiments were performed by monitoring the UV-Visible absorbance (Cary 100, Agilent) and CD spectra (Applied Photophysics) in the 220-320 nm wavelength range at 25 °C. Oligonucleotides were dissolved at a final concentration of 5.0 μM in 20 mM B-R buffer at a pH varying from 5.0 to 8.0 with 0.25 pH unit intervals (i.e., 13 different pH values were tested) in the presence of 140 mM KCl. All samples in the corresponding pH solutions were denatured at 95 °C for 3 min, slowly cooled down to room temperature, then stored at 4 °C for at least overnight. All samples were then incubated at 25 °C for at least two hours prior to spectral measurements. Each sample scan was subtracted by the corresponding buffer scan before data processing. The changes in signal intensities at 295 and 288 nm for UV absorbance and CD ellipticity, respectively, were used to calculate the pH transition midpoint (pH_T) of the structure switching from stable i-DNA to random coil. pH_T were obtained by fitting the signals from UV or CD vs. pH values, by using a Boltzman sigmoidal function.

UV-melting/annealing experiments^[4]. Samples were prepared at 5.0 μM oligonucleotide concentration in 20 mM B-R buffers containing 140 mM KCl. UV-absorbance at 295 nm was recorded at pH 5.0 (for all sequences, 0.5 °C/min rate in 5 to 95 °C temperature range) or 7.0 (for sequences with C₅- and C₆-tracts, using a slower temperature gradient of 0.2 °C/min to limit hysteresis). Absorbance was normalized between 1 and 0 to compare the profiles. Half transition temperatures (T_m or $T_{1/2}$) were calculated by fitting the plot of UV absorbance vs. temperature with a Boltzman sigmoidal function. $T_{1/2}$ is used rather than T_m when hysteresis is present.

Differential scanning calorimetry (DSC)

DSC measurements were carried out using a Nano DSC equipment. Oligonucleotides were prepared at 100 μM strand concentration in 20 mM B-R buffer (pH 5.0 or 7.0). All heating and cooling scans were recorded at 1.0 °C/min rate, and in the 0-100 °C and 0-65 °C temperature ranges for pH 5.0 and 7.0 supplemented with 140 mM KCl, respectively. The DNA sample versus buffer scan was subtracted by the previously performed buffer versus buffer for all the scans. T_m or $T_{1/2}$ was calculated by using *TwoStateScaled* model to fit the heat capacity vs. temperature curve.

SUPPORTING INFORMATION

Gel electrophoresis

Non-denaturing polyacrylamide gel electrophoresis (PAGE) experiments were performed to check the molecularity of sequences with C₅-tracts. Oligonucleotides were dissolved in B-R buffer (pH 5.0 or 7.0) at 100 μ M strand concentration, denatured at 95 °C for 3 min, then slowly cooled to room temperature. Samples were stored at 4 °C overnight before incubation. Oligonucleotides were incubated for two hours at room temperature, then 30% (w/v) sucrose was added before loading and final oligo concentration was 25.0 μ M. Gels (7 × 10 × 0.1 cm) were prepared with 15% acrylamide (acrylamide:bisacrylamide, 19:1) in 50 mM B-R buffer (pH 5.0 or 7.0) which was also used as the running buffer. Gels were run at room temperature (ca. 25 °C) with 80 V for 90 min and stained by Stains-all (Sigma, 95%). Oligothymidylate DNA single-strands (dT_n, n = 90, 60, 30, 21, 15, 10) were used as internal migration standards, and bromophenol blue was added to act as an indicator of migration.

In vitro 1D ¹H NMR

100 μ M oligonucleotide was prepared in 20 mM pH 7.0 potassium phosphate (KPi) buffer supplemented with 10% (v/v) D₂O and KCl (total potassium in solution is 140 mM), then denatured at 95 °C for 3 min, slowly cooled down to room temperature, and stored at 4 °C overnight. Prior to experiments, samples were incubated at room temperature for at least two hours. ¹H NMR experiments were carried out on a 400 (Figure S2) or 600 MHz (Figure 7) Bruker spectrometer at 20 °C, unless stated otherwise. The jump-and-return pulse program was used in recording proton spectra and suppressing the water signal.

In-cell 1D ¹H NMR

Preparation of DNA oligonucleotides. Oligonucleotides used for in-cell NMR experiments were ordered from Sigma-Aldrich (USA). Non-labelled oligonucleotides were purchased as pre-purified by desalting at a 10- μ mol scale, while the fluorescently-labelled oligonucleotides were purified by HPLC and ordered at a 1-nmol scale. For oligonucleotide labelling, FAM dye was used at the 5' end. The fluorescently (FAM) labelled oligonucleotides were dissolved in H₂O to yield 100.0 μ M stock solutions. Desalted oligonucleotides were further subjected to *n*-butanol precipitation, to remove contaminants from the solid-state synthesis. At first, they were dissolved in 1 mL Milli-Q H₂O. Then, 30 mL of *n*-butanol was added, the samples were mixed thoroughly for ~ 10 min and transferred into centrifuge tubes (Beckman Coulter, USA). The centrifugation parameters were set to 30,000 × g, 4 °C and 1 h. After centrifugation, the supernatant was carefully drained and the samples were left open to dry at room temperature. The dried pellets were resuspended in 1 mL Milli-Q H₂O again and annealed by heating the solution for 5 min at 95 °C and allowing the samples to cool down to room temperature. Finally, the concentration was determined by UV absorbance, using NanoDrop 2000c (Thermo Fisher Scientific, USA).

Preparation of in-cell NMR samples. The in-cell NMR samples were prepared according to the protocol by Krafcikova *et al.* [5]. For purpose of in-cell NMR experiments, HeLa cells (Sigma-Aldrich, USA) were cultured in Dulbecco's modified Eagle's medium (DMEM) (Gibco, USA) supplemented with 10 % fetal bovine serum (HyClone, GE Life Sciences) and penicillin-streptomycin solution (100 units penicillin and 0.10 mg streptomycin/mL) (Sigma-Aldrich, USA) at 37 °C in a 5 % CO₂ atmosphere.

The DNA was introduced inside the cells via electroporation using the BTX-ECM 830 system (Harvard Apparatus, USA). Prior to electroporation, cells were washed with 1 x Dulbecco's Phosphate Buffered Saline (PBS) (Sigma-Aldrich, USA) and harvested using 1 x Trypsin/EDTA (Sigma-Aldrich, USA) in PBS. Cells were then centrifuged at 1,000 rpm for 5 min and resuspended in 1 x PBS. To estimate the number of cells per mL, cells were counted in a Bürker counting chamber and approximately 1.1 × 10⁸ cells were used to prepare the NMR sample. The proper amount of cells was centrifuged (1,000 rpm for 5 min) and resuspended in 2.8 mL of the Electroporation buffer (EC buffer) (140 mM NaPO₄, 5 mM KCl, 10 mM MgCl₂, pH 7.0) containing 400 μ M DNA and 10 μ M FAM-labelled DNA. The cell suspension was then divided into 4-mm electroporation cuvettes (Cell Projects, UK) and incubated on ice for 5 min. The used electroporation procedure consisted of two square-wave pulses (100 μ s/1000 V and 30 ms/350 V) separated by a 5 s interval. After electroporation, cells were incubated at room temperature for 2 min, then transferred into Leibovitz L15 ^{-/-} medium (no FBS/no antibiotics) (Gibco, USA) and centrifuged (1000 rpm, 5 min). Cells were resuspended in fresh L15 ^{-/-} medium and a small portion of the suspension (~ 6 × 10⁵ cells) was used for flow cytometry (FCM) and confocal microscopy analysis (see below) to evaluate the cell viability, electroporation efficiency and DNA localization. The rest of the suspension was centrifuged (1000 rpm, 5 min) and after removing the supernatant, the cell pellet was resuspended in 550 μ L of Leibovitz L15 ^{-/-} medium containing 10 % D₂O and placed into a 5-mm Shigemi NMR tube (Shigemi Co., Tokyo, Japan). Prior to performing the NMR experiment, cells in the NMR tube were manually centrifuged using a "hand centrifuge" (CortecNet, France) to form a fluffy pellet at the bottom of the NMR tube. Finally, 450 μ L of L15 ^{-/-} medium (with 10 % D₂O) was carefully added into the tube.

Flow cytometry. For FCM analysis, ~ 10⁵ cells were resuspended in 200 μ L of PBS buffer (Sigma-Aldrich, USA) and 1 μ L (stock solution was 1 mg/mL) of propidium iodide (PI) (Exbio, Czech Republic) was added for distinguishing the living cells from the apoptotic population, dead cells, or cells with compromised membrane integrity. Subsequently, 10⁴ HeLa cells were analyzed using a BD FACSVerser flow cytometer with BD FACSuite software (BD Biosciences, San Jose, CA, USA). To measure cell viability, excitation wavelength for PI was set to 488 nm, and the emission was detected at 700/54 nm. To evaluate the transfection efficiency, the fluorescently (FAM) labelled DNA was excited at 488 nm, and the emission was detected at 527/532 nm.

Confocal microscopy. For confocal microscopy, ~ 5 × 10⁵ cells were placed in one drop onto a 35-mm glass dish (ibidi GmbH, Germany) pre-coated with 0.01 % poly-L-lysine (Sigma-Aldrich, USA). The cell drop was then immersed in 2 mL of Leibovitz L15 ^{-/-}

SUPPORTING INFORMATION

medium containing 1 $\mu\text{g/mL}$ Hoechst dye (Sigma-Aldrich, USA) to stain the cell nuclei. All microscopy images were obtained using a Zeiss LSM 800 confocal microscope with a 63x/1.2 C-Apo-chromat objective.

In-cell NMR spectra acquisition. For in-cell NMR spectroscopy analysis, a 600 MHz Bruker Avance III HD spectrometer (Bruker, Corporation, Billerica, MA, USA) equipped with a quadruple-resonance cryogenic probe was used. In-cell 1D ^1H NMR spectra were acquired at 20 $^\circ\text{C}$ in Leibovitz L15 -/- medium containing 10 % D_2O , with 5 x 256 scans, using a 1D ^1H JR-echo (1-1 echo) pulse sequence [6] with zero excitation set to the resonance of water and the excitation maximum set to 13 ppm. The spectra were corrected for baseline and processed with the exponential apodization function with the line-broadening parameter set to 14. Data were processed using MNova v12.0.0 (Mestrelab Research, Spain).

Immediately after the acquisition of the in-cell NMR spectrum, 1D ^1H NMR spectrum of the supernatant was measured (using the same parameters as were used for acquiring the in-cell NMR spectra) to control for possible leakage of the transfected DNA from the cells. Meanwhile, a fraction of cells in the NMR tube was taken for FCM analysis to evaluate the cell mortality in the course of the NMR experiment, and the rest of the cells were subjected to lysis (see below) in order to control for possible DNA degradation and to acquire higher resolution spectra in a more homogenous sample [5, 7]. Finally, 1D ^1H NMR spectrum of the cell lysate was measured using the same NMR parameters as mentioned above.

Cell lysis. Following the acquisition of the in-cell NMR spectrum, the cellular pellet was resuspended in 200 μL of the Lysation buffer (10 mM NaPO_4 , 1.5 mM MgCl_2 , 10 mM KCl, 0.5 % NP-40, pH 6.8), sonicated on ice with a micro-tip (3 x 10 s at amplitude of 50 %; then 1 x 5 s at amplitude of 85 %), and heated at 95 $^\circ\text{C}$ for 2 min. The sample was then centrifuged at max speed (15 000 rpm) for 10 min and the pH of the resulting supernatant was adjusted to pH < 6.5. After 10 % D_2O enrichment, the sample was finally placed into a 5-mm Shigemi NMR tube (Shigemi Co., Tokyo, Japan) and taken for NMR measurement.

Modeling studies for stability prediction

Modeling studies have been constructed, to separately predict melting temperatures (T_m at pH 5.0) or the pH transition mid-points (pH_T), by adhering to three general strategies. Unless otherwise stated, all the calculations were done *via* custom scripts written in R programming language.

Modifying the G4-Hunter algorithm to make it applicable for i-DNAs. First, a model was generated by modifying the existing G4Hunter algorithm [8], adapting that to the given sequence space of C-based i-DNAs with T-only spacers. In the original G4Hunter, designated for G-quadruplex sequences, a sole G singleton acquires a score of 1 (a scoring coefficient), each G in a GG tract acquires 2 and so on. In the modified version, the base that adds positive scoring was set to be C, instead of G, with the maximum cutoff for the length of the tract set to 6. The contribution from the T bases, along with any other possible bases, was set to be 0. Furthermore, the individual non-0 scoring coefficients, for each C in CC tract, each C in CCC tract and so on, were optimized to values different from the conventional G4Hunter integer numbers. The optimization was done to fit the provided i-DNA dataset (T_m or pH_T), using the *Optimus* optimization engine [9], *via* an acceptance ratio annealing Monte Carlo technique. Acceptance ratio values were allowed to linearly reduce from 90 % to 5 % in 4 cycles, each using 250,000 optimization steps. In each step, a random scoring coefficient was selected, altering its value by 0.1, with a sign of alteration (*i.e.* whether adding or subtracting) also randomly determined. The new configuration was then either retained or rejected based on the Metropolis criterion, with the acceptance probabilities conforming the above-mentioned linear regiment of the acceptance ratio annealing through a special self-adjusting pseudo-temperature bath [9].

This approach of creating a G4Hunter analogue for i-DNAs, while accounting for C-tract-based (instead of G4Hunter G-tracts) scores and optimizing the scoring coefficients, resulted in models that assign overall scores (iM_{score}) to i-DNAs while capturing the T_m ($T_m \text{ pred} = 55.15 + 0.6440 iM_{\text{score}}^{T_m}$, Pearson's R = 0.958, **Figure S34A**) and pH_T ($pH_T \text{ pred} = 6.13 + 0.0188 iM_{\text{score}}^{pH_T}$, Pearson's R = 0.915, **Figure S34B**) dependencies. In general, the above approach resulted in all the scoring coefficients for the C-tracts of length 3 and shorter to be optimized to 0, retaining only the coefficients for the tracts of length 4 (24.1 for $iM_{\text{score}}^{T_m}$, 20.2 for $iM_{\text{score}}^{pH_T}$), 5 (37.0 for $iM_{\text{score}}^{T_m}$, 31.4 for $iM_{\text{score}}^{pH_T}$) and at-or-above-6 (45.1 for $iM_{\text{score}}^{T_m}$, 38.3 for $iM_{\text{score}}^{pH_T}$). The 0 coefficients reflected the fact that all our sequences had at least 3 Cs in their C-tracts, thus eliminating the need to have a differentiating contributor from C tracts of length 3 or below. The model for T_m and pH_T reached a good performance, however, due to all the training sequences having C-tracts with at least three Cs within, the scoring coefficients for the C-tracts of length 3 and shorter were optimized into 0.

Gradient boosting machines (GBM). The second strategy was to develop a novel sequence-only machine learning model for the restricted C- and T-based sequence space used in this study. Due to the simplicity of the explored sub-universe of i-DNA structures, we were able to use only four features to fully abstract the sequence in our dataset. Those features were C-tract length (denoted as C, same for all C-tracts in a given i-DNA candidate sequence), and the lengths of all three T-based loops (denoted as T_1 , T_2 and T_3 , from 5' to 3' direction). All features were next checked against the presence of a strong cross-correlation, and were centered and scaled. Those were then used for machine learning, by adopting the XGBoost [10] implementation of the Gradient Boosting Machines [11], as interfaced through R via the Caret library [12]. Gradient boosting machines have been successfully applied for modelling G-quadruplex structures before [13], hence a similar strategy was used here, but with simple initial feature set. To tune the machine learning architecture, five hyperparameters (in the XGBoost implementation denoted as *eta* - learning rate or shrinkage, *max_depth* - interaction depth, *min_child_weight* - final leave characteristics in the trees, *subsample* - bag fraction or subsampling ratio, and *nrounds* - number

SUPPORTING INFORMATION

of trees) were optimized on all 196 sequences data, using root mean squared errors of predictions (RMSE) in a repeated cross-validation (5-fold, repeated thrice) setup for the performance evaluation. Using the architecture-defining optimal hyperparameters separately identified for the modeling of T_m and pH_T , the GBM models were then trained on randomly chosen 80 % of data, further testing on the 20 % left out test set. This resulted in two models, one with 1.210 RMSE and 0.990 Pearson's R for T_m predictions, and the second with 0.053 RMSE and 0.973 Pearson's R for pH_T .

Defining a simple analytical equation expressing T_m / pH_T as a function of the primary sequence. In the third approach, we searched for more transparent mathematical models to express T_m and pH_T measurements as a function of C-tract (C) and loop (T_1 , T_2 and T_3) lengths. To search for such non-linear equations, we used Eureqa^[14], a program for an unrestricted search for analytical forms in provided data. We used the default absolute error as a performance metric for the search, and, for the sake of the lucidity of the resulting equations, allowed only constant, input variable, addition, subtraction, multiplication, division and exponentiation terms and operations in the equations. All sequences were inputted to the program, making use of Eureqa's internal capability to split the data for training and validation.

In this approach, we searched for a simple and interpretable non-linear analytical equation for both T_m and pH_T , expressing those as a function of C-tract and T-spacer lengths. With some compromises in the model performance, we arrived to the following mathematical expressions:

$$T_m = 102 - T_3 - (137 - T_2T_3 + T_1)/C \quad (\text{equation 1})$$

$$pH_T = 7.38 - 3.70/C - (0.00565 L)/T_2 \quad (\text{equation 2})$$

in which L is the total sequence length:

$$L = 4C + T_1 + T_2 + T_3 \quad (\text{equation 3})$$

C is the C-tract length (common for all four C-tracts), T_1 , T_2 and T_3 are the lengths of the first, second and third spacers respectively (in 5'-to-3' direction), and the equations result in Pearson R values of 0.979 and 0.960 for T_m and pH_T values respectively, based on Eureqa's internal validation. The equations are all simple dependences from unitless base-counts that reflect spacer, C-tract and i-motif lengths, also bearing a constant that can bear any unit to conform the dimensional consistency of the equations. As for all the other models above, these mathematical models are applicable for only the C/T-based sequence space with equally sized C-tracts used in this study for most experimental measurements. Furthermore, the found other Eureqa solutions show comparable performance, due to the internal restrictions on the spacer lengths in the used experimental dataset (in most cases, two spacers being equal in length, hence some candidate solutions eliminating some of the spacers). The equations are consistent with our observations in the explored i-DNA subspace, and capture the stabilizing role of the lengthy middle spacer length (T_2) within a given overall length of i-motifs. Both equations capture the interplay between the C-tract length and the spacer lengths 1-3 in modulating the T_m of i-DNAs in the given sub-universe. For pH_T , the chosen equation outlines the observed stabilizing role of the length of the central spacer. Overall, equations would perform better as we expand the investigated space of i-DNA sequences in future, by including sequences with varying C-tract lengths and spacer length relations.

Results and Discussion

Table S1 271 sequences information and BLAST results.

Name	Sequence (5'→3')	nt	Total Loop Length	$\epsilon_{260}/L \cdot \text{mole}^{-1} \cdot \text{cm}^{-1}$	pH_T^{UV}	Human Genome (Chromosome) ^a
<i>C₃ Tract</i>						
T111-3	CCCTCCCTCCCTCCC	15	3	110900	6.27	1-22,x,y
T222-3	CCCTCCCTCCCTCCC	18	6	135200	6.09	1-22,x,y
T333-3	CCCTTCCCTTCCCTTCCC	21	9	159500	6.16	1-13,17-20,22,x,y
T444-3	CCCTTTCCCTTTCCCTTTCCC	24	12	183800	6.23	10,16
T112-3	CCCTCCCTCCCTCCC	16	4	119000	6.07	1-22,x,y
T121-3	CCCTCCCTCCCTCCC	16	4	119000	6.26	1-22,x,y
T211-3	CCCTCCCTCCCTCCC	16	4	119000	6.10	1-22,x,y
T113-3	CCCTCCCTCCCTTCCC	17	5	127100	6.12	1-22,x,y
T131-3	CCCTCCCTTCCCTCCC	17	5	127100	6.10	1-7,8-17,19,20,y
T311-3	CCCTTCCCTCCCTCCC	17	5	127100	6.11	1-20,22,y
T114-3	CCCTCCCTCCCTTCCC	18	6	135200	6.12	1,3,5-11,19,20,22
T141-3	CCCTCCCTTTCCCTCCC	18	6	135200	6.11	3,5,10,12,16

SUPPORTING INFORMATION

T411-3	CCCTTTCCCTCCCTCCC	18	6	135200	6.12	1,2,4,6,7,11-13,17,20,x
T115-3	CCCTCCCTCCCTTTTCCC	19	7	143300	6.03	3,7,12-15,17,20,22
T151-3	CCCTCCCTTTTCCCTCCC	19	7	143300	6.10	1,2,5-11,17,18,x,y
T511-3	CCCTTTTCCCTCCCTCCC	19	7	143300	6.01	1,2,7,10,11,12
T116-3	CCCTCCCTCCCTTTTCCC	20	8	151400	6.30	5,12,15,17
T161-3	CCCTCCCTTTTCCCTCCC	20	8	151400	6.01	2,5,17
T611-3	CCCTTTTCCCTCCCTCCC	20	8	151400	6.08	7,10,12
					--	
T221-3	CCCTCCCTCCCTCCC	17	5	127100	6.14	1-21,x,y
T212-3	CCCTCCCTCCCTCCC	17	5	127100	6.19	1-19,22,x
T122-3	CCCTCCCTCCCTCCC	17	5	127100	6.14	1-21,x,y
					--	
T223-3	CCCTCCCTCCCTTTCCC	19	7	143300	6.16	1-12,15-17,19,10,x
T232-3	CCCTCCCTTTCCCTCCC	19	7	143300	6.21	1-7,10-16,19-21,x
T322-3	CCCTTCCCTCCCTCCC	19	7	143300	6.19	1-12,16-20,x
					--	
T224-3	CCCTCCCTCCCTTTCCC	20	8	151400	5.99	2,4,5,7,10,15,21,x,y
T242-3	CCCTCCCTTTCCCTCCC	20	8	151400	6.13	1,2,4,5,7,10,11,15,x
T422-3	CCCTTTCCCTCCCTCCC	20	8	151400	6.05	1,2,4,6,7,10,15,x
					--	
T225-3	CCCTCCCTCCCTTTTCCC	21	9	159500	5.85	10,11
T252-3	CCCTCCCTTTTCCCTCCC	21	9	159500	6.09	5,7,8,10
T522-3	CCCTTTTCCCTCCCTCCC	21	9	159500	5.88	4,7,10
					--	
T226-3	CCCTCCCTCCCTTTTCCC	22	10	167600	5.93	none
T262-3	CCCTCCCTTTTCCCTCCC	22	10	167600	6.07	none
T622-3	CCCTTTTCCCTCCCTCCC	22	10	167600	5.84	8
					--	
T331-3	CCCTTCCCTTCCCTCCC	19	7	143300	6.07	2,6,7,10,11,16,19,20,x,y
T313-3	CCCTTCCCTCCCTTTCCC	19	7	143300	6.00	1,2,3,5,9,12,13,17,20
T133-3	CCCTCCCTTCCCTTTCCC	19	7	143300	6.10	1,11,15,18,19,20
					--	
T332-3	CCCTTCCCTTCCCTTTCCC	20	8	151400	6.29	1-12,14,16,19,20,22,x
T323-3	CCCTTCCCTTCCCTTTCCC	20	8	151400	6.25	7,9-11,15-17,20,22
T233-3	CCCTTCCCTTCCCTTTCCC	20	8	151400	6.28	1-12,14,16,19,20,22,x
					--	
T334-3	CCCTTCCCTTCCCTTTCCC	22	10	167600	6.20	1,13
T343-3	CCCTTCCCTTTCCCTTTCCC	22	10	167600	6.19	13
T433-3	CCCTTCCCTTCCCTTTCCC	22	10	167600	6.19	3,8,x
					--	
T335-3	CCCTTCCCTTCCCTTTTCCC	23	11	175700	6.11	none
T353-3	CCCTTCCCTTTTCCCTTTCCC	23	11	175700	6.18	6
T533-3	CCCTTTTCCCTTCCCTTTCCC	23	11	175700	6.11	9
					--	
T336-3	CCCTTCCCTTCCCTTTTCCC	24	12	183800	6.11	none
T363-3	CCCTTCCCTTTTCCCTTTCCC	24	12	183800	6.15	none

SUPPORTING INFORMATION

T633-3	CCCTTTTCCCTTTCCCTTTCCC	24	12	183800	6.15	none
	<i>C₄ Tract</i>					
T111-4	CCCCTCCCCTCCCCTCCCC	19	3	139700	6.23	1-22,x,y
T222-4	CCCCTCCCCTTCCCCTCCCC	22	6	164000	6.27	1-12,14-22,x,y
T333-4	CCCCTTCCCCTTTCCCCTTTCCCC	25	9	188300	6.37	15
T444-4	CCCCTTTCCCCTTTTCCCCTTTTCCCC	28	12	212600	6.52	none
					--	
T112-4	CCCCTCCCCTCCCCTTCCCC	20	4	147800	6.25	1-10,12-14,16-22,x,y
T121-4	CCCCTCCCCTTCCCCTCCCC	20	4	147800	6.29	2,4-10,13,14,16,17,19,20,22,x,y
T211-4	CCCCTCCCCTCCCCTCCCC	20	4	147800	6.26	1-17,19,20,x,y
					--	
T113-4	CCCCTCCCCTCCCCTTTCCCC	21	5	155900	6.22	2,3,8,13,20
T131-4	CCCCTCCCCTTTCCCCTCCCC	21	5	155900	6.37	2,5,8,15,21,22
T311-4	CCCCTTCCCCTCCCCTCCCC	21	5	155900	6.30	2,16,21
					--	
T114-4	CCCCTCCCCTCCCCTTTTCCCC	22	6	164000	6.32	none
T141-4	CCCCTCCCCTTTTCCCCTCCCC	22	6	164000	6.32	none
T411-4	CCCCTTTTCCCCTCCCCTCCCC	22	6	164000	6.28	19
					--	
T115-4	CCCCTCCCCTCCCCTTTTCCCC	23	7	172100	6.27	none
T151-4	CCCCTCCCCTTTTCCCCTCCCC	23	7	172100	6.33	none
T511-4	CCCCTTTTCCCCTCCCCTCCCC	23	7	172100	6.30	11
					--	
T116-4	CCCCTCCCCTCCCCTTTTCCCC	24	8	180200	6.14	none
T161-4	CCCCTCCCCTTTTCCCCTCCCC	24	8	180200	6.33	none
T611-4	CCCCTTTTCCCCTCCCCTCCCC	24	8	180200	6.15	none
					--	
T221-4	CCCCTCCCCTTCCCCTCCCC	21	5	155900	6.25	1-5,7,8,11,16,19,x
T212-4	CCCCTCCCCTCCCCTTCCCC	21	5	155900	6.22	2,4-7,9,10,13,15,16,19,21
T122-4	CCCCTCCCCTTCCCCTTCCCC	21	5	155900	6.28	2,3,7,8,10,13,16,17,19,21
					--	
T223-4	CCCCTCCCCTTCCCCTTTCCCC	23	7	172100	6.35	2,7
T232-4	CCCCTCCCCTTTCCCCTTCCCC	23	7	172100	6.36	12
T322-4	CCCCTTCCCCTTCCCCTTCCCC	23	7	172100	6.29	3
					--	
T224-4	CCCCTCCCCTTCCCCTTTCCCC	24	8	180200	6.28	none
T242-4	CCCCTCCCCTTTTCCCCTTCCCC	24	8	180200	6.34	none
T422-4	CCCCTTTTCCCCTTCCCCTTCCCC	24	8	180200	6.30	none
					--	
T225-4	CCCCTCCCCTTCCCCTTTTCCCC	24	9	188300	6.26	none
T252-4	CCCCTCCCCTTTTCCCCTTCCCC	25	9	188300	6.35	none
T522-4	CCCCTTTTCCCCTTCCCCTTCCCC	25	9	188300	6.27	none
					--	
T226-4	CCCCTCCCCTTCCCCTTTTCCCC	26	10	196400	6.23	none
T262-4	CCCCTCCCCTTTTCCCCTTCCCC	26	10	196400	6.29	none
T622-4	CCCCTTTTCCCCTTCCCCTTCCCC	26	10	196400	6.22	none
					--	
T331-4	CCCCTTCCCCTTTCCCCTCCCC	23	7	172100	6.35	none

SUPPORTING INFORMATION

T313-4	CCCCCTTCCCTTCCCTTTC	23	7	172100	6.26	none
T133-4	CCCCTCCCTTTCCTTTC	23	7	172100	6.33	none
					--	
T332-4	CCCCCTTCCCTTTCCTTTC	24	8	180200	6.35	none
T323-4	CCCCCTTCCCTTTCCTTTC	24	8	180200	6.36	none
T233-4	CCCCCTCCCTTTCCTTTC	24	8	180200	6.34	none
					--	
T334-4	CCCCCTTCCCTTTCCTTTC	26	10	196400	6.40	None
T343-4	CCCCCTTCCCTTTCCTTTC	26	10	196400	6.36	none
T433-4	CCCCCTTCCCTTTCCTTTC	26	10	196400	6.39	none
					--	
T335-4	CCCCCTTCCCTTTCCTTTC	27	11	204500	6.33	none
T353-4	CCCCCTTCCCTTTCCTTTC	27	11	204500	6.35	none
T533-4	CCCCCTTTCCTTTCCTTTC	27	11	204500	6.32	none
					--	
T336-4	CCCCCTTCCCTTTCCTTTC	28	12	212600	6.31	none
T363-4	CCCCCTTCCCTTTCCTTTC	28	12	212600	6.41	none
T633-4	CCCCCTTTCCTTTCCTTTC	28	12	212600	6.32	none
	<i>C₅ Tract</i>					
T111-5	CCCCCTCCCTTCCCTTTC	23	3	168500	6.44	1-20,22,x
T222-5	CCCCCTCCCTTCCCTTTC	26	6	192800	6.48	4,10,11
T333-5	CCCCCTTCCCTTTCCTTTC	29	9	217100	6.56	none
T444-5	CCCCCTTTCCTTTCCTTTC	32	12	241400	6.71	none
					--	
T112-5	CCCCCTCCCTTCCCTTTC	24	4	176600	6.41	21
T121-5	CCCCCTCCCTTCCCTTTC	24	4	176600	6.44	7,9,21
T211-5	CCCCCTCCCTTCCCTTTC	24	4	176600	6.43	8,9,15
					--	
T113-5	CCCCCTCCCTTCCCTTTC	25	5	184700	6.62	none
T131-5	CCCCCTCCCTTTCCTTTC	25	5	184700	6.75	1,13
T311-5	CCCCCTTCCCTTCCCTTTC	25	5	184700	6.62	none
					--	
T114-5	CCCCCTCCCTTCCCTTTC	26	6	192800	6.41	none
T141-5	CCCCCTCCCTTTCCTTTC	26	6	192800	6.57	none
T411-5	CCCCCTTTCCTTTCCTTTC	26	6	192800	6.39	none
					--	
T115-5	CCCCCTCCCTTCCCTTTC	27	7	200900	6.34	none
T151-5	CCCCCTCCCTTTCCTTTC	27	7	200900	6.45	none
T511-5	CCCCCTTTCCTTTCCTTTC	27	7	200900	6.37	none
					--	
T116-5	CCCCCTCCCTTCCCTTTC	28	8	209000	6.40	none
T161-5	CCCCCTCCCTTTCCTTTC	28	8	209000	6.41	none
T611-5	CCCCCTTTCCTTTCCTTTC	28	8	209000	6.32	none
					--	
T221-5	CCCCCTCCCTTCCCTTTC	25	5	184700	6.65	none
T212-5	CCCCCTCCCTTCCCTTTC	25	5	184700	6.64	1,21
T122-5	CCCCCTCCCTTCCCTTTC	25	5	184700	6.80	15
					--	

SUPPORTING INFORMATION

T223-5	CCCCCTCCCCCTCCCCCTTTCCCCC	27	7	200900	6.64	none
T232-5	CCCCCTCCCCCTTTCCCCCTCCCCC	27	7	200900	6.54	none
T322-5	CCCCCTTTCCCCCTTCCCCCTCCCCC	27	7	200900	6.51	none
					--	
T224-5	CCCCCTCCCCCTCCCCCTTTTCCCCC	28	8	209000	6.57	none
T242-5	CCCCCTCCCCCTTTTCCCCCTCCCCC	28	8	209000	6.44	none
T422-5	CCCCCTTTCCCCCTTCCCCCTCCCCC	28	8	209000	6.51	none
					--	
T225-5	CCCCCTCCCCCTCCCCCTTTTCCCCC	29	9	217100	6.55	none
T252-5	CCCCCTCCCCCTTTTCCCCCTCCCCC	29	9	217100	6.56	none
T522-5	CCCCCTTTTCCCCCTTCCCCCTCCCCC	29	9	217100	6.47	none
					--	
T226-5	CCCCCTCCCCCTTCCCCCTTTTCCCCC	30	10	225200	6.40	none
T262-5	CCCCCTCCCCCTTTTCCCCCTCCCCC	30	10	225200	6.52	none
T622-5	CCCCCTTTTCCCCCTTCCCCCTCCCCC	30	10	225200	6.44	none
					--	
T331-5	CCCCCTTTCCCCCTTCCCCCTCCCCC	27	7	200900	6.49	none
T313-5	CCCCCTTTCCCCCTCCCCCTTTCCCCC	27	7	200900	6.40	none
T133-5	CCCCCTCCCCCTTCCCCCTTTCCCCC	27	7	200900	6.42	none
					--	
T332-5	CCCCCTTTCCCCCTTTCCCCCTCCCCC	28	8	209000	6.48	none
T323-5	CCCCCTTTCCCCCTTCCCCCTTTCCCCC	28	8	209000	6.56	none
T233-5	CCCCCTCCCCCTTCCCCCTTTCCCCC	28	8	209000	6.56	none
					--	
T334-5	CCCCCTTTCCCCCTTTCCCCCTTTCCCCC	30	10	225200	6.69	none
T343-5	CCCCCTTTCCCCCTTTTCCCCCTTTCCCCC	30	10	225200	6.54	none
T433-5	CCCCCTTTTCCCCCTTCCCCCTTTCCCCC	30	10	225200	6.60	none
					--	
T335-5	CCCCCTTTCCCCCTTTCCCCCTTTTCCCCC	31	11	233300	6.50	none
T353-5	CCCCCTTTCCCCCTTTTCCCCCTTTCCCCC	31	11	233300	6.66	none
T533-5	CCCCCTTTTCCCCCTTCCCCCTTTCCCCC	31	11	233300	6.58	none
					--	
T336-5	CCCCCTTTCCCCCTTTCCCCCTTTTCCCCC	32	12	241400	6.74	none
T363-5	CCCCCTTTCCCCCTTTTCCCCCTTTCCCCC	32	12	241400	6.77	none
T633-5	CCCCCTTTTCCCCCTTTCCCCCTTTCCCCC	32	12	241400	6.67	none
	<i>C₆ Tract</i>					
T111-6	CCCCCTCCCCCTCCCCCTCCCCC	27	3	197300	6.57	1,3,5,7,8,12
T222-6	CCCCCTTCCCCCTTCCCCCTCCCCC	30	6	221600	6.66	none
T333-6	CCCCCTTCCCCCTTCCCCCTTTCCCCC	33	9	245900	6.79	none
T444-6	CCCCCTTTTCCCCCTTTCCCCCTTTCCCCC	36	12	270200	6.84	none
					--	
T112-6	CCCCCTCCCCCTCCCCCTTCCCCC	28	4	205400	6.66	none
T121-6	CCCCCTCCCCCTTCCCCCTCCCCC	28	4	205400	6.65	4
T211-6	CCCCCTTCCCCCTCCCCCTCCCCC	28	4	205400	6.60	none
					--	
T113-6	CCCCCTCCCCCTCCCCCTTTCCCCC	29	5	213500	6.51	none
T131-6	CCCCCTCCCCCTTTCCCCCTCCCCC	29	5	213500	6.68	none
T311-6	CCCCCTTTCCCCCTCCCCCTCCCCC	29	5	213500	6.64	none

SUPPORTING INFORMATION

					--	
T114-6	CCCCCTCCCCCTCCCCCTTTTCCCCC	30	6	221600	6.57	none
T141-6	CCCCCTCCCCCTTTTCCCCCTCCCCC	30	6	221600	6.69	none
T411-6	CCCCCTTTTCCCCCTCCCCCTCCCCC	30	6	221600	6.59	none
					--	
T115-6	CCCCCTCCCCCTCCCCCTTTTCCCCC	31	7	229700	6.59	none
T151-6	CCCCCTCCCCCTTTTCCCCCTCCCCC	31	7	229700	6.63	none
T511-6	CCCCCTTTTCCCCCTCCCCCTCCCCC	31	7	229700	6.50	none
					--	
T116-6	CCCCCTCCCCCTCCCCCTTTTCCCCC	32	8	237800	6.58	none
T161-6	CCCCCTCCCCCTTTTCCCCCTCCCCC	32	8	237800	6.63	none
T611-6	CCCCCTTTTCCCCCTCCCCCTCCCCC	32	8	237800	6.53	none
					--	
T221-6	CCCCCTCCCCCTTCCCCCTCCCCC	29	5	221600	6.69	none
T212-6	CCCCCTCCCCCTCCCCCTTCCCCC	29	5	221600	6.64	none
T122-6	CCCCCTCCCCCTTCCCCCTTCCCCC	29	5	221600	6.65	none
					--	
T223-6	CCCCCTCCCCCTTCCCCCTTTCCCCC	31	7	229700	6.88	none
T232-6	CCCCCTCCCCCTTTCCCCCTTCCCCC	31	7	229700	6.84	none
T322-6	CCCCCTTCCCCCTTCCCCCTTCCCCC	31	7	229700	6.81	none
					--	
T224-6	CCCCCTCCCCCTTCCCCCTTTTCCCCC	32	8	237800	6.86	none
T242-6	CCCCCTCCCCCTTTTCCCCCTTCCCCC	32	8	237800	6.79	none
T422-6	CCCCCTTTTCCCCCTTCCCCCTTCCCCC	32	8	237800	6.80	none
					--	
T225-6	CCCCCTCCCCCTTCCCCCTTTTCCCCC	33	9	245900	6.71	none
T252-6	CCCCCTCCCCCTTTTCCCCCTTCCCCC	33	9	245900	6.75	none
T522-6	CCCCCTTTTCCCCCTTCCCCCTTCCCCC	33	9	245900	6.70	none
					--	
T226-6	CCCCCTCCCCCTTCCCCCTTTTCCCCC	34	10	254000	6.66	none
T262-6	CCCCCTCCCCCTTTTCCCCCTTCCCCC	34	10	254000	6.71	none
T622-6	CCCCCTTTTCCCCCTTCCCCCTTCCCCC	34	10	254000	6.67	none
					--	
T331-6	CCCCCTTCCCCCTTCCCCCTTCCCCC	31	7	229700	6.76	none
T313-6	CCCCCTTCCCCCTTCCCCCTTCCCCC	31	7	229700	6.72	none
T133-6	CCCCCTCCCCCTTCCCCCTTCCCCC	31	7	229700	6.74	none
					--	
T332-6	CCCCCTTCCCCCTTCCCCCTTCCCCC	32	8	237800	6.75	none
T323-6	CCCCCTTCCCCCTTCCCCCTTCCCCC	32	8	237800	6.75	none
T233-6	CCCCCTTCCCCCTTCCCCCTTCCCCC	32	8	237800	6.73	none
					--	
T334-6	CCCCCTTCCCCCTTCCCCCTTTTCCCCC	34	10	254000	6.82	none
T343-6	CCCCCTTCCCCCTTTTCCCCCTTCCCCC	34	10	254000	6.80	none
T433-6	CCCCCTTTTCCCCCTTCCCCCTTCCCCC	34	10	254000	6.81	none
					--	
T335-6	CCCCCTTCCCCCTTCCCCCTTTTCCCCC	35	11	262100	6.77	none
T353-6	CCCCCTTCCCCCTTTTCCCCCTTCCCCC	35	11	262100	6.92	none
T533-6	CCCCCTTTTCCCCCTTCCCCCTTCCCCC	35	11	262100	6.81	none

SUPPORTING INFORMATION

					--		
T336-6	CCCCCTTCCCCCTTCCCCCTTTTTCCCC	36	12	270200	6.77	none	
T363-6	CCCCCTTCCCCCTTCCCCCTTCCCC	36	12	270200	6.81	none	
T633-6	CCCCCTTTTTCCCCCTTCCCCCTTCC	36	12	270200	6.74	none	

75 extended sequences with C₅-tract*Longer (7-15) central loop*

T171-5	CCCCCTCCCTTTTTTCCCTCC	29	9	217100		none	
T181-5	CCCCCTCCCTTTTTTCCCTCC	30	10	225200		none	
T1101-5	CCCCCTCCCC T ₁₀ CCCCCTCC	32	12	241400		none	
T1151-5	CCCCCTCCCC T ₁₅ CCCCCTCC	37	17	281900		none	

Adenine in loop

AA115-5	CCCCACCCACCCCTTTTTCC	27	7	209500		none	
AA151-5	CCCCACCCCTTTTTCCCA	27	7	209500		none	
AA511-5	CCCCTTTTCCCA	27	7	209500		none	

--

1A15-5	CCCCACCCCTCCCTTTTTCC	27	7	205200		none	
11A5-5	CCCCCTCCCA	27	7	205200		none	
1A51-5	CCCCACCCCTTTTTCCCTCC	27	7	205200		none	
151A-5	CCCCCTCCCTTTTTCCCA	27	7	205200		none	
51A1-5	CCCCTTTTCCCA	27	7	205200		none	
511A-5	CCCCTTTTCCCTCCCA	27	7	205200		none	

--

115_1A-5	CCCCCTCCCTCCCA	27	7	206200		none	
151_1A-5	CCCCCTCCCA	27	7	206200		none	
511_1A-5	CCCCATTTCCCTCCCTCC	27	7	206200		none	
115_2A-5	CCCCCTCCCTCCCTATTTCC	27	7	206800		none	
151_2A-5	CCCCCTCCCTATTTCCCTCC	27	7	206800		none	
511_2A-5	CCCCATTTCCCTCCCTCC	27	7	206800		none	
115_3A-5	CCCCCTCCCTCCCTTATTTCC	27	7	206800		none	
151_3A-5	CCCCCTCCCTTATTTCCCTCC	27	7	206800		none	
511_3A-5	CCCCCTATTTCCCTCCCTCC	27	7	206800		none	
115_4A-5	CCCCCTCCCTCCCTTTATCC	27	7	206800		none	
151_4A-5	CCCCCTCCCTTTATCCCTCC	27	7	206800		none	
511_4A-5	CCCCTTATCCCTCCCTCC	27	7	206800		none	
115_5A-5	CCCCCTCCCTCCCTTTTAC	27	7	206800		none	
151_5A-5	CCCCCTCCCTTTTACCCCTCC	27	7	206800		none	
511_5A-5	CCCCTTTTACCCCTCCCTCC	27	7	206800		none	

Two short loops of different length

T152-5	CCCCCTCCCTTTTTCCCTCC	28	8	209000		none	
T251-5	CCCCCTCCCTTTTTCCCTCC	28	8	209000		none	
T153-5	CCCCCTCCCTTTTTCCCTCC	29	9	217100		none	
T351-5	CCCCCTTCCCTTTTTCCCTCC	29	9	217100		none	
T253-5	CCCCCTCCCTTTTTCCCTCC	30	10	225200		none	
T352-5	CCCCCTTCCCTTTTTCCCTCC	30	10	225200		none	
T162-5	CCCCCTCCCTTTTTCCCTCC	29	9	217100		none	
T261-5	CCCCCTCCCTTTTTCCCTCC	29	9	217100		none	
T163-5	CCCCCTCCCTTTTTCCCTCC	30	10	225200		none	

SUPPORTING INFORMATION

T361-5	CCCCCTTCCCCCTTTTTCCCCCTCCCC	30	10	225200	none
T263-5	CCCCCTCCCCCTTTTTCCCCCTTCCCC	31	11	233300	none
T362-5	CCCCCTTCCCCCTTTTTCCCCCTCCCC	31	11	233300	none

Flanking sequences

TT252-5	T CCCCC TT CCCCC TTTT CCCCC TT CCCCC	30	9	225900
T252-5T	CCCCC TT CCCCC TTTT CCCCC TT CCCCC T	30	9	224900
TT252-5T	T CCCCC TT CCCCC TTTT CCCCC TT CCCCC T	31	9	233700

AT252-5	A CCCCC TT CCCCC TTTT CCCCC TT CCCCC	30	9	230900
T252-5A	CCCCC TT CCCCC TTTT CCCCC TT CCCCC A	30	9	230900
AT252-5A	A CCCCC TT CCCCC TTTT CCCCC TT CCCCC A	31	9	244700

GT252-5	G CCCCC TT CCCCC TTTT CCCCC TT CCCCC	30	9	227300
T252-5G	CCCCC TT CCCCC TTTT CCCCC TT CCCCC G	30	9	227700
GT252-5G	G CCCCC TT CCCCC TTTT CCCCC TT CCCCC G	31	9	237900

Loop contents

252-5_A1	CCCCC AT CCCCC TTTT CCCCC TT CCCCC	29	9	222400
252-5_A2	CCCCC TA CCCCC TTTT CCCCC TT CCCCC	29	9	222000
252-5_A3	CCCCC TT CCCCC ATTTT CCCCC TT CCCCC	29	9	222400
252-5_A4	CCCCC TT CCCCC TTTTA CCCCC TT CCCCC	29	9	222000
252-5_A5	CCCCC TT CCCCC TTTT CCCCC AT CCCCC	29	9	222400
252-5_A6	CCCCC TT CCCCC TTTT CCCCC TA CCCCC	29	9	222000

252-5_AA1	CCCCC AA CCCCC TTTT CCCCC TT CCCCC	29	9	225300
252-5_AA2	CCCCC TT CCCCC AAAAA CCCCC TT CCCCC	29	9	237000
252-5_AA3	CCCCC TT CCCCC TTTT CCCCC AA CCCCC	29	9	225300
A252-5	CCCCC AA CCCCC AAAAA CCCCC AA CCCCC	29	9	253400

252-5_G1	CCCCC GT CCCCC TTTT CCCCC TT CCCCC	29	9	220300
252-5_G2	CCCCC TG CCCCC TTTT CCCCC TT CCCCC	29	9	217900
252-5_G3	CCCCC TT CCCCC GTTTT CCCCC TT CCCCC	29	9	220300
252-5_G4	CCCCC TT CCCCC TTTTG CCCCC TT CCCCC	29	9	217900
252-5_G5	CCCCC TT CCCCC TTTT CCCCC GT CCCCC	29	9	220300
252-5_G6	CCCCC TT CCCCC TTTT CCCCC TG CCCCC	29	9	217900

252-5_GG1	CCCCC GG CCCCC TTTT CCCCC TT CCCCC	29	9	220500
252-5_GG2	CCCCC TT CCCCC GGGGG CCCCC TT CCCCC	29	9	226500
252-5_GG3	CCCCC TT CCCCC TTTT CCCCC GG CCCCC	29	9	220500
G252-5	CCCCC GG CCCCC GGGGG CCCCC GG CCCCC	29	9	233300

Odd number of C-C base pair*

T225-45	CCCC TT CCCCC TT CCCC TTTT CCCCC	27	9	202700
T252-45	CCCC TT CCCCC TTTT CCCC TT CCCCC	27	9	202700
T522-45	CCCC TTTT CCCCC TT CCCC TT CCCCC	27	9	202700
T225-56	CCCCC TT CCCCC TT CCCCC TTTT CCCCC	31	9	231500
T252-56	CCCCC TT CCCCC TTTT CCCCC TT CCCCC	31	9	231500
T522-56	CCCCC TTTT CCCCC TT CCCCC TT CCCCC	31	9	231500

^a If a sequence is found in human genome, chromosome number is given here; 'None' means that it does not been found in human genomes by BLAST ^[15].

SUPPORTING INFORMATION

Table S2 pH transition midpoint and thermal stability of 196 pyrimidine sequences containing thymidine spacers (T_1 to T_6) and C-tracts (C_3 to C_6) of variable lengths.^a

Name ^b	Spacer Permutation ^c	pH_T^{CD}	$T_m^{pH 5.0}$	Name ^b	Spacer Permutation ^c	pH_T^{CD}	$T_m^{pH 5.0}$	$T_m^{pH 7.0d}$		
								$T_{heating}$	$T_{cooling}$	T_m
<i>C₃ Tract</i>				<i>C₅ Tract</i>						
T111-3	--	6.22	57.8	T111-5	--	6.48	72.0	14.6	13.7	14.1
T222-3	--	6.16	53.2	T222-5	--	6.58	73.3	18.0	15.8	16.9
T333-3	--	6.22	56.9	T333-5	--	6.68	73.4	22.3	14.3	18.3
T444-3	--	6.27	58.8	T444-5	--	6.71	73.4	25.8	9.3	17.6
			--			--	--	--	--	--
T112-3	SSL	6.11	53.5	T112-5	SSL	6.51	71.1	14.8	13.8	14.3
T121-3	SLS	6.30	58.0	T121-5	SLS	6.56	73.6	16.9	15.6	16.2
T211-3	LSS	6.12	54.5	T211-5	LSS	6.50	71.9	15.4	13.9	14.7
			--			--	--	--	--	--
T113-3	SSL	6.15	54.9	T113-5	SSL	6.56	74.4	17.6	15.5	16.5
T131-3	SLS	6.20	54.3	T131-5	SLS	6.58	74.7	17.7	16.1	16.9
T311-3	LSS	6.10	58.3	T311-5	LSS	6.50	73.9	15.7	14.2	15.0
			--			--	--	--	--	--
T114-3	SSL	6.24	54.3	T114-5	SSL	6.52	69.5	15.2	12.1	13.6
T141-3	SLS	6.11	59.2	T141-5	SLS	6.60	74.2	18.2	15.9	17.0
T411-3	LSS	6.12	54.3	T411-5	LSS	6.47	70.6	15.7	13.8	14.8
			--			--	--	--	--	--
T115-3	SSL	6.07	52.2	T115-5	SSL	6.40	69.3	13.7	11.6	12.7
T151-3	SLS	6.11	57.5	T151-5	SLS	6.60	74.4	18.4	15.2	16.8
T511-3	LSS	6.03	51.7	T511-5	LSS	6.45	70.5	14.4	12.0	13.2
			--			--	--	--	--	--
T116-3	SSL	6.24	50.3	T116-5	SSL	6.45	66.6	13.1	10.6	11.8
T161-3	SLS	6.00	57.0	T161-5	SLS	6.60	73.1	17.9	14.3	16.1
T611-3	LSS	6.00	50.0	T611-5	LSS	6.45	68.0	14.0	11.4	12.7
			--			--	--	--	--	--
T221-3	LLS	6.07	54.6	T221-5	LLS	6.56	76.3	17.9	16.2	17.0
T212-3	LSL	6.05	54.9	T212-5	LSL	6.52	74.3	16.1	14.6	15.4
T122-3	SLL	6.07	54.6	T122-5	SLL	6.55	75.7	17.3	15.8	16.6
			--			--	--	--	--	--
T223-3	SSL	6.13	52.5	T223-5	SSL	6.62	72.3	19.0	15.4	17.2
T232-3	SLS	6.04	57.3	T232-5	SLS	6.57	74.0	19.2	15.6	17.4
T322-3	LSS	6.07	53.7	T322-5	LSS	6.58	73.2	19.5	15.8	17.6
			--			--	--	--	--	--
T224-3	SSL	5.97	52.2	T224-5	SSL	6.59	72.8	20.8	14.8	17.8
T242-3	SLS	6.07	59.1	T242-5	SLS	6.60	74.7	20.6	15.4	18.0
T422-3	LSS	6.00	53.3	T422-5	LSS	6.58	74.2	20.3	14.0	17.2
			--			--	--	--	--	--
T225-3	SSL	5.96	48.3	T225-5	SSL	6.55	69.1	18.4	12.7	15.6
T252-3	SLS	6.16	58.3	T252-5	SLS	6.59	73.4	20.8	14.0	17.4
T522-3	LSS	5.98	49.5	T522-5	LSS	6.53	70.5	18.8	13.3	16.1
			--			--	--	--	--	--
T226-3	SSL	6.02	48.0	T226-5	SSL	6.50	70.8	18.3	11.7	15.0
T262-3	SLS	6.16	57.1	T262-5	SLS	6.59	73.7	20.5	12.9	16.7

SUPPORTING INFORMATION

Name ^b	Spacer Permutation ^c	pH_T^{CD}	$T_m^{pH 5.0}$	Name ^b	Spacer Permutation ^c	pH_T^{CD}	$T_m^{pH 5.0}$	$T_m^{pH 7.0_d}$		
								$T_{heating}$	$T_{cooling}$	T_m
T622-3	LSS	5.97	48.8	T622-5	LSS	6.50	66.5	18.3	11.2	14.7
		--	--			--	--	--	--	--
T331-3	LLS	6.09	56.4	T331-5	LLS	6.50	73.5	19.7	15.9	17.8
T313-3	LSL	6.08	53.2	T313-5	LSL	6.47	71.8	18.2	14.4	16.3
T133-3	SLL	6.14	56.7	T133-5	SLL	6.50	73.7	20.6	16.3	18.4
		--	--			--	--	--	--	--
T332-3	LLS	6.16	59.1	T332-5	LLS	6.54	75.4	20.7	15.4	18.1
T323-3	LSL	6.05	55.3	T323-5	LSL	6.60	73.7	21.6	15.8	18.7
T233-3	SLL	6.08	58.7	T233-5	SLL	6.62	76.5	20.9	15.5	18.2
		--	--			--	--	--	--	--
T334-3	SSL	6.23	56.6	T334-5	SSL	6.69	72.3	23.9	13.1	18.5
T343-3	SLS	6.23	57.6	T343-5	SLS	6.67	73.5	23.7	13.0	18.4
T433-3	LSS	6.21	57.0	T433-5	LSS	6.67	73.2	23.7	13.1	18.4
		--	--			--	--	--	--	--
T335-3	SSL	6.12	55.5	T335-5	SSL	6.57	73.0	22.7	11.4	17.0
T353-3	SLS	6.16	57.5	T353-5	SLS	6.65	73.5	24.0	11.6	17.8
T533-3	LSS	6.10	55.6	T533-5	LSS	6.62	73.1	22.5	11.3	16.9
		--	--			--	--	--	--	--
T336-3	SSL	6.11	52.6	T336-5	SSL	6.57	69.2	22.8	10.0	16.4
T363-3	SLS	6.15	56.1	T363-5	SLS	6.63	71.2	24.1	10.3	17.2
T633-3	LSS	6.08	53.0	T633-5	LSS	6.56	69.7	22.6	10.0	16.3
	C₄ Tract				C₆ Tract					
T111-4	--	6.44	66.4	T111-6	--	6.64	77.5	20.9	18.7	19.8
T222-4	--	6.28	66.0	T222-6	--	6.68	78.2	24.1	17.5	20.8
T333-4	--	6.45	68.0	T333-6	--	6.76	77.9	28.4	13.1	20.7
T444-4	--	6.52	68.6	T444-6	--	6.75	75.3	29.7	9.0	19.4
		--	--			--	--	--	--	--
T112-4	SSL	6.42	64.0	T112-6	SSL	6.64	76.9	21.6	18.4	20.0
T121-4	SLS	6.52	67.0	T121-6	SLS	6.66	79.1	22.7	19.3	21.0
T211-4	LSS	6.48	65.0	T211-6	LSS	6.59	77.9	21.8	18.6	20.2
		--	--			--	--	--	--	--
T113-4	SSL	6.33	65.5	T113-6	SSL	6.60	77.9	21.9	17.3	19.6
T131-4	SLS	6.35	68.5	T131-6	SLS	6.67	79.4	23.8	18.9	21.4
T311-4	LSS	6.38	65.6	T311-6	LSS	6.64	77.9	22.4	17.8	20.1
		--	--			--	--	--	--	--
T114-4	SSL	6.49	62.1	T114-6	SSL	6.47	75.2	21.9	15.9	18.9
T141-4	SLS	6.32	68.6	T141-6	SLS	6.67	78.1	24.1	17.8	20.9
T411-4	LSS	6.40	63.3	T411-6	LSS	6.60	76.2	22.4	16.5	19.5
		--	--			--	--	--	--	--
T115-4	SSL	6.35	62.5	T115-6	SSL	6.58	76.5	20.8	14.7	17.7
T151-4	SLS	6.41	68.8	T151-6	SLS	6.66	78.7	24.2	16.9	20.6
T511-4	LSS	6.30	60.7	T511-6	LSS	6.54	76.0	21.4	15.1	18.2
		--	--			--	--	--	--	--
T116-4	SSL	6.24	59.0	T116-6	SSL	6.54	73.1	20.3	13.1	16.7
T161-4	SLS	6.38	66.5	T161-6	SLS	6.62	77.4	23.7	15.8	19.7
T611-4	LSS	6.25	59.7	T611-6	LSS	6.54	74.1	21.3	13.7	17.5

SUPPORTING INFORMATION

Name ^b	Spacer Permutation ^c	pH_T^{CD}	$T_m^{pH\ 5.0}$	Name ^b	Spacer Permutation ^c	pH_T^{CD}	$T_m^{pH\ 5.0}$	$T_m^{pH\ 7.0d}$		
								$T_{heating}$	$T_{cooling}$	T_m
--	--	--	--	--	--	--	--	--	--	--
T221-4	LLS	6.34	67.6	T221-6	LLS	6.67	81.9	23.5	18.6	21.0
T212-4	LSL	6.29	65.0	T212-6	LSL	6.67	78.7	22.3	17.4	19.8
T122-4	SLL	6.37	67.4	T122-6	SLL	6.69	79.8	23.4	18.4	20.9
--	--	--	--	--	--	--	--	--	--	--
T223-4	SSL	6.38	64.9	T223-6	SSL	6.66	77.5	25.5	15.9	20.7
T232-4	SLS	6.39	67.4	T232-6	SLS	6.74	78.4	25.9	16.6	21.2
T322-4	LSS	6.33	67.5	T322-6	LSS	6.74	78.4	25.9	16.2	21.1
--	--	--	--	--	--	--	--	--	--	--
T224-4	SSL	6.33	65.2	T224-6	SSL	6.74	77.1	26.6	14.4	20.5
T242-4	SLS	6.40	68.5	T242-6	SLS	6.74	79.1	25.9	14.6	20.2
T422-4	LSS	6.37	66.2	T422-6	LSS	6.78	78.4	26.4	15.2	20.8
--	--	--	--	--	--	--	--	--	--	--
T225-4	SSL	6.30	60.6	T225-6	SSL	6.59	75.1	25.0	12.8	18.9
T252-4	SLS	6.41	67.4	T252-6	SLS	6.68	77.2	26.2	13.3	19.8
T522-4	LSS	6.33	63.1	T522-6	LSS	6.63	76.1	25.4	12.9	19.2
--	--	--	--	--	--	--	--	--	--	--
T226-4	SSL	6.27	61.6	T226-6	SSL	6.64	75.0	24.8	12.1	18.4
T262-4	SLS	6.35	68.4	T262-6	SLS	6.67	77.3	25.7	12.7	19.2
T622-4	LSS	6.27	63.1	T622-6	LSS	6.65	76.0	25.3	11.8	18.5
--	--	--	--	--	--	--	--	--	--	--
T331-4	LLS	6.43	67.2	T331-6	LLS	6.74	78.4	25.9	16.6	21.2
T313-4	LSL	6.30	67.4	T313-6	LSL	6.71	76.4	25.8	16.0	20.9
T133-4	SLL	6.38	64.4	T133-6	SLL	6.73	78.4	26.9	16.5	21.7
--	--	--	--	--	--	--	--	--	--	--
T332-4	LLS	6.42	69.5	T332-6	LLS	6.72	78.6	26.8	14.8	20.8
T323-4	LSL	6.39	66.9	T323-6	LSL	6.73	78.3	27.4	15.0	21.2
T233-4	SLL	6.41	69.7	T233-6	SLL	6.70	79.1	27.1	14.8	20.9
--	--	--	--	--	--	--	--	--	--	--
T334-4	SSL	6.53	66.4	T334-6	SSL	6.74	76.5	28.8	11.9	20.4
T343-4	SLS	6.59	67.1	T343-6	SLS	6.74	77.3	29.1	11.3	20.2
T433-4	LSS	6.53	66.7	T433-6	LSS	6.70	77.0	28.7	11.4	20.1
--	--	--	--	--	--	--	--	--	--	--
T335-4	SSL	6.44	66.2	T335-6	SSL	6.74	76.1	27.7	10.9	19.3
T353-4	SLS	6.50	67.6	T353-6	SLS	6.77	77.4	28.7	10.4	19.6
T533-4	LSS	6.43	67.1	T533-6	LSS	6.71	77.4	27.8	9.5	18.6
--	--	--	--	--	--	--	--	--	--	--
T336-4	SSL	6.39	65.7	T336-6	SSL	6.76	74.6	27.9	8.8	18.4
T363-4	SLS	6.49	66.7	T363-6	SLS	6.90	75.8	28.7	9.6	19.2
T633-4	LSS	6.39	66.4	T633-6	LSS	6.78	75.5	27.5	8.5	18.0

^aDetailed information for all sequences is presented in **Table S1**. pH transition midpoints were identified by pH-dependent CD (pH_T^{CD}) spectra at 288 nm and pH-dependent UV absorption (pH_T^{UV} , given in **Table S1**) spectra at 295 nm. Thermal stabilities (T_m , °C) were characterized by UV-melting curves at 295 nm. Standard deviations of pH_T and T_m of two independent measurements were less than 0.2 and 1.0 °C, respectively. pH_T obtained by CD and UV absorbance were in excellent agreement ($pH_T^{CD} - pH_T^{UV} < 0.25$). No melting experiment was performed for the C_3 and C_4 tracts since most of these sequences do not form an i-DNA at pH 7.0 (see TDS in Figure S1), or their melting temperatures is too low to be measured accurately.

^bName: The first 'T' letter means that all spacers are composed of thymine bases only; three consecutive numbers refer to lengths of the three spacers in the 5' to 3' direction; '-3, -4, -5 and -6' refer to sequences with four C_3 , C_4 , C_5 , and C_6 tracts (all of equal length), respectively. For example, the T112-3 sequence is 5'-CCCTCCCTCCCTCCC-3' (four repeats of 3 cytosines separated by one, one, and two thymines). Each *group* is composed of sequences which differ only in

SUPPORTING INFORMATION

spacer permutation; it is named after the first sequence in the group. For example, the *T112-3* group is composed of three sequences: *T112-3*, *T121-3*, and *T211-3*.

^c Spacer permutation is defined as the swap between two sequences of an intramolecular i-DNA keeping length and overall base composition constant^[1]. These sequences belong to the same group. Each group contains three sequences. In this study, as two spacers are of identical length by design, the spacer pattern can either be *SSL*, *SLS*, *LLS*, or *LLS*, *LSL*, *SLL*. Herein, *S* and *L* are short for relatively *short* and *long* spacers, respectively.

^d As a first approximation^[16], T_m at pH 7.0 is assumed to be equal to the average of half-transition values for heating and cooling curves, provided by the heating and cooling profiles which are recorded with the same temperature gradient: $T_m^{pH\ 7.0} = \frac{T_{heating} + T_{cooling}}{2}$.

SUPPORTING INFORMATION

Table S3 pH transition and thermal stability at pH 5.0 of extended sequences with four C_5 -tracts. ^a

Name ^b	Spacer Permutation ^c	pH_T^{CD}	$T_m^{pH\ 5.0}$	Name ^b	Spacer Permutation ^c	pH_T^{CD}	$T_m^{pH\ 5.0}$
Longer (7-15) central spacer				Adenine in spacer			
T171-5	SLS	6.54	72.7	AA115-5	SSL	6.38	69.5
T181-5	SLS	6.52	72.3	AA151-5	SLS	6.43	74.6
T1101-5	SLS	6.47	71.0	AA511-5	LSS	6.42	69.3
T1151-5	SLS	6.34	69.2	--	--	--	--
Two short spacers of different length				1A15-5	SSL	6.46	69.8
T152-5	SLM	6.71	75.3	11A5-5	SSL	6.41	70.1
T251-5	MLS	6.62	75.7	1A51-5	SLS	6.50	75.1
		--		151A-5	SLS	6.59	74.8
T153-5	SLM	6.60	75.6	51A1-5	LSS	6.43	71.1
T351-5	MLS	6.86	73.5	511A-5	LSS	6.50	70.5
		--		--	--	--	--
T253-5	SLM	6.84	73.6	115_1A-5	SSL	6.70	69.2
T352-5	MLS	6.79	74.6	151_1A-5	SLS	6.59	73.5
		--		511_1A-5	LSS	6.49	70.5
T162-5	SLM	6.70	74.2	--	--	--	--
T261-5	MLS	6.70	76.1	115_2A-5	SSL	6.36	68.7
		--		151_2A-5	SLS	6.49	76.2
T163-5	SLM	6.71	73.3	511_2A-5	LSS	6.36	69.2
T361-5	MLS	6.72	72.6	--	--	--	--
		--		115_3A-5	SSL	6.42	67.2
T263-5	SLM	6.74	72.8	151_3A-5	SLS	6.57	73.2
T362-5	MLS	6.70	74.2	511_3A-5	LSS	6.35	68.5
		--		--	--	--	--
		--		115_4A-5	SSL	6.48	68.5
		--		151_4A-5	SLS	6.69	76.1
		--		511_4A-5	LSS	6.33	70.8
		--		--	--	--	--
		--		115_5A-5	SSL	6.49	70.7
		--		151_5A-5	SLS	6.75	75.1
		--		511_5A-5	LSS	6.43	70.3

^a Detailed information for all sequences is provided in **Table S1**. pH transition midpoints were identified by pH-dependent CD (pH_T^{CD}) spectra at 288 nm. Thermal stabilities (T_m) were characterized by UV-melting curves at 295 nm. Standard deviations of pH_T and T_m of two independent measurements were below 0.2 and 1.0 °C, respectively.

^b Name: 'T' means that all spacers are composed of thymine base only; 'A' and 'AA' means that one or two thymine(s) in the spacer are replaced by one or two adenines, respectively; three consecutive numbers refer to lengths of the three spacers in the 5' to 3' direction; '-5' refers to sequences with four C_5 -tracts.

^c Loop permutation is defined as the swap between two sequences of an intramolecular i-DNA keeping length and overall base composition constant. These sequences belong to a same group. Their spacer pattern can be either SSL, SLS, LLS, or SLM, MLS. Herein, S, M and L are short for relatively short, middle, long spacer length, respectively.

SUPPORTING INFORMATION

Table S4 Thermal stability (°C) measured by DSC-melting and annealing experiments using a temperature gradient of 1°C/min (**Figure S19**).

Sequence	pH 5.0	pH 7.0			
	T_m	$T_{heating}$	$T_{cooling}$	T_m	$T_{Hysteresis}$
T112-5	75.6	21.2	15.6	18.4	5.6
T121-5	77.6	23.9	17.2	20.6	6.7
T211-5	71.8	22.6	17.0	19.8	5.6
T225-5	71.8	28.3	5.4	16.9	22.9
T252-5	76.1	32.1	7.4	19.8	24.6
T522-5	72.0	30.0	5.4	17.7	24.7
T112-6	81.0	33.0	16.1	24.6	16.9
T121-6	82.4	32.4	14.5	23.5	17.9
T211-6	80.2	31.4	14.5	23.0	16.9
T225-6	76.9	35.8	7.2	21.5	28.6
T252-6	79.8	38.8	8.2	23.5	30.6
T522-6	77.5	36.4	7.5	22.0	28.9

SUPPORTING INFORMATION

Table S5 Thermal stability (°C) of sequences with flanking sequences, different spacer contents and odd number of C·C⁺ base pairs (Figures S30-31) and description of the results.

Sequence	pH 5.0	pH 7.0			
	T_m	$T_{heating}$	$T_{cooling}$	T_m	$T_{hysteresis}$
T252-5	73.4	20.8	14.0	17.4	6.8
TT252-5	74.3	25.4	12.4	18.9	13.0
T252-5T	75.2	20.1	12.3	16.2	7.8
TT252-5T	74.9	25.9	10.3	18.1	15.6
AT252-5	75.6	23.6	14.5	19.0	9.1
T252-5A	75.9	22.0	13.7	17.9	8.3
AT252-5A	74.1	25.2	13.5	19.3	11.7
GT252-5	73.2	22.0	13.3	17.7	8.7
T252-5G	73.9	22.3	14.4	18.4	8.0
GT252-5G	74.5	22.7	13.3	18.0	9.5
252-5_A1	75.9	20.9	13.3	17.1	7.6
252-5_A2	75.0	18.4	12.4	15.4	6.0
252-5_A3	74.2	20.7	14.8	17.8	5.9
252-5_A4	74.6	23.2	15.4	19.3	7.8
252-5_A5	74.2	20.8	12.4	16.6	8.4
252-5_A6	75.9	18.2	12.7	15.4	5.5
252-5_AA1	74.1	17.9	9.6	13.8	8.3
252-5_AA2	75.1	18.5	10.1	14.3	8.4
252-5_AA3	72.4	18.0	10.8	14.4	7.2
A252-5	68.3	a	a		
252-5_G1	76.3	20.1	14.3	17.2	5.8
252-5_G2	71.9	17.9	13.1	15.5	4.9
252-5_G3	73.8	20.6	16.5	18.5	4.1
252-5_G4	74.5	19.3	16.0	17.7	3.3
252-5_G5	75.8	20.7	14.7	17.7	6.0
252-5_G6	75.2	17.9	13.1	15.5	4.8
252-5_GG1	73.0	16.3	10.7	13.5	5.5
252-5_GG2	74.3	a	a		
252-5_GG3	74.6	17.1	11.1	14.1	6.0
G252-5	66.0	a	a		
T225-45	68.5	12.5	11.1	11.8	1.3
T252-45	71.7	15.4	12.5	13.9	2.9
T522-45	69.7	13.1	11.6	12.4	1.5
T225-56	74.9	20.4	12.7	16.5	7.7
T252-56	77.4	21.6	13.5	17.5	8.1
T522-56	76.1	20.4	12.3	16.4	8.1

^a, The stability at pH 7.0 is not enough to obtain the thermal stability under the experimental conditions.

Expanding the sequence diversity: 35 sequence variants are designed based the T252-5 and sequences are given in **Table S1**.

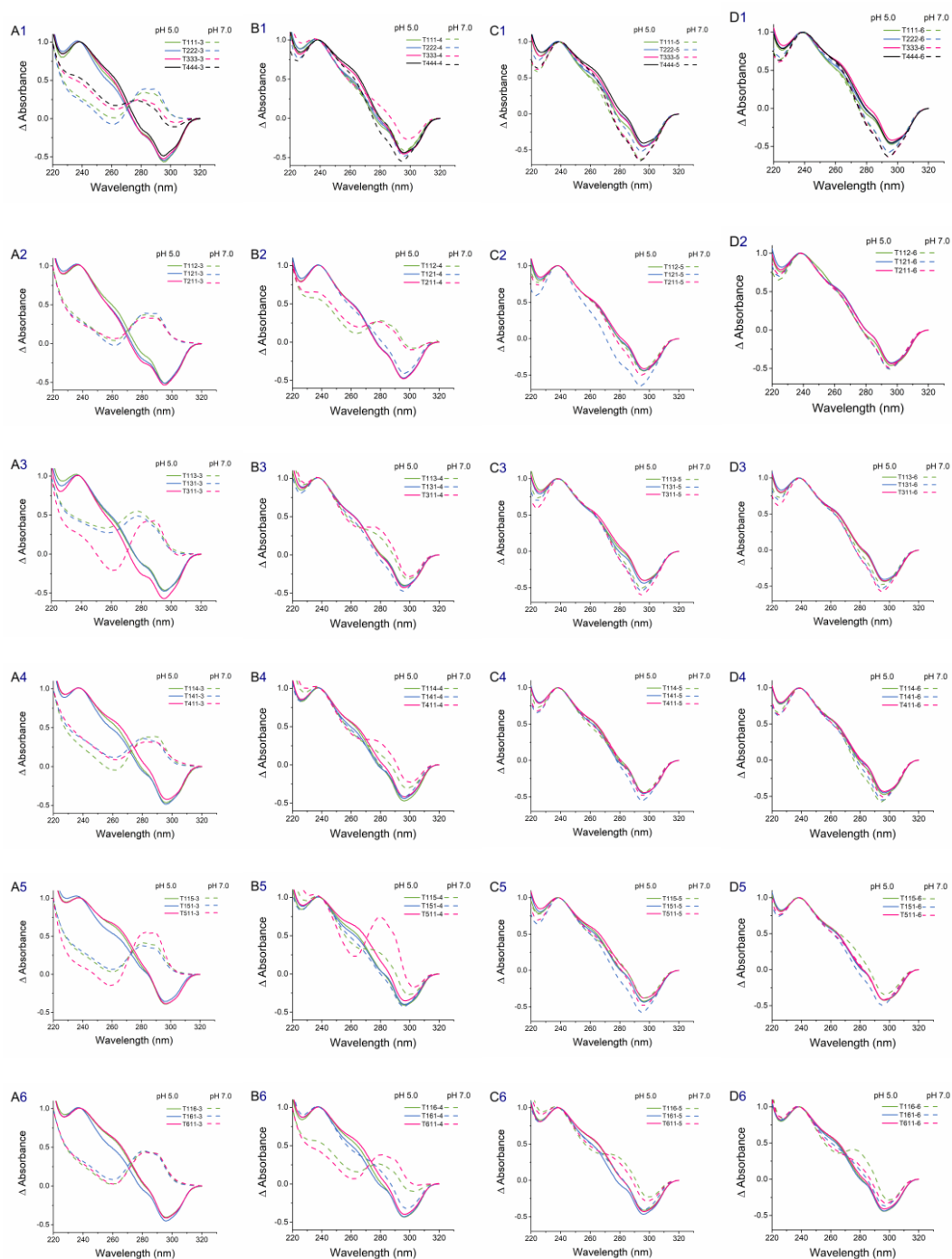
1) Regarding the addition of terminal nucleotides (A, T or G) either 5' or 3' end, or both ends: these capping nucleotides induce a modest change in T_m (less than 3 °C at both pH 5.0 and 7.0) but also affect the hysteresis between melting and annealing processes at pH 7.0. These results indicate that caps do not affect the thermodynamic stability obviously but are able to change the folding kinetics of i-DNAs.

2) Regarding the replacement of one, two, or all thymines in the spacer by adenines or guanines: i) Generally, adenines and guanines in the spacers can change the thermal stability, which decreases along with the increasing number of adenines and guanines; ii) Replacement of single thymine in the second spacer increases the thermal stability, whereas an opposite effect was observed for the first and third spacers.

3) Odd number of C·C⁺ base pairs: we compared the stabilities of T252-5 variants, potentially forming 9, 10 and 11 C·C⁺ base pairs. Overall, thermal stability increases along with the increasing in C·C⁺ base pairs and the "long central spacer is better" rule also applies to i-DNAs with an odd number of C·C⁺ base pairs.

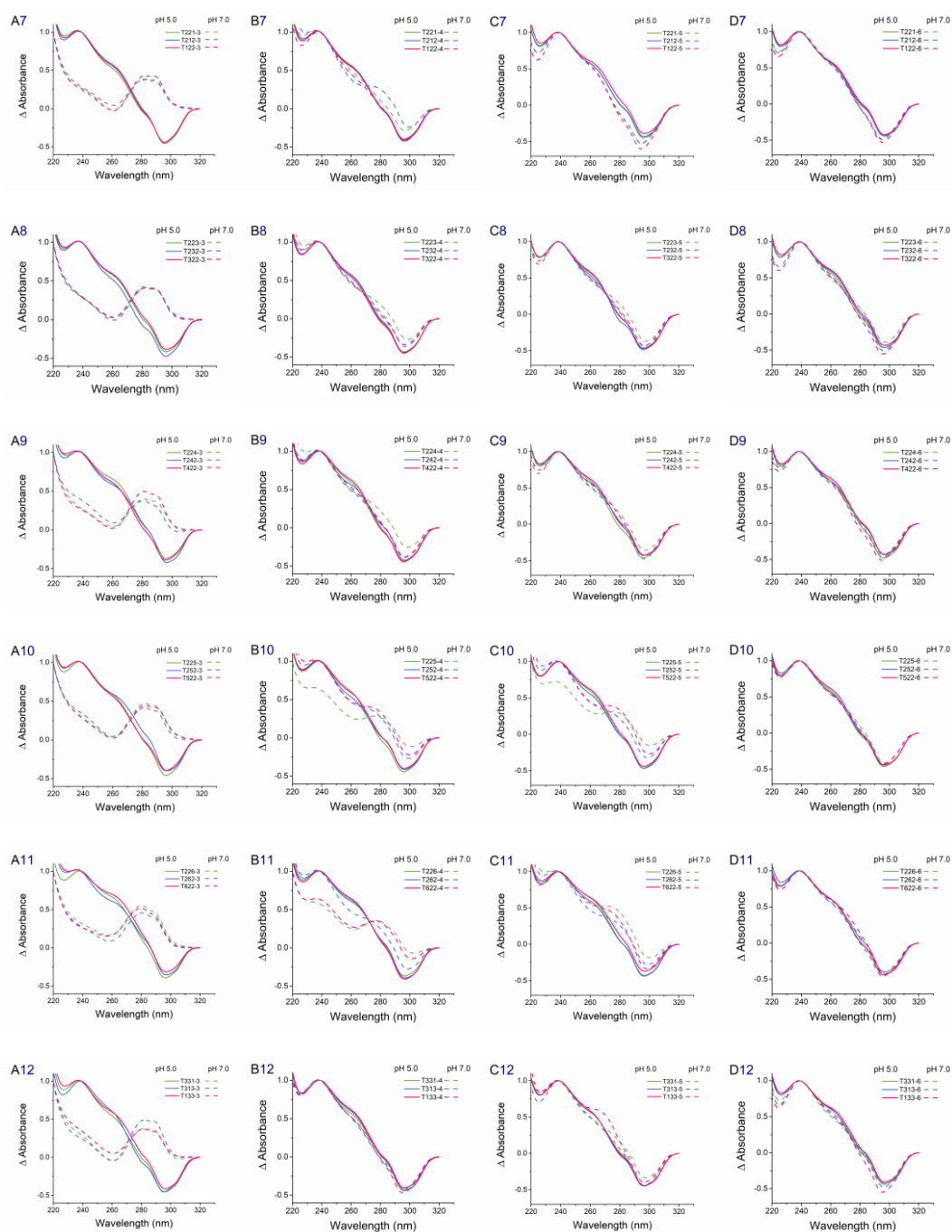
SUPPORTING INFORMATION

Figure S1 Thermal difference spectra (TDS).



SUPPORTING INFORMATION

Figure S1 Thermal difference spectra (TDS). (Continued_01)



SUPPORTING INFORMATION

Figure S1 Thermal difference spectra (TDS). (Continued_02)

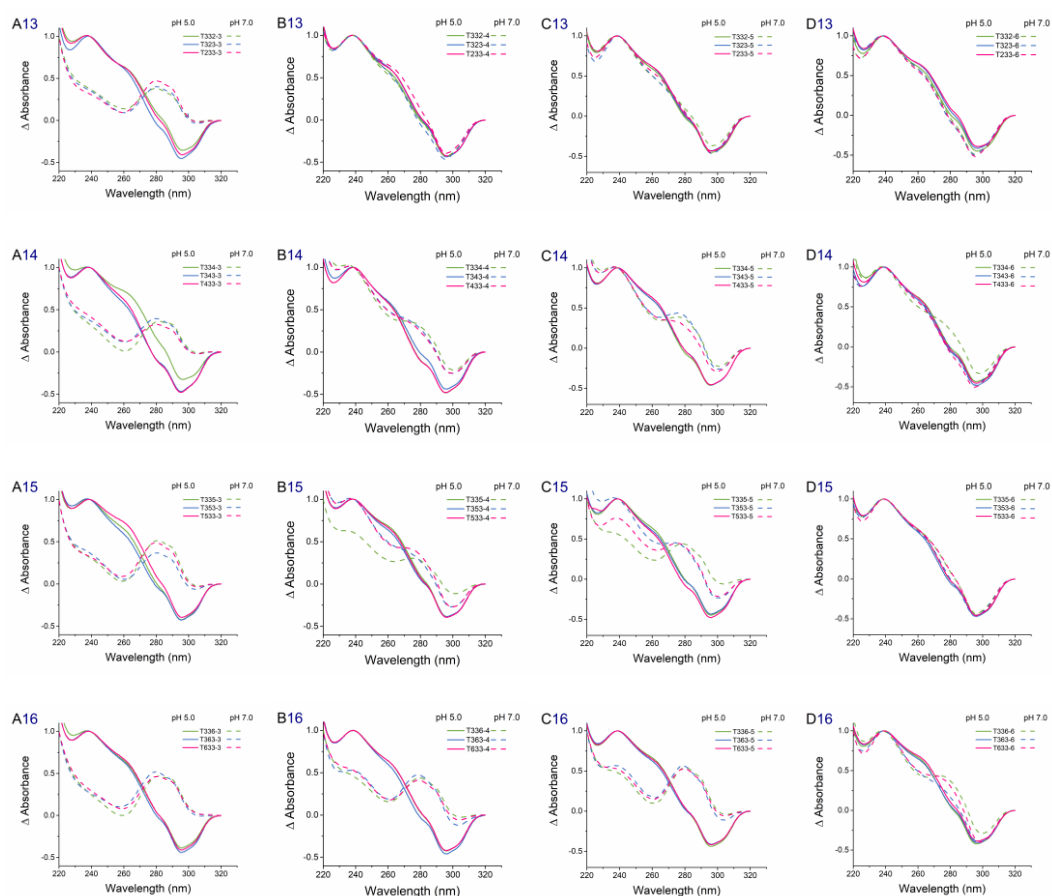


Figure S1 Normalized thermal difference spectra (TDS) of (A) i-DNAs with C_3 tract (first column, A1~A16), (B) i-DNAs with C_4 tract (second column, B1~B16), (C) i-DNAs with C_5 tract (third column, C1~C16), and (D) i-DNAs with C_6 tract (fourth column, D1~D16), resulting from the subtraction of UV absorbance spectra at 5 °C from the spectra at 95 °C (for pH 5.0) or 65 °C (for pH 7.0). 5 μ M DNA in pH 5.0 (solid line) and 7.0 (dashed line).

SUPPORTING INFORMATION

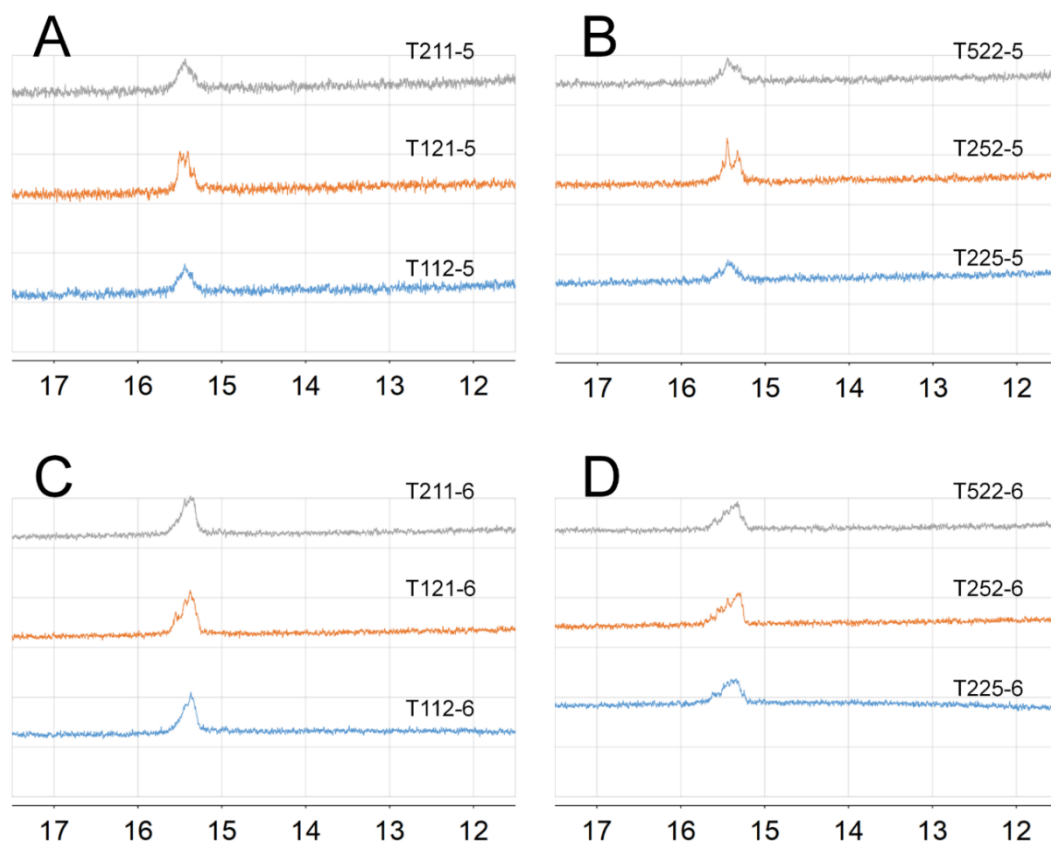
Figure S2 ^1H 1D NMR spectra.

Figure S2 1D ^1H NMR spectra of 12 selected sequences at pH 7.0 in the region assigned to imino protons of protonated cytosines at 20 °C. (A) T112-5, T121-5 and T211-5 sequences; (B) T225-5, T252-5 and T522-5 sequences; (C) T112-6, T121-6 and T211-6 sequences; (D) T225-6, T252-6 and T522-6 sequences.

SUPPORTING INFORMATION

Figures S3-S4 Non-denaturing PAGEs.

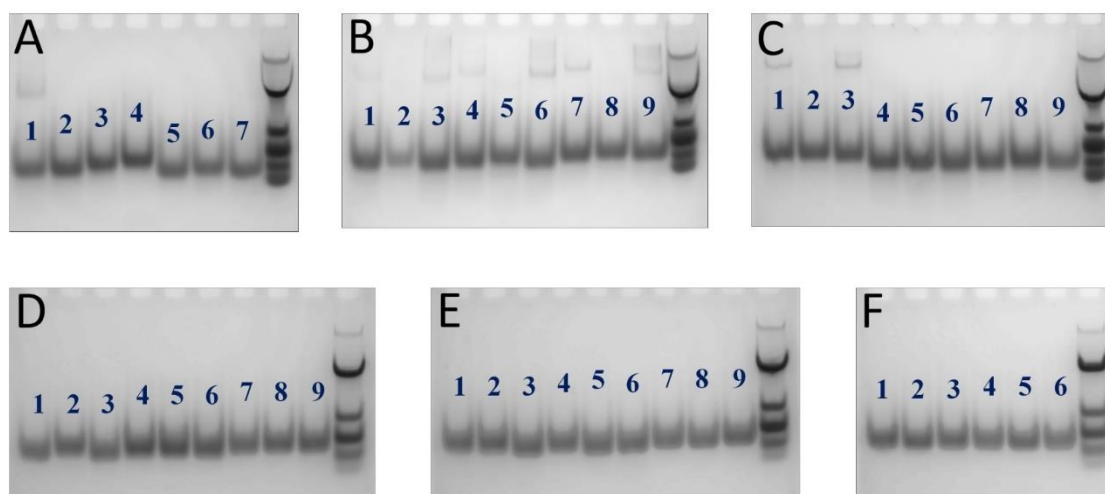


Figure S3 Non-denaturing PAGE of i-DNA with C_5 -tract at pH 5.0. Samples concentration is 25 μ M. (A-F) 49 sequences with C_5 -tract in **Table 1**. Last lane in each gel is dTn ($n = 90, 60, 30, 21, 15, 10$) ladder.

(A) Lane A1: T111-5; Lane A2: T222-5; Lane A3: T333-5; Lane A4: T444-5; Lane A5: T112-5; Lane A6: T121-5; Lane A7: T211-5.

(B) Lane B1: T113-5; Lane B2: T131-5; Lane B3: T311-5; Lane B4: T114-5; Lane B5: T141-5; Lane B6: T411-5; Lane B7: T115-5; Lane B8: T151-5; Lane B9: T511-5.

(C) Lane C1: T116-5; Lane C2: T161-5; Lane C3: T611-5; Lane C4: T221-5; Lane C5: T212-5; Lane C6: T122-5; Lane C7: T223-5; Lane C8: T232-5; Lane C9: T322-5.

(D) Lane D1: T224-5; Lane D2: T242-5; Lane D3: T422-5; Lane D4: T225-5; Lane D5: T252-5; Lane D6: T522-5; Lane D7: T226-5; Lane D8: T262-5; Lane D9: T622-5.

(E) Lane E1: T331-5; Lane E2: T313-5; Lane E3: T133-5; Lane E4: T332-5; Lane E5: T323-5; Lane E6: T233-5; Lane E7: T334-5; Lane E8: T343-5; Lane E9: T433-5.

(F) Lane F1: T335-5; Lane F2: T353-5; Lane F3: T533-5; Lane F4: T336-5; Lane F5: T363-5; Lane F6: T633-5.

SUPPORTING INFORMATION

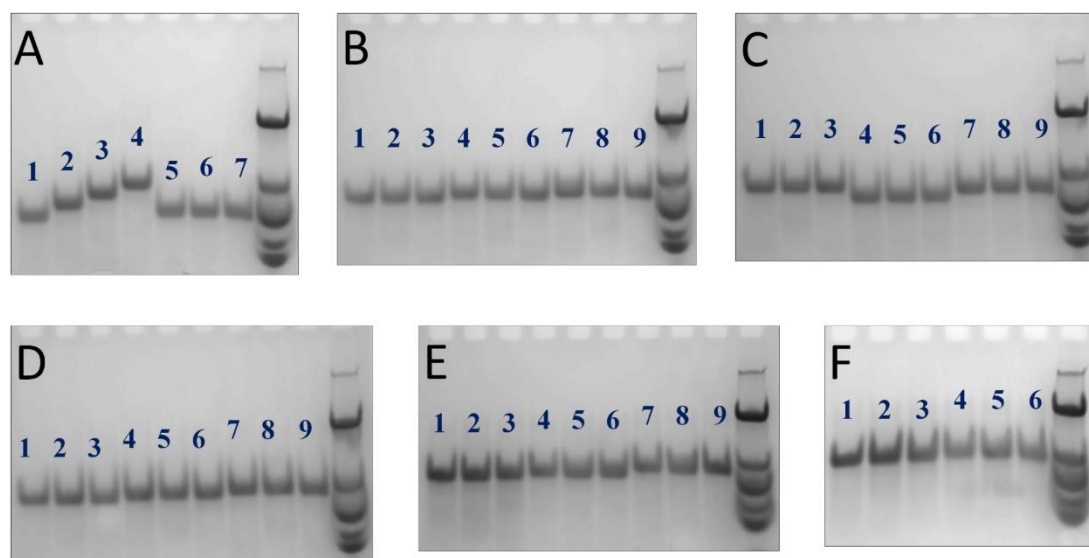


Figure S4 Non-denaturing PAGE of i-DNA with C_5 -tract at pH 7.0. Samples concentration is 25 μ M. (A-F) 49 sequences with C_5 -tract in **Table 1**. Last lane in each gel is dTn (n = 90, 60, 30, 21, 15, 10) ladder.

(A) Lane A1: T111-5; Lane A2: T222-5; Lane A3: T333-5; Lane A4: T444-5; Lane A5: T112-5; Lane A6: T121-5; Lane A7: T211-5.

(B) Lane B1: T113-5; Lane B2: T131-5; Lane B3: T311-5; Lane B4: T114-5; Lane B5: T141-5; Lane B6: T411-5; Lane B7: T115-5; Lane B8: T151-5; Lane B9: T511-5.

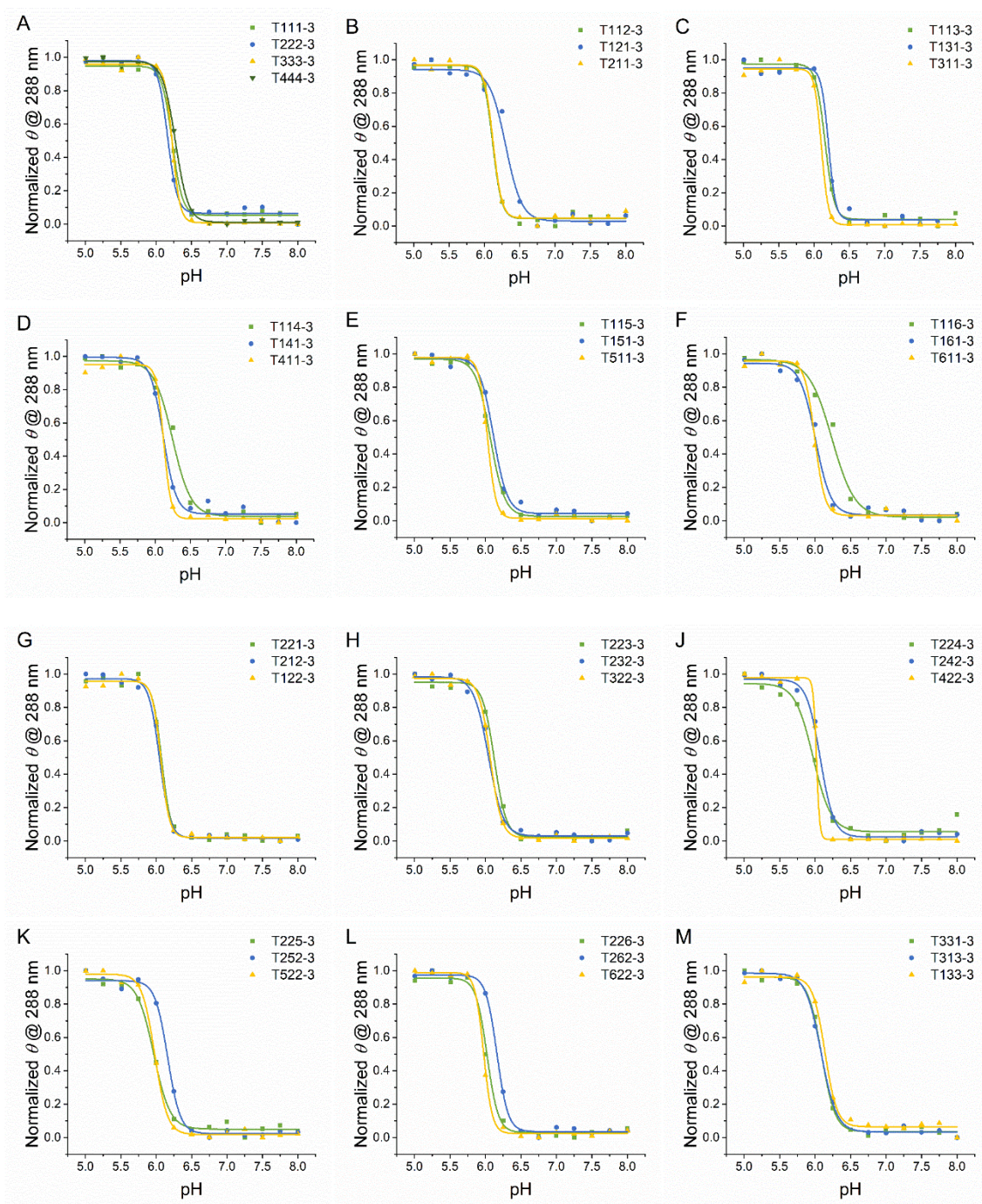
(C) Lane C1: T116-5; Lane C2: T161-5; Lane C3: T611-5; Lane C4: T221-5; Lane C5: T212-5; Lane C6: T122-5; Lane C7: T223-5; Lane C8: T232-5; Lane C9: T322-5.

(D) Lane D1: T224-5; Lane D2: T242-5; Lane D3: T422-5; Lane D4: T225-5; Lane D5: T252-5; Lane D6: T522-5; Lane D7: T226-5; Lane D8: T262-5; Lane D9: T622-5.

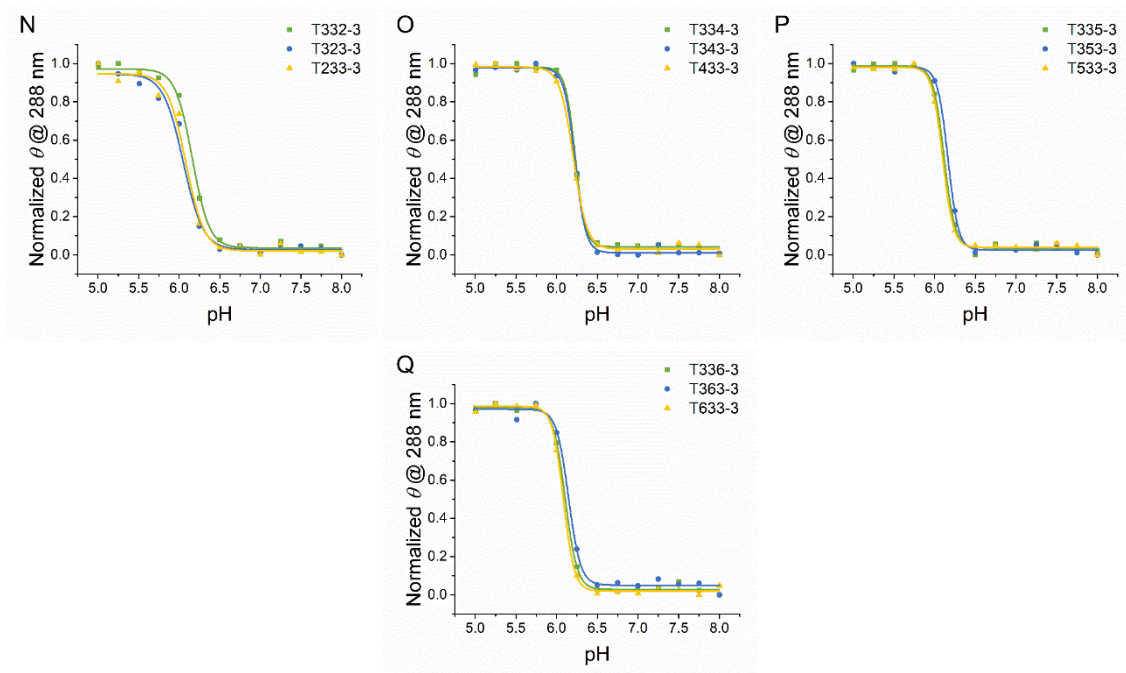
(E) Lane E1: T331-5; Lane E2: T313-5; Lane E3: T133-5; Lane E4: T332-5; Lane E5: T323-5; Lane E6: T233-5; Lane E7: T334-5; Lane E8: T343-5; Lane E9: T433-5.

(F) Lane F1: T335-5; Lane F2: T353-5; Lane F3: T533-5; Lane F4: T336-5; Lane F5: T363-5; Lane F6: T633-5.

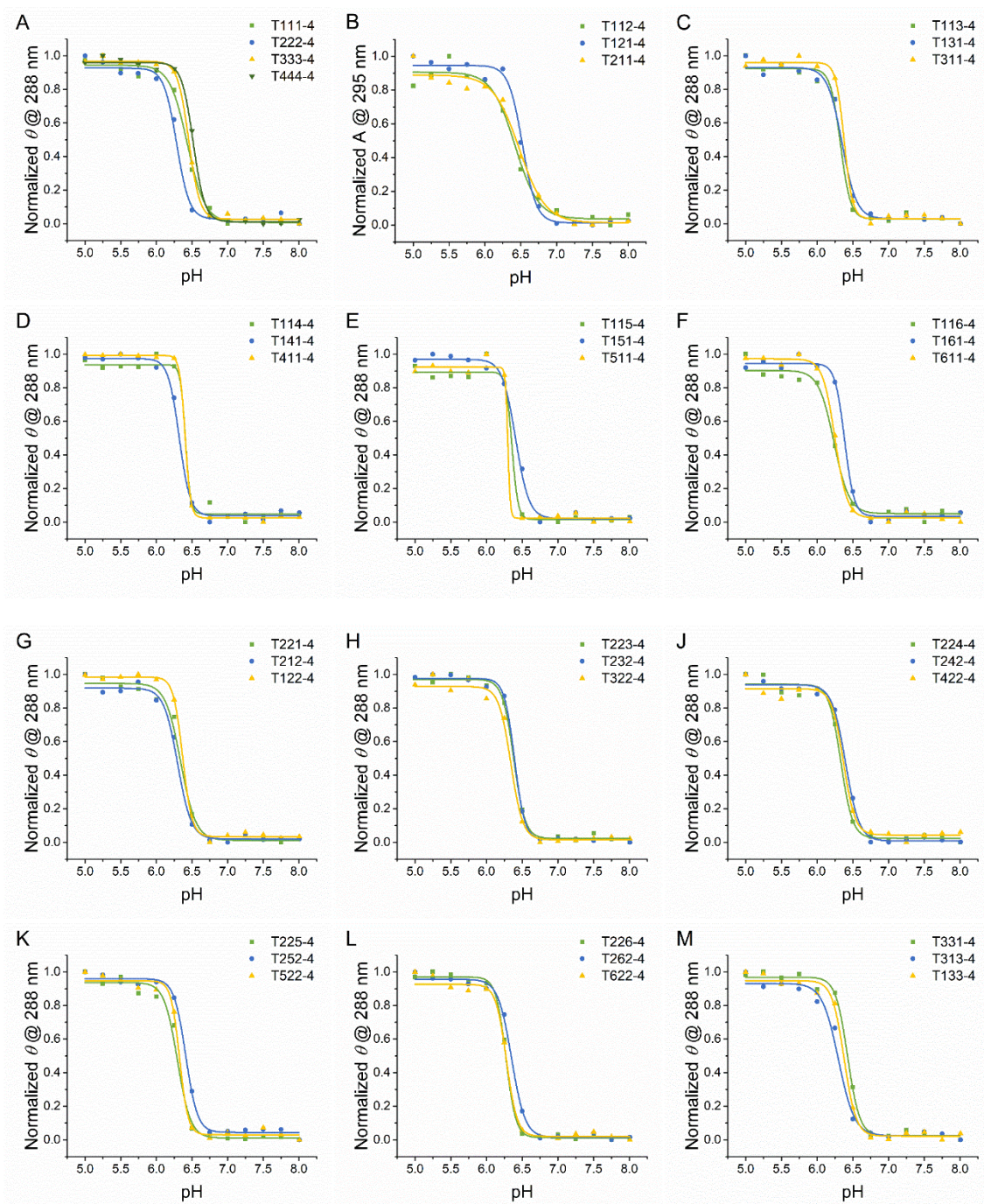
SUPPORTING INFORMATION

Figure S5 pH-dependent normalized ellipticities at 288 nm for sequences with C₃ tract.

SUPPORTING INFORMATION

Figure S5 pH-dependent normalized ellipticities at 288 nm of sequences with C_3 tract. (Continued_01)**Figure S5** pH-transition by CD spectra at 288 nm of i-DNAs with C_3 tract. (A) *T111-3* group, (B) *T112-3* group, (C) *T113-3* group, (D) *T114-3* group, (E) *T115-3* group, (F) *T116-3* group, (G) *T221-3* group, (H) *T223-3* group, (J) *T224-3* group, (K) *T225-3* group, (L) *T226-3* group, (M) *T331-3* group, (N) *T332-3* group, (O) *T334-3* group, (P) *T335-3* group, and (Q) *T336-3* group.

SUPPORTING INFORMATION

Figure S6 pH-dependent normalized ellipticities at 288 nm of sequences with C₄ tract.

SUPPORTING INFORMATION

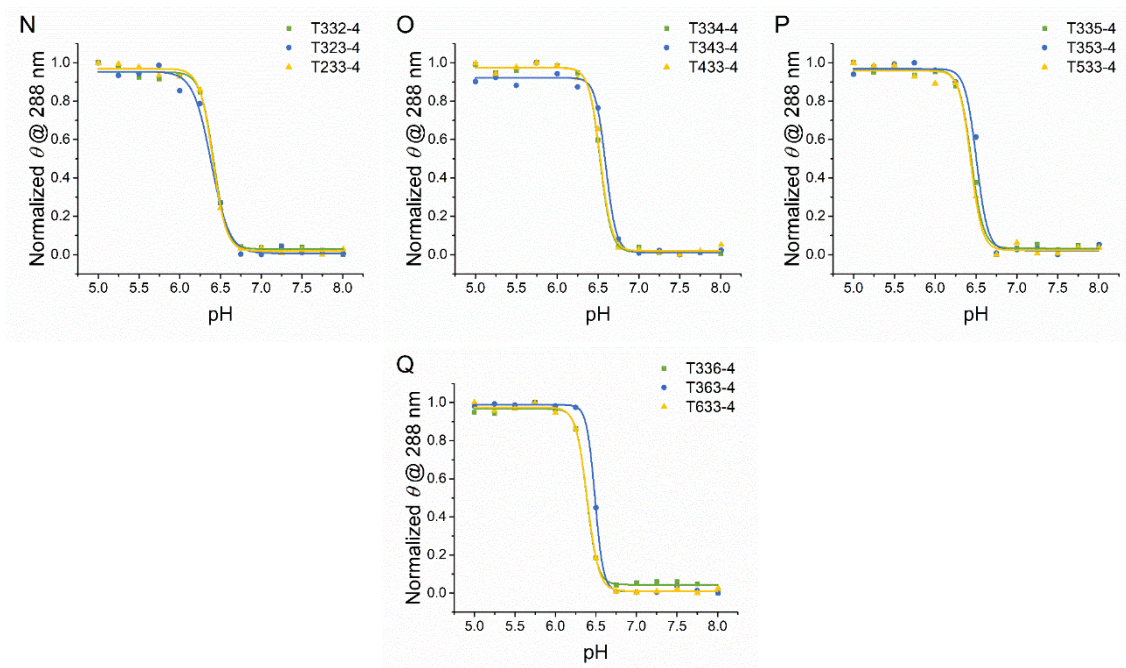
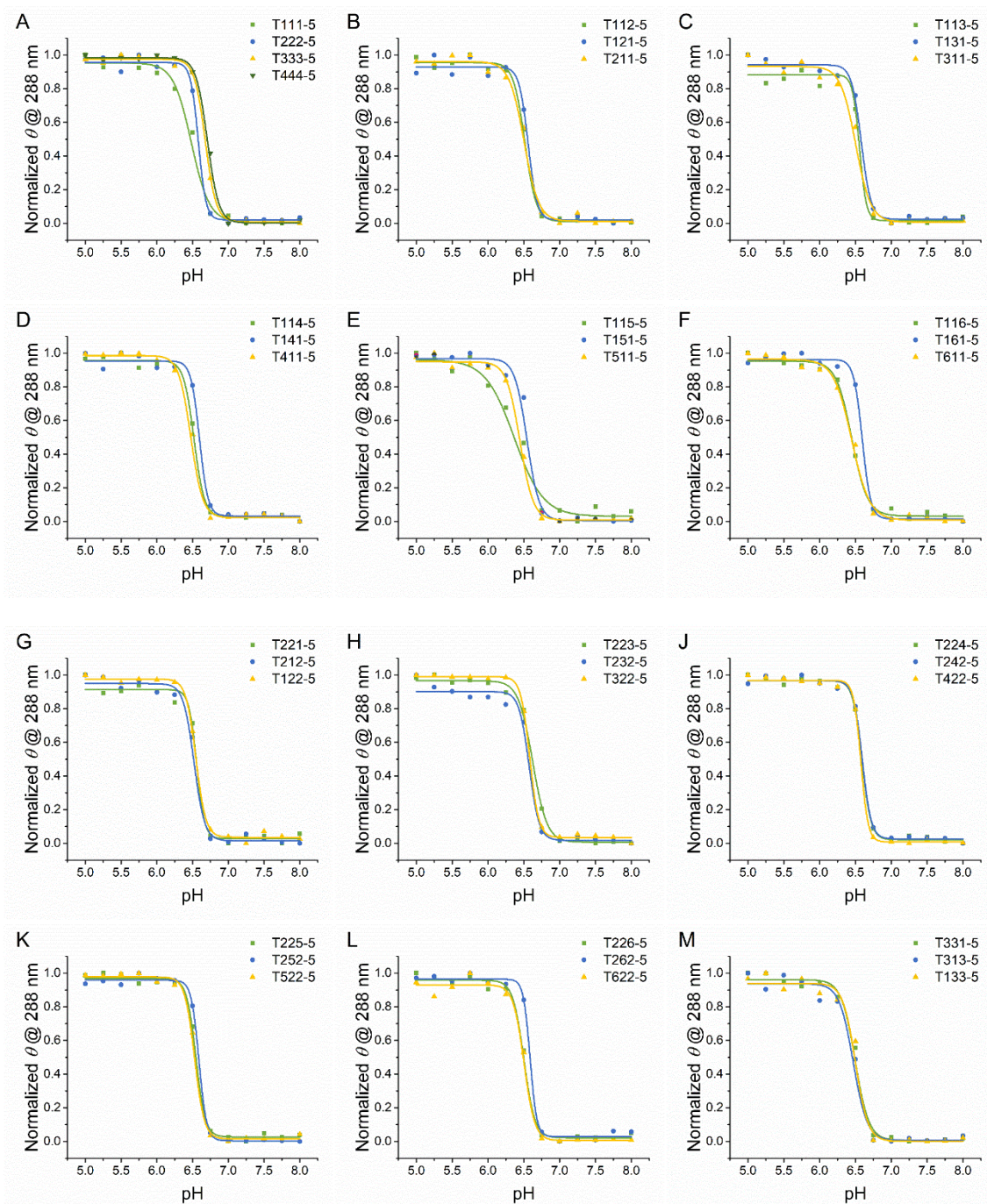
Figure S6 pH-dependent CD spectra of sequences with C_4 tract. (Continued_01)

Figure S6 pH-transition by CD spectra at 288 nm of i-DNAs with C_4 tract. (A) $T111-4$ group, (B) $T112-4$ group, (C) $T113-4$ group, (D) $T114-4$ group, (E) $T115-4$ group, (F) $T116-4$ group, (G) $T221-4$ group, (H) $T223-4$ group, (J) $T224-4$ group, (K) $T225-4$ group, (L) $T226-4$ group, (M) $T331-4$ group, (N) $T332-4$ group, (O) $T334-4$ group, (P) $T335-4$ group, and (Q) $T336-4$ group.

SUPPORTING INFORMATION

Figure S7 pH-dependent normalized ellipticities at 288 nm of sequences with C₅ tract.

SUPPORTING INFORMATION

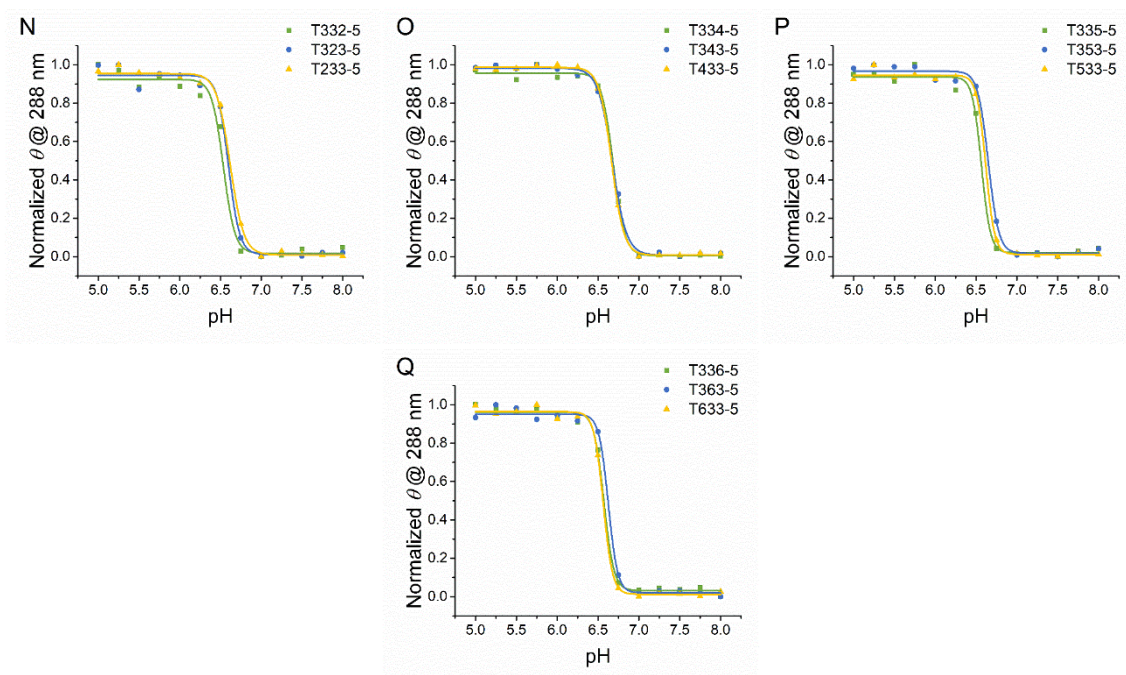
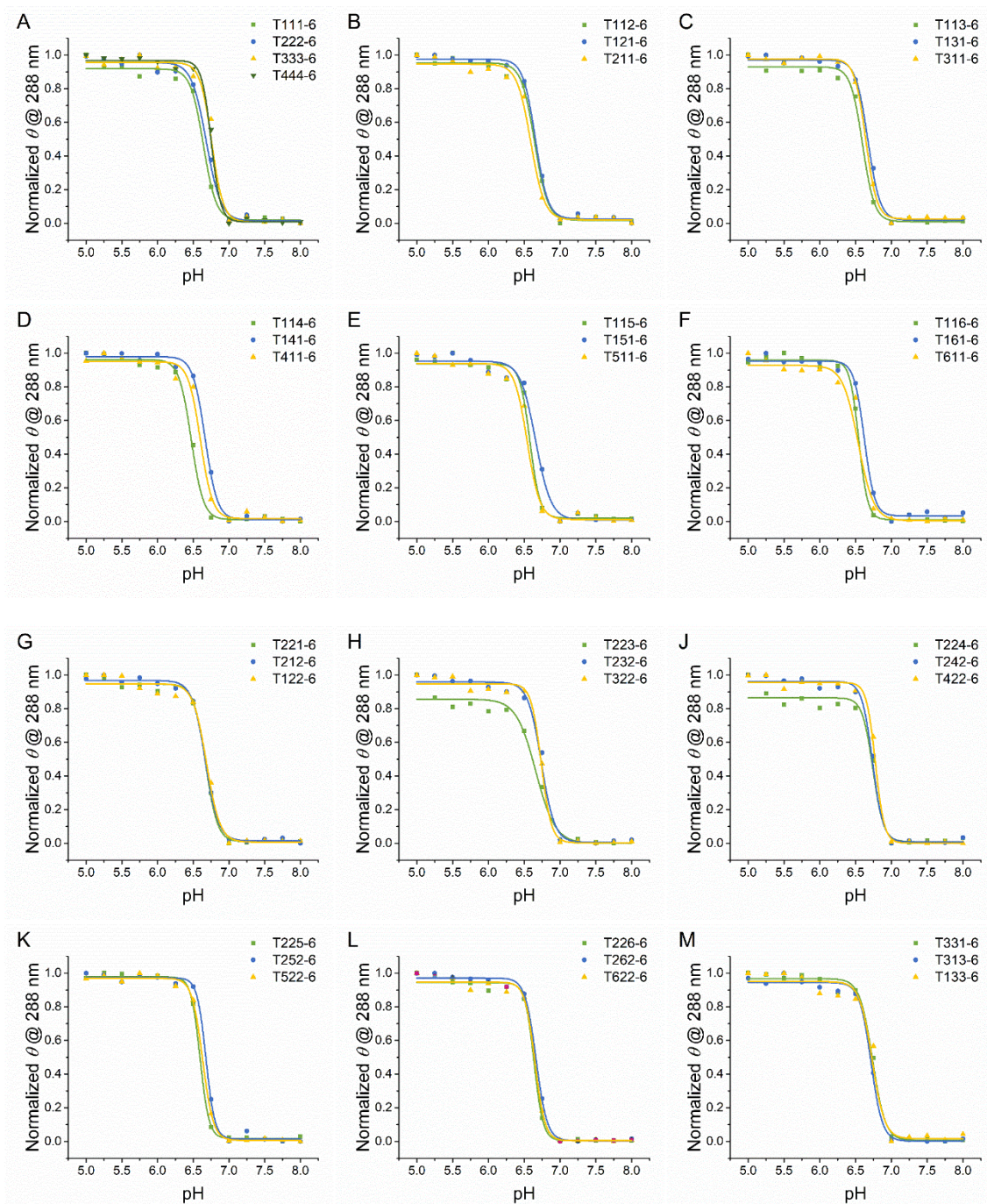
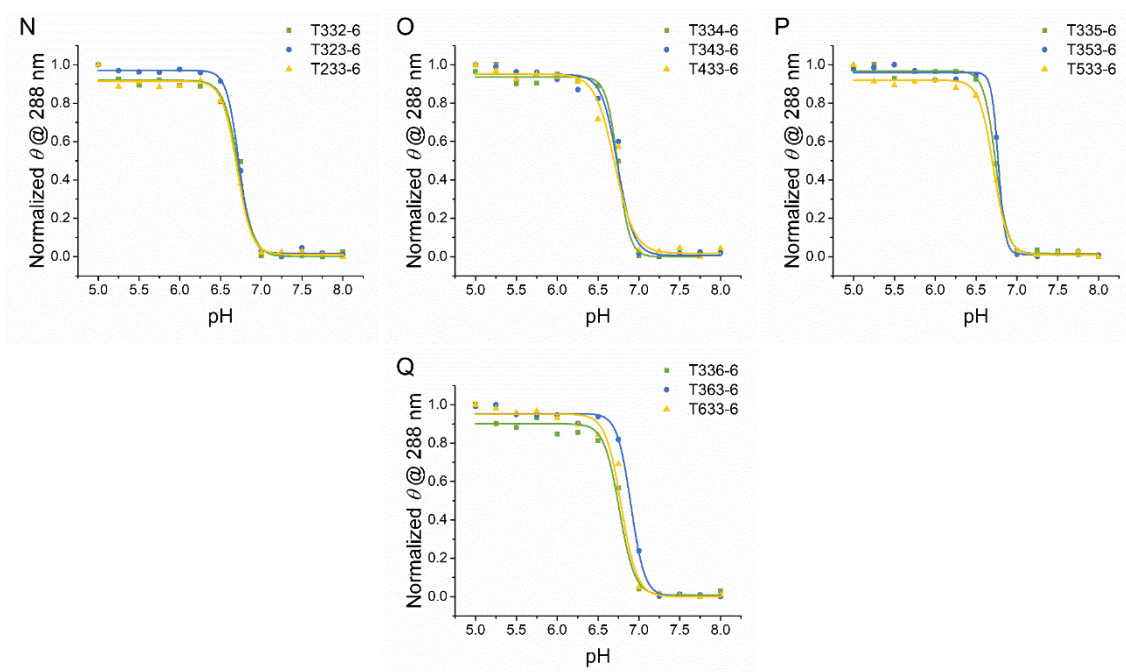
Figure S7 pH-dependent normalized ellipticities at 288 nm of sequences with C_5 tract. (Continued_01)

Figure S7 pH-transition by CD spectra at 288 nm of i-DNAs with C_5 tract. (A) $T111-5$ group, (B) $T112-5$ group, (C) $T113-5$ group, (D) $T114-5$ group, (E) $T115-5$ group, (F) $T116-5$ group, (G) $T221-5$ group, (H) $T223-5$ group, (J) $T224-5$ group, (K) $T225-5$ group, (L) $T226-5$ group, (M) $T331-5$ group, (N) $T332-5$ group, (O) $T334-5$ group, (P) $T335-5$ group, and (Q) $T336-5$ group.

SUPPORTING INFORMATION

Figure S8 pH-dependent normalized ellipticities at 288 nm of sequences with C₆ tract.

SUPPORTING INFORMATION

Figure S8 pH-dependent normalized ellipticities at 288 nm of sequences with C_6 tract. (*Continued_01*)**Figure S8** pH-transition by CD spectra at 288 nm of i-DNAs with C_6 tract. (A) $T111-6$ group, (B) $T112-6$ group, (C) $T113-6$ group, (D) $T114-6$ group, (E) $T115-6$ group, (F) $T116-6$ group, (G) $T221-6$ group, (H) $T223-6$ group, (J) $T224-6$ group, (K) $T225-6$ group, (L) $T226-6$ group, (M) $T331-6$ group, (N) $T332-6$ group, (O) $T334-6$ group, (P) $T335-6$ group, and (Q) $T336-6$ group.

SUPPORTING INFORMATION

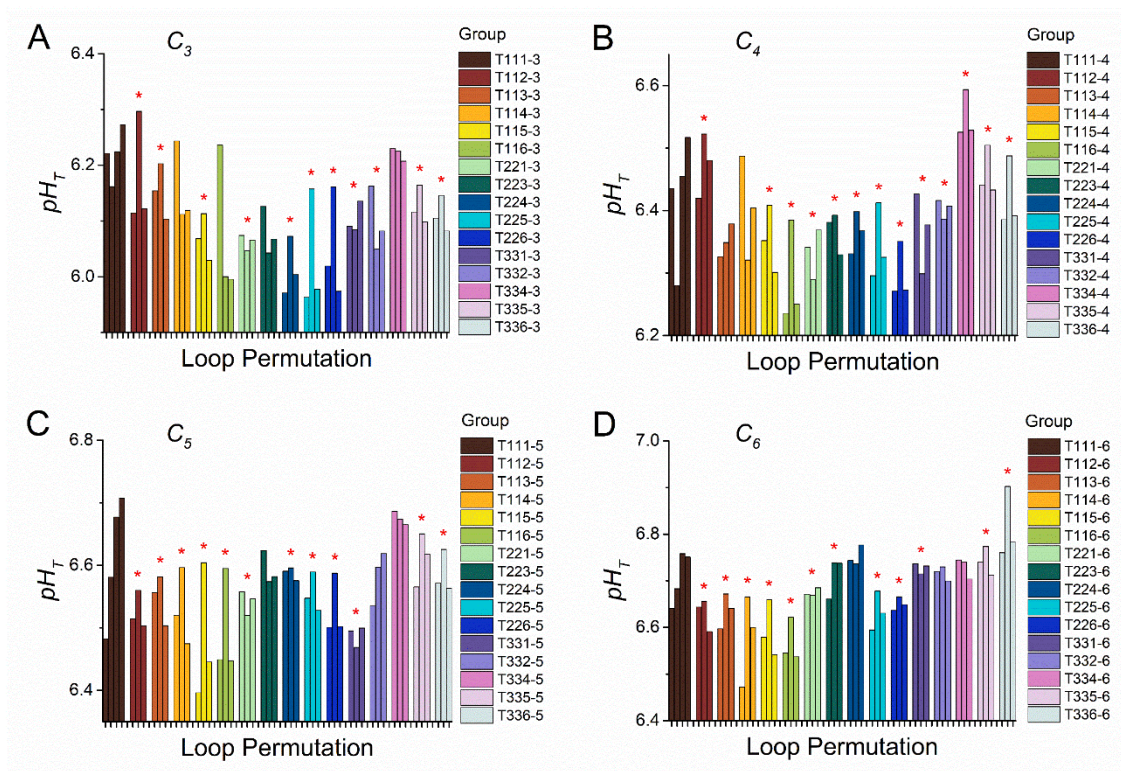
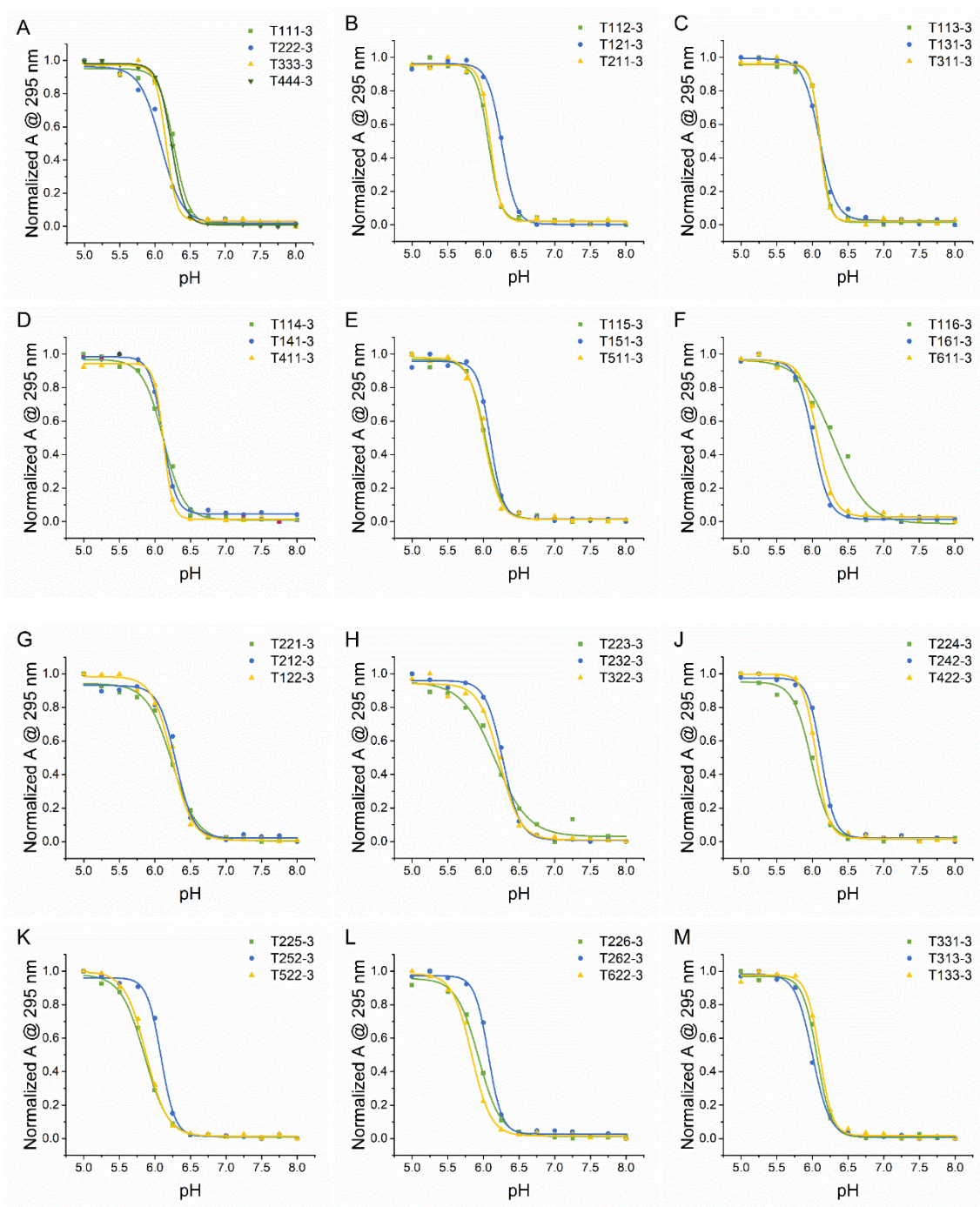
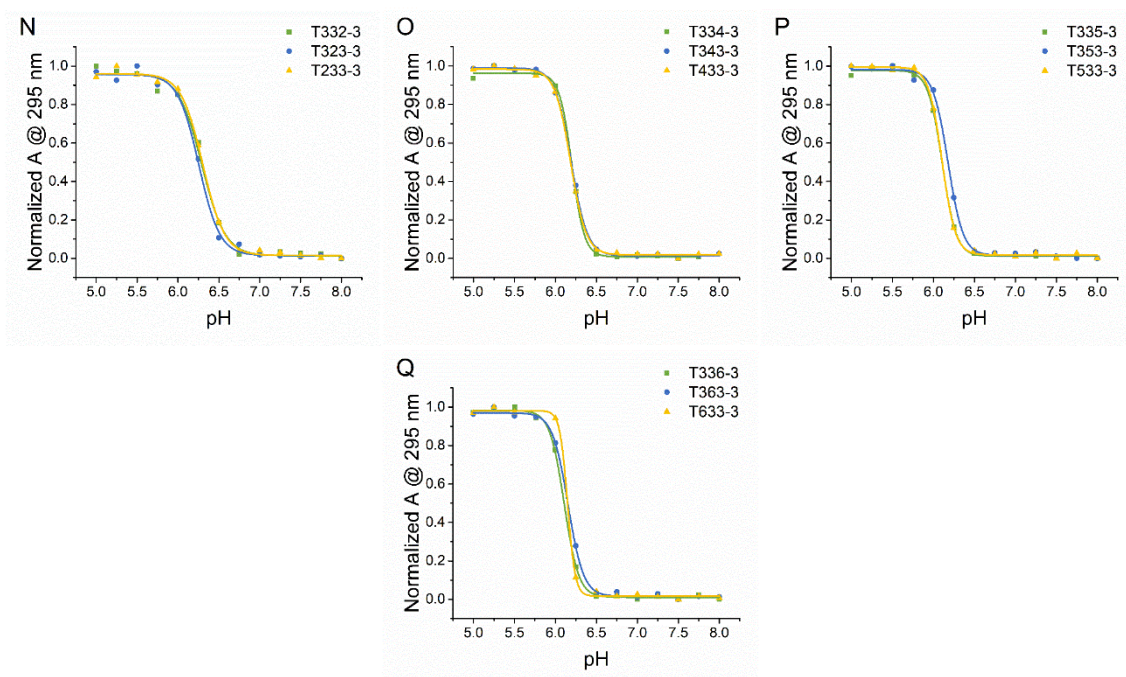
Figure S9 pH transition midpoint (pH_T) of i-DNA determined by CD.

Figure S9 pH transition midpoint (pH_T) of i-DNA determined by CD: (A) I-DNAs with four C_3 tracts; (B) I-DNAs with four C_4 tracts; (C) I-DNAs with four C_5 tracts; (D) I-DNAs with four C_6 tracts. The experiments were carried out in 20 mM Britton-Robinson buffer with 140 mM KCl and 20 mM NaCl at room temperature (25 °C). pH titrations are shown in the supplementary information; pH varied from 5.00 to 8.00 with 0.25 pH unit intervals. All oligonucleotide strand concentrations were 5 μ M. Symbol * at top of the bar indicates that this group obeys the rule that the sequence with longer central loop exhibits a higher pH_T .

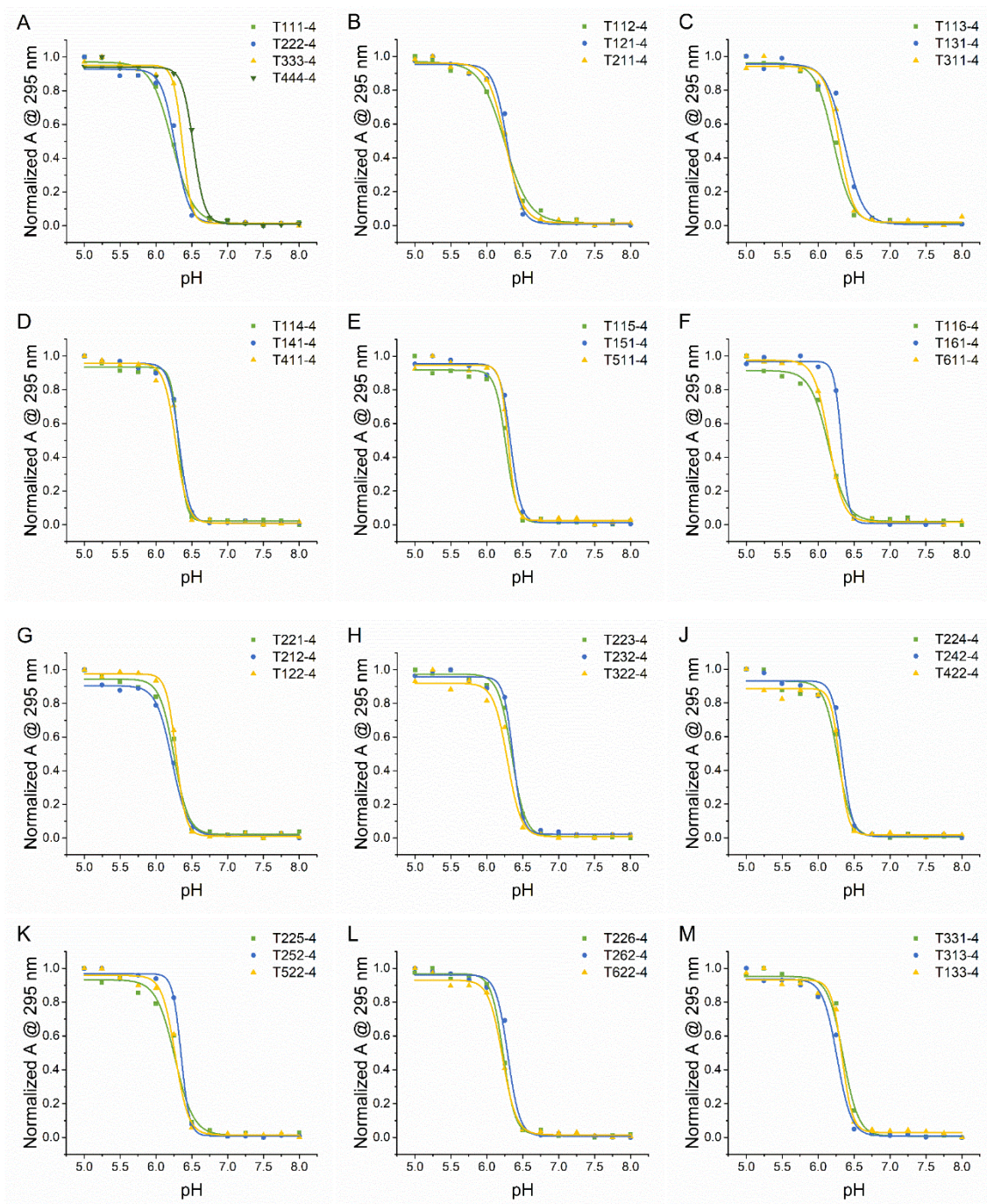
SUPPORTING INFORMATION

Figure S10 pH-dependent normalized absorbances at 295 nm for sequences with C₃ tract.

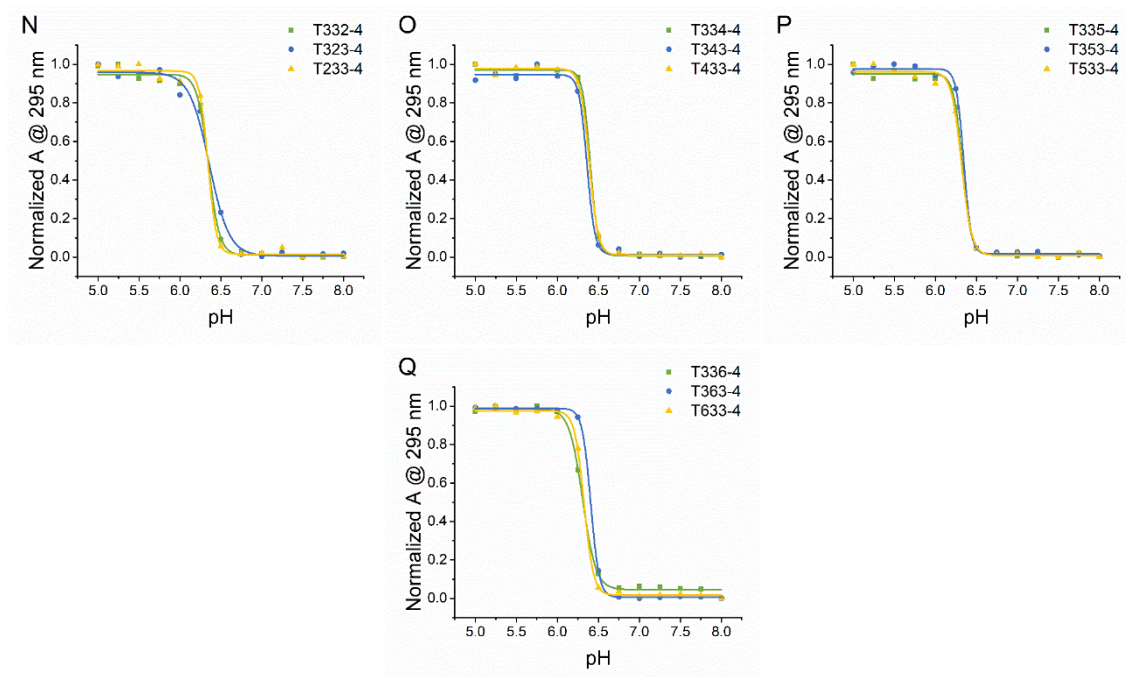
SUPPORTING INFORMATION

Figure S10 pH-dependent normalized absorbances at 295 nm for sequences with C_3 tract. (Continued_01)**Figure S10** pH-transition by UV absorbance spectra at 295 nm of i-DNAs with C_3 tract. (A) $T111$ -3 group, (B) $T112$ -3 group, (C) $T113$ -3 group, (D) $T114$ -3 group, (E) $T115$ -3 group, (F) $T116$ -3 group, (G) $T221$ -3 group, (H) $T223$ -3 group, (J) $T224$ -3 group, (K) $T225$ -3 group, (L) $T226$ -3 group, (M) $T331$ -3 group, (N) $T332$ -3 group, (O) $T334$ -3 group, (P) $T335$ -3 group, and (Q) $T336$ -3 group.

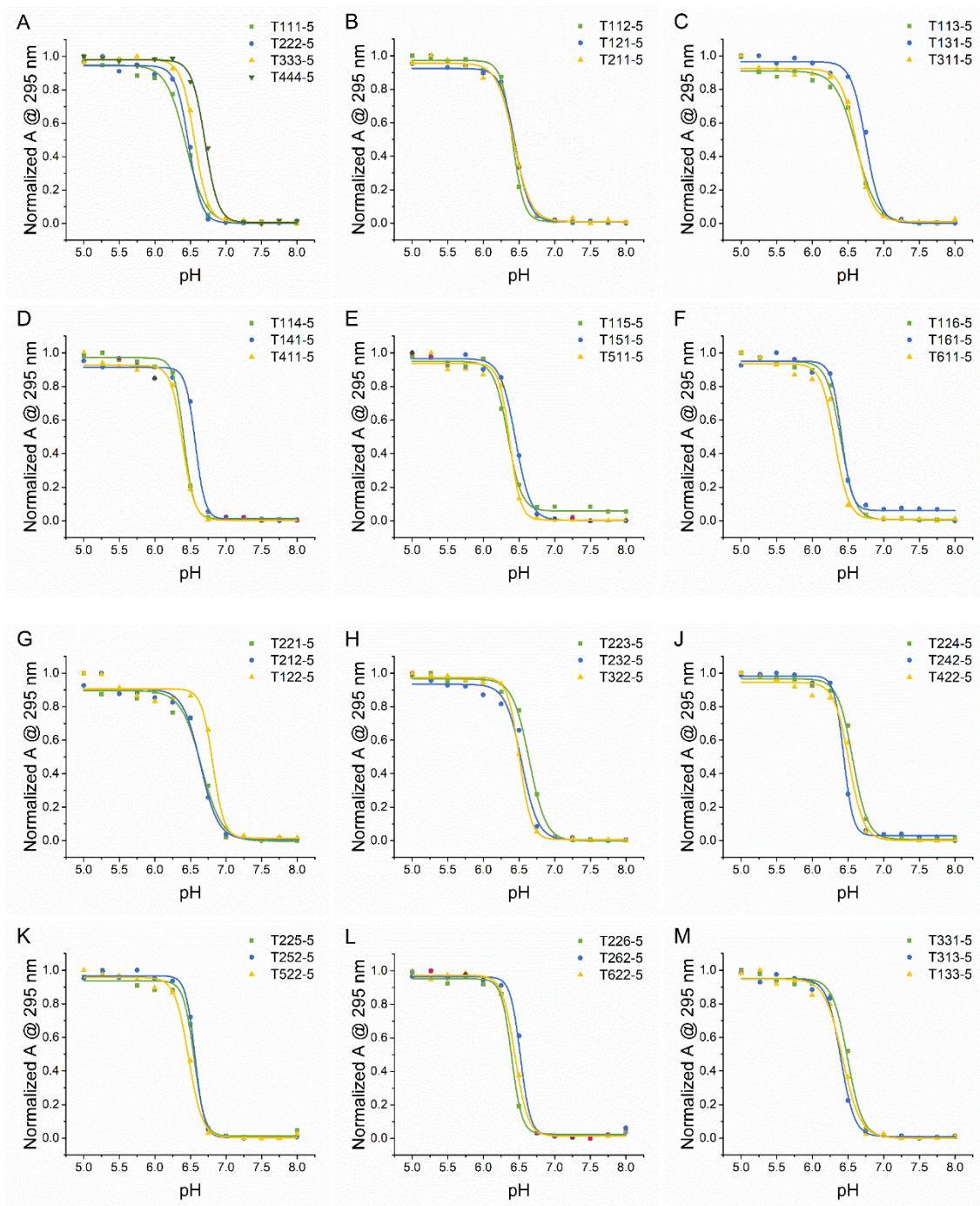
SUPPORTING INFORMATION

Figure S11 pH-dependent normalized absorbances at 295 nm for sequences with C₄ tract.

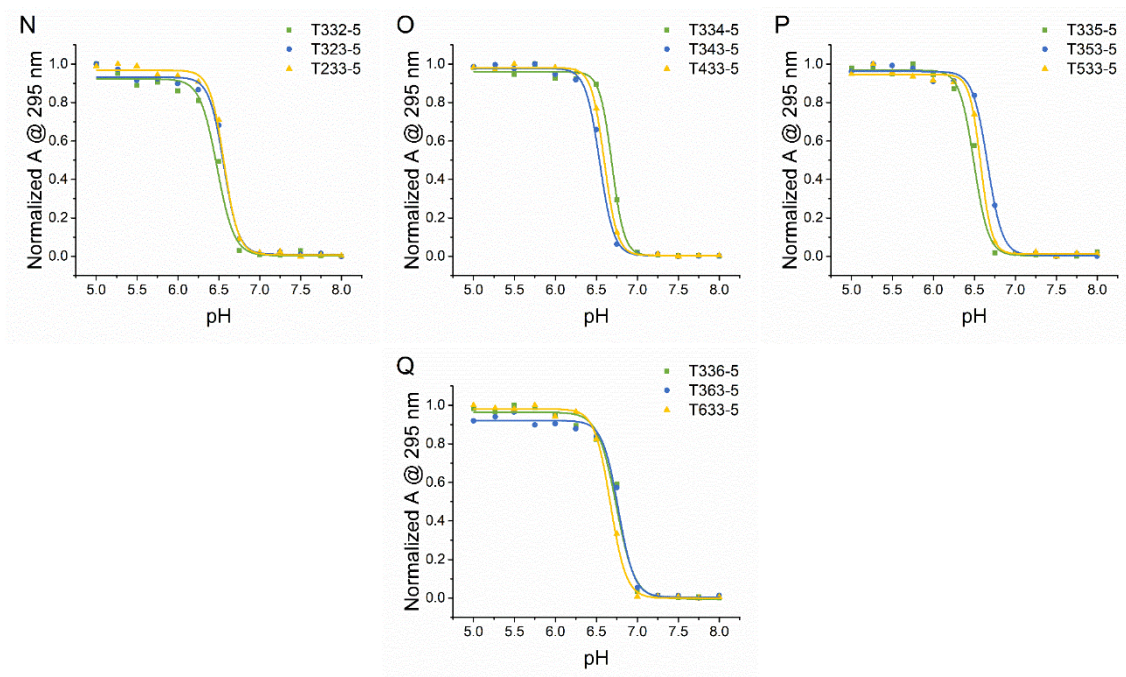
SUPPORTING INFORMATION

Figure S11 pH-dependent normalized absorbances at 295 nm for sequences with C_4 tract. (Continued_01)**Figure S11** pH-transition by UV absorbance spectra at 295 nm of i-DNAs with C_4 tract. (A) $T111-4$ group, (B) $T112-4$ group, (C) $T113-4$ group, (D) $T114-4$ group, (E) $T115-4$ group, (F) $T116-4$ group, (G) $T221-4$ group, (H) $T223-4$ group, (J) $T224-4$ group, (K) $T225-4$ group, (L) $T226-4$ group, (M) $T331-4$ group, (N) $T332-4$ group, (O) $T334-4$ group, (P) $T335-4$ group, and (Q) $T336-4$ group.

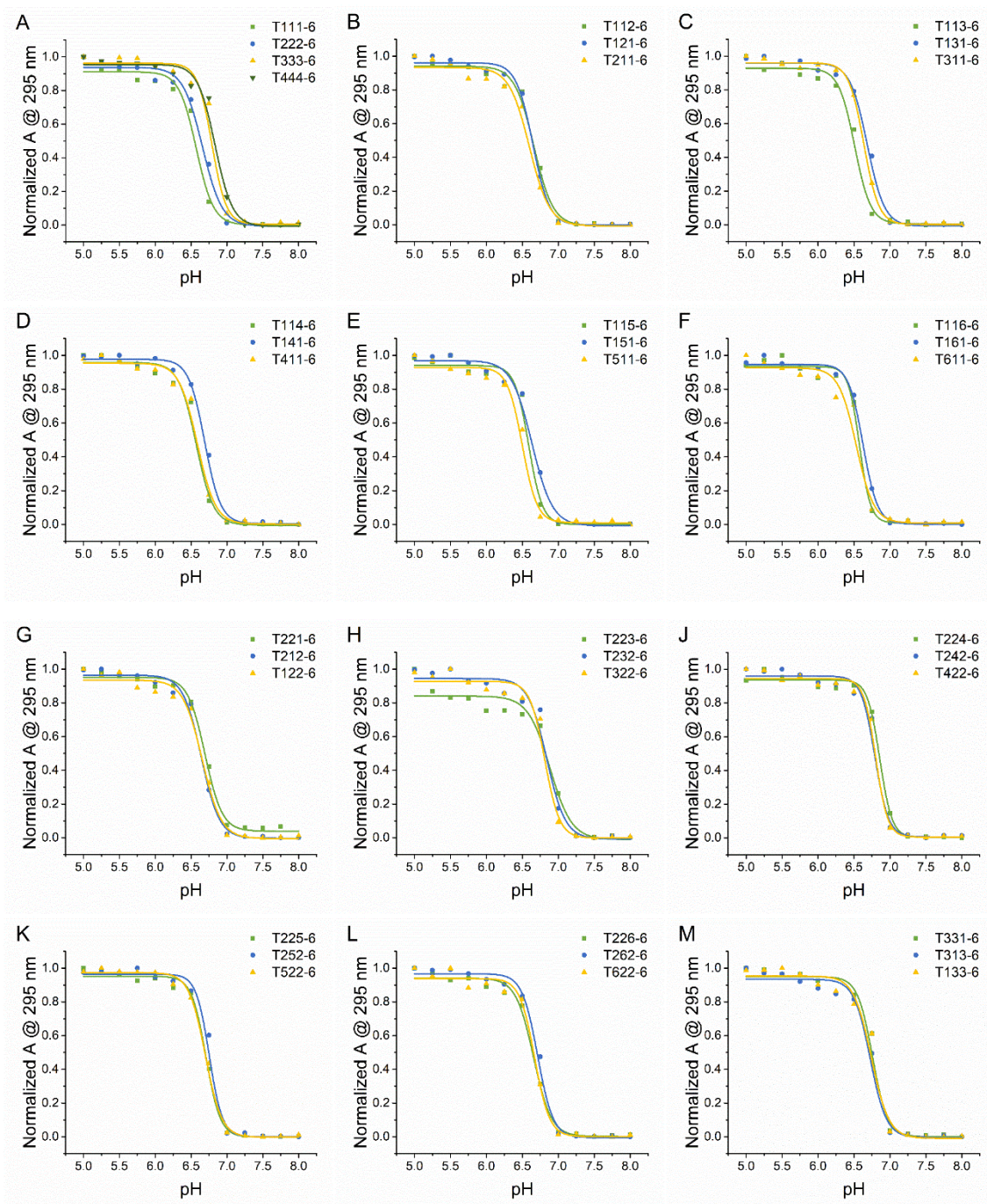
SUPPORTING INFORMATION

Figure S12 pH-dependent normalized absorbances at 295 nm for sequences with C₅ tract.

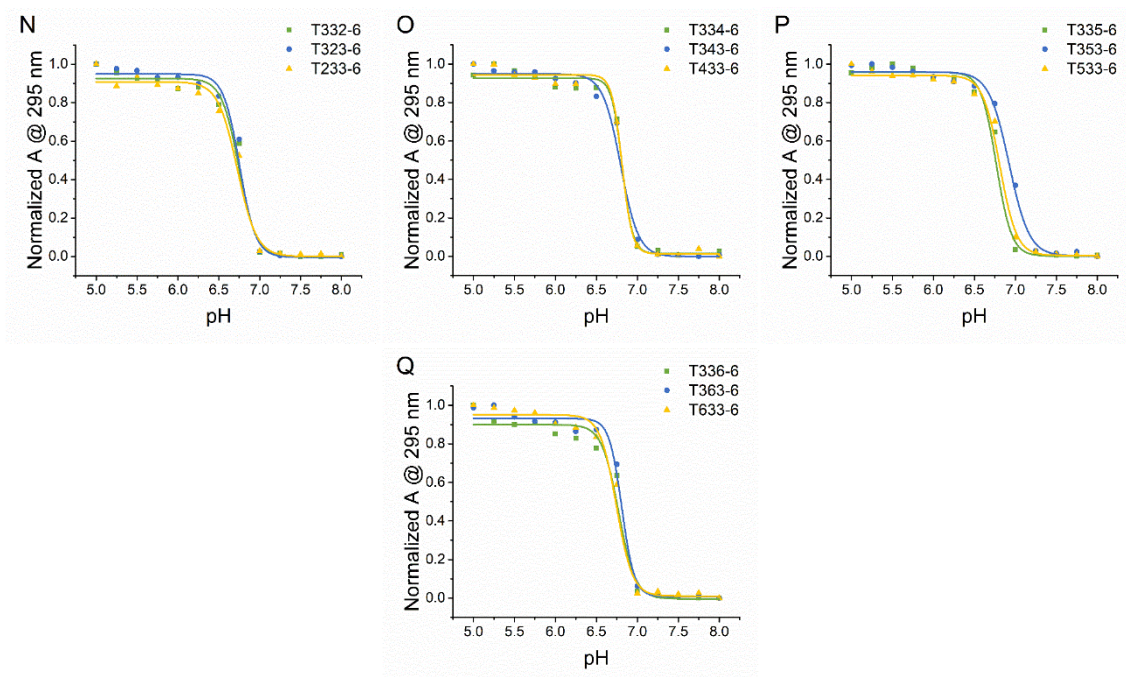
SUPPORTING INFORMATION

Figure S12 pH-dependent normalized absorbances at 295 nm for sequences with C_5 tract. (*Continued_01*)**Figure S12** pH-transition by UV absorbance spectra at 295 nm of i-DNAs with C_5 tract. (A) *T111-5* group, (B) *T112-5* group, (C) *T113-5* group, (D) *T114-5* group, (E) *T115-5* group, (F) *T116-5* group, (G) *T221-5* group, (H) *T223-5* group, (J) *T224-5* group, (K) *T225-5* group, (L) *T226-5* group, (M) *T331-5* group, (N) *T332-5* group, (O) *T334-5* group, (P) *T335-5* group, and (Q) *T336-5* group.

SUPPORTING INFORMATION

Figure S13 pH-dependent normalized absorbances at 295 nm for sequences with C₆ tract.

SUPPORTING INFORMATION

Figure S13 pH-dependent normalized absorbances at 295 nm for sequences with C_6 tract. (Continued_01)**Figure S13** pH-transition by UV absorbance spectra at 295 nm of i-DNAs with C_6 tract. (A) T111-6 group, (B) T112-6 group, (C) T113-6 group, (D) T114-6 group, (E) T115-6 group, (F) T116-6 group, (G) T221-6 group, (H) T223-6 group, (J) T224-6 group, (K) T225-6 group, (L) T226-6 group, (M) T331-6 group, (N) T332-6 group, (O) T334-6 group, (P) T335-6 group, and (Q) T336-6 group.

SUPPORTING INFORMATION

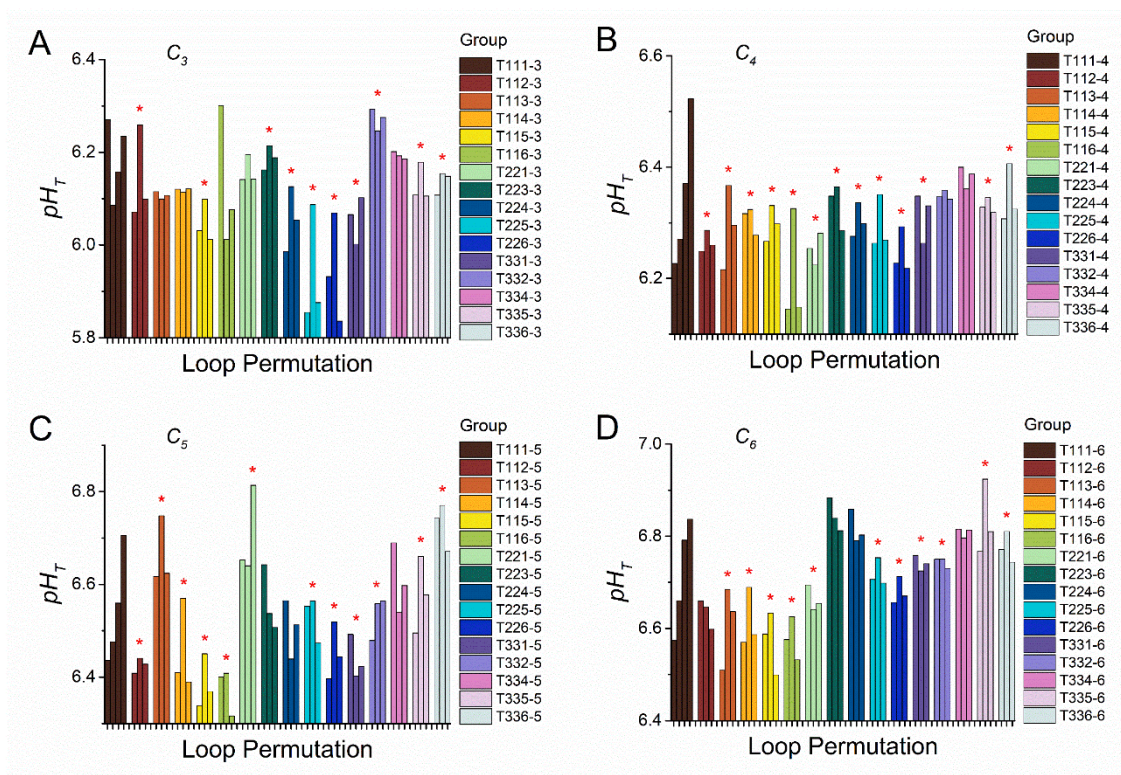
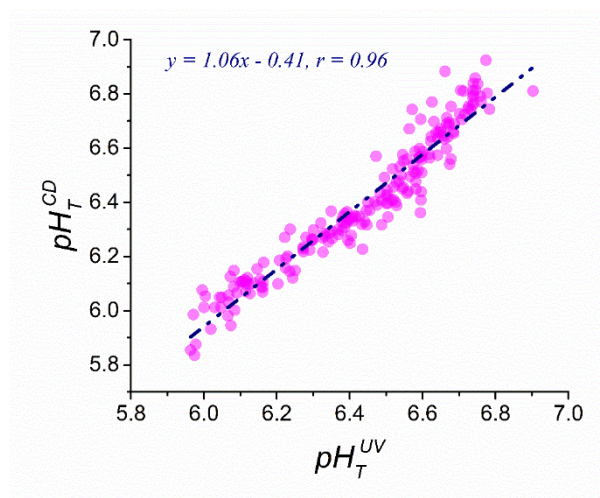
Figure S14 pH of mid-transition (pH_T) determined by UV absorbance data.

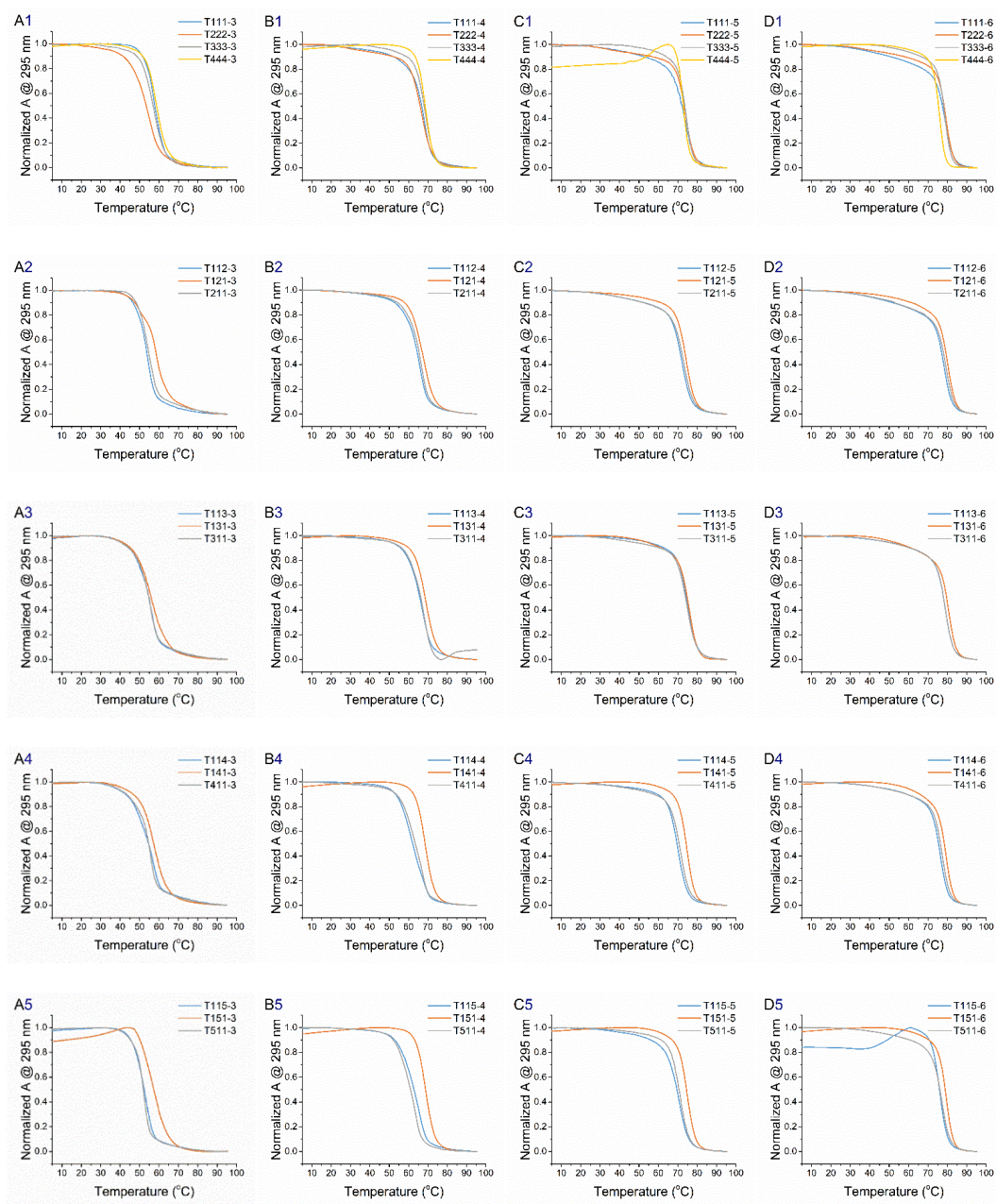
Figure S14 pH transition midpoint (pH_T) of i-DNAs identified by UV absorption spectra: (A) i-DNAs with four C_3 tracts; (B) i-DNAs with four C_4 tracts; (C) i-DNAs with four C_5 tracts; (D) i-DNAs with four C_6 tracts. The experiments were carried out in 20 mM Britton-Robinson buffer with 140 mM KCl and 20 mM NaCl at room temperature (25 °C). The pH varied from 5.00 to 8.00 at the interval of 0.25 pH unit and strand concentrations of oligonucleotides were 5 μ M. Symbol * at top of the bar indicates that this group obeys the rule that the sequence with longer central loop exhibits a higher pH_T .

SUPPORTING INFORMATION

Figure S15 Comparison of pH_T obtained by pH-dependent CD and UV absorbance spectra.**Figure S15** pH_T obtained by CD spectra as a function of pH_T deduced from UV absorbance spectra.

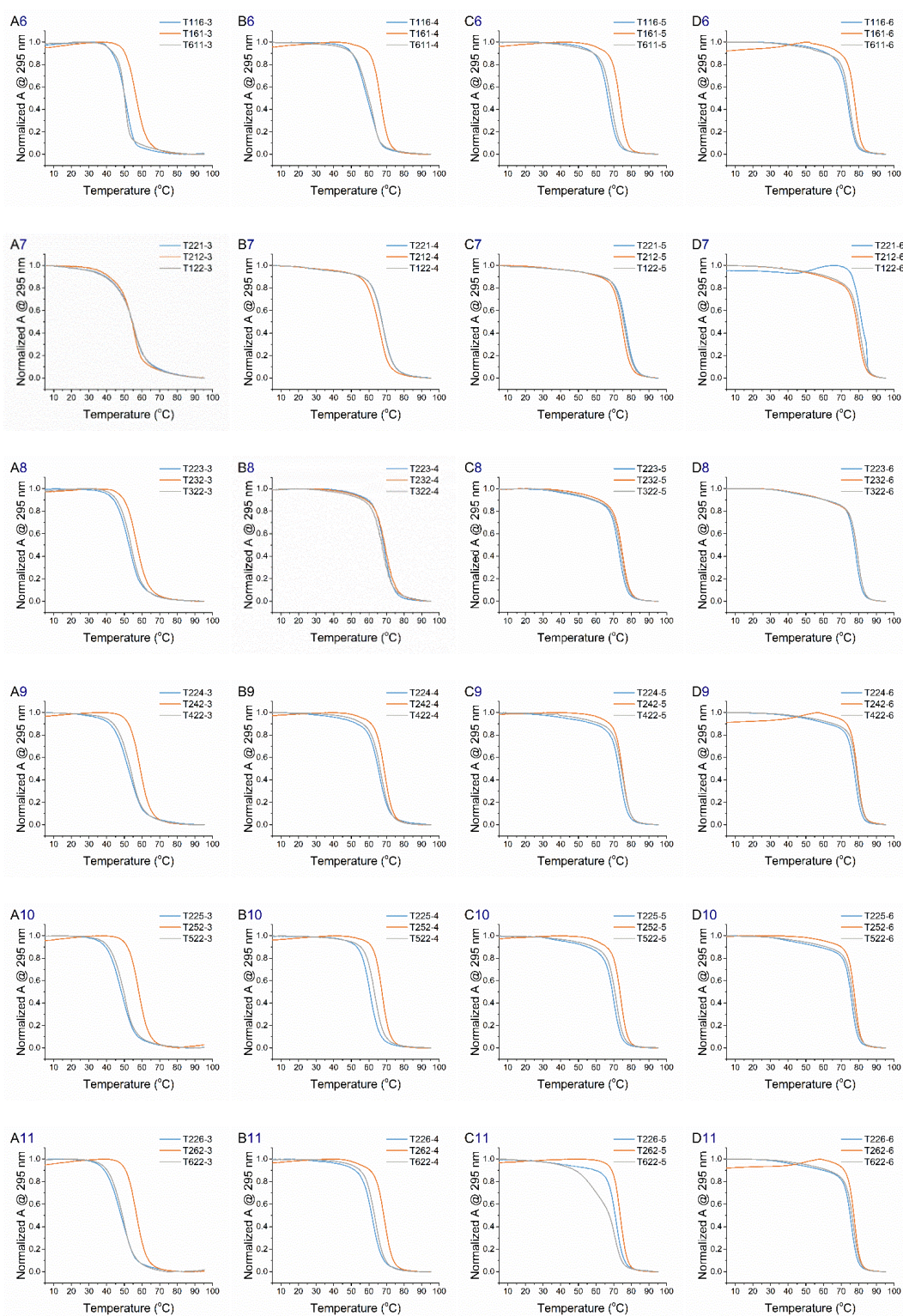
SUPPORTING INFORMATION

Figure S16 UV-melting curves at pH 5.0.



SUPPORTING INFORMATION

Figure S16 UV-melting curves at pH 5.0. (Continued_01)



SUPPORTING INFORMATION

Figure S16 UV-melting curves at pH 5.0. (Continued_02)

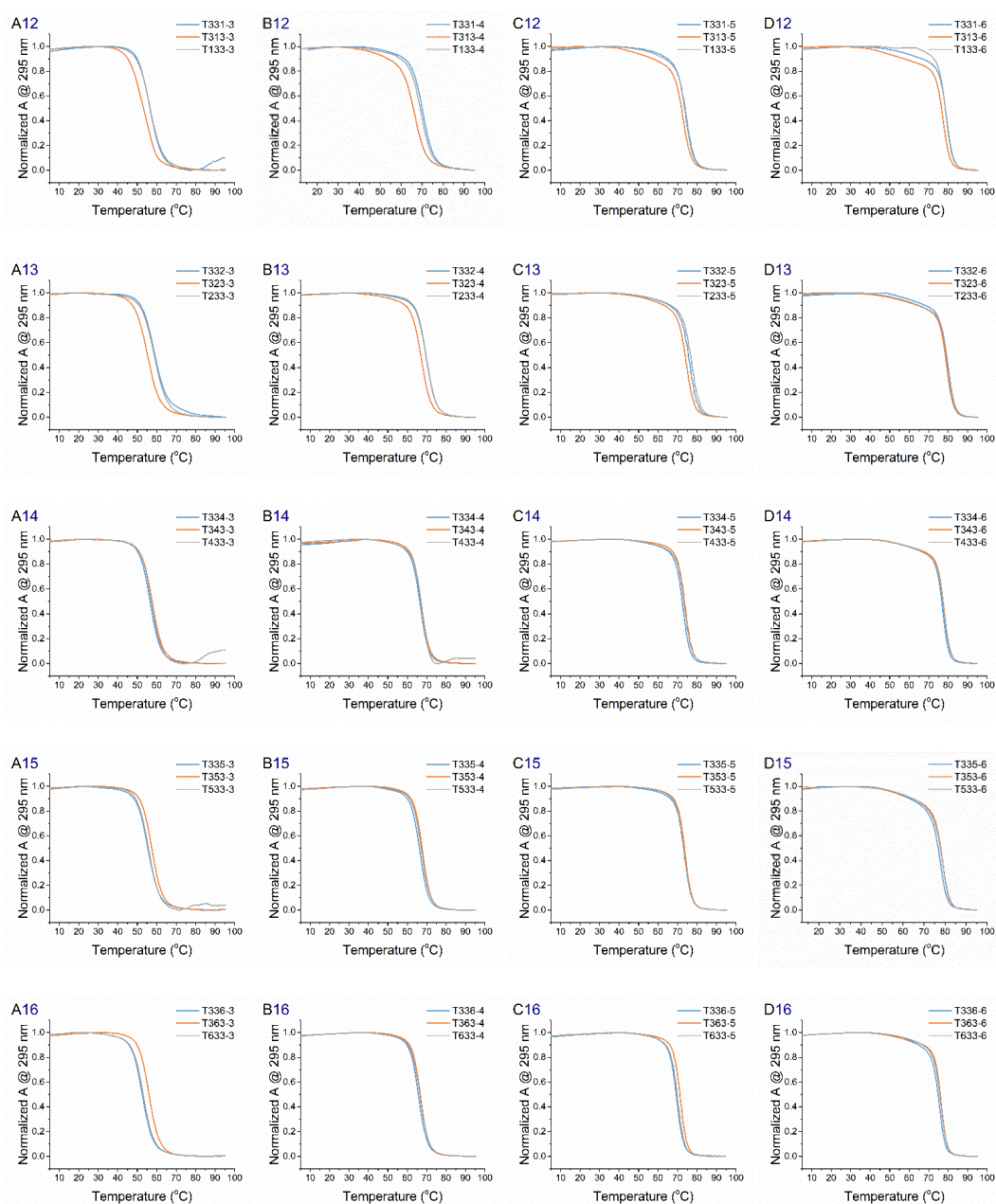
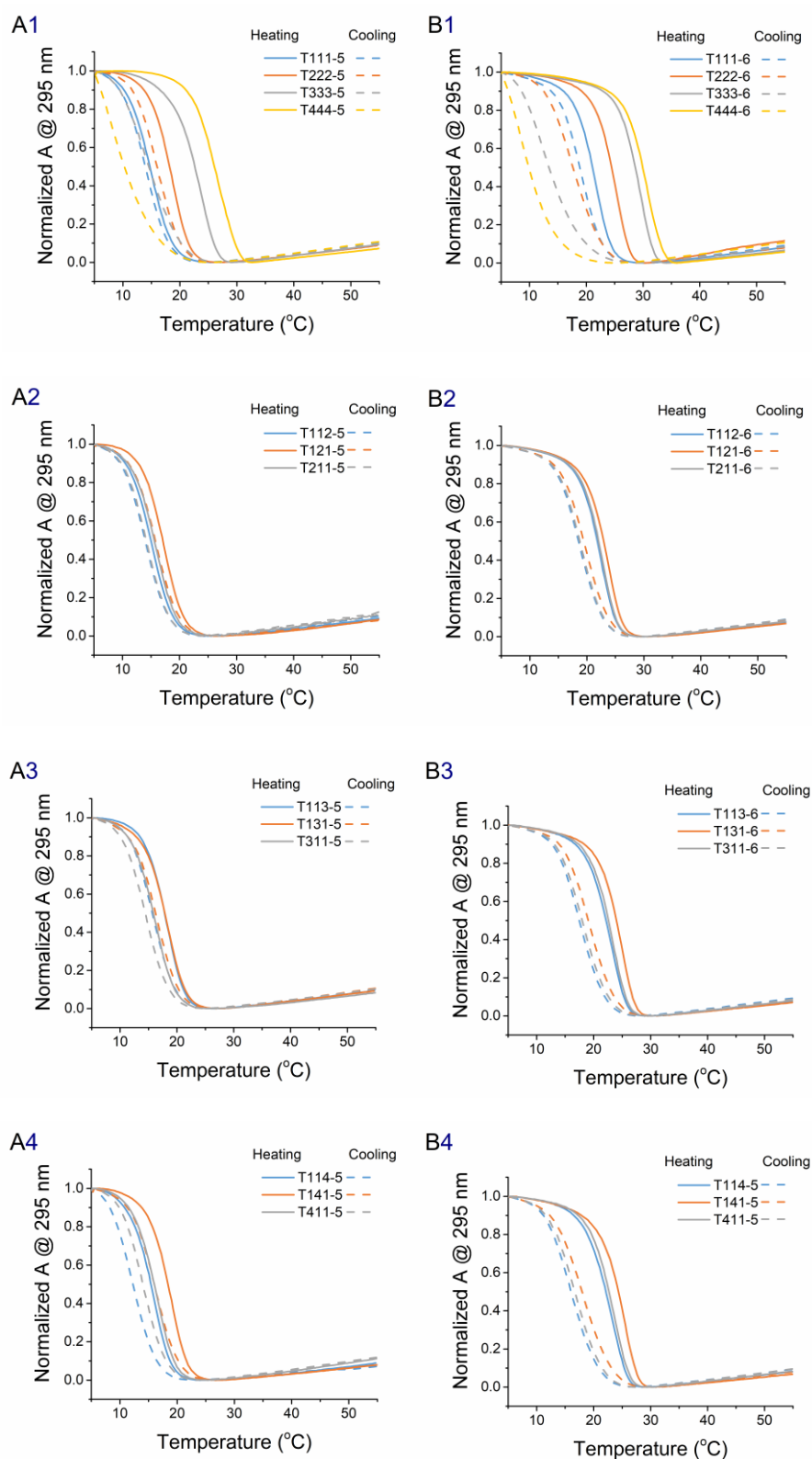


Figure S16 UV-melting curves at pH 5.0 of (A) i-DNAs with C_3 tract (first column, A1~A16), (B) i-DNAs with C_4 tract (second column, B1~B16), (C) i-DNAs with C_5 tract (third column, C1~C16), and (D) i-DNAs with C_6 tract (fourth column, D1~D16). Temperatures varied from 5 to 95 °C.

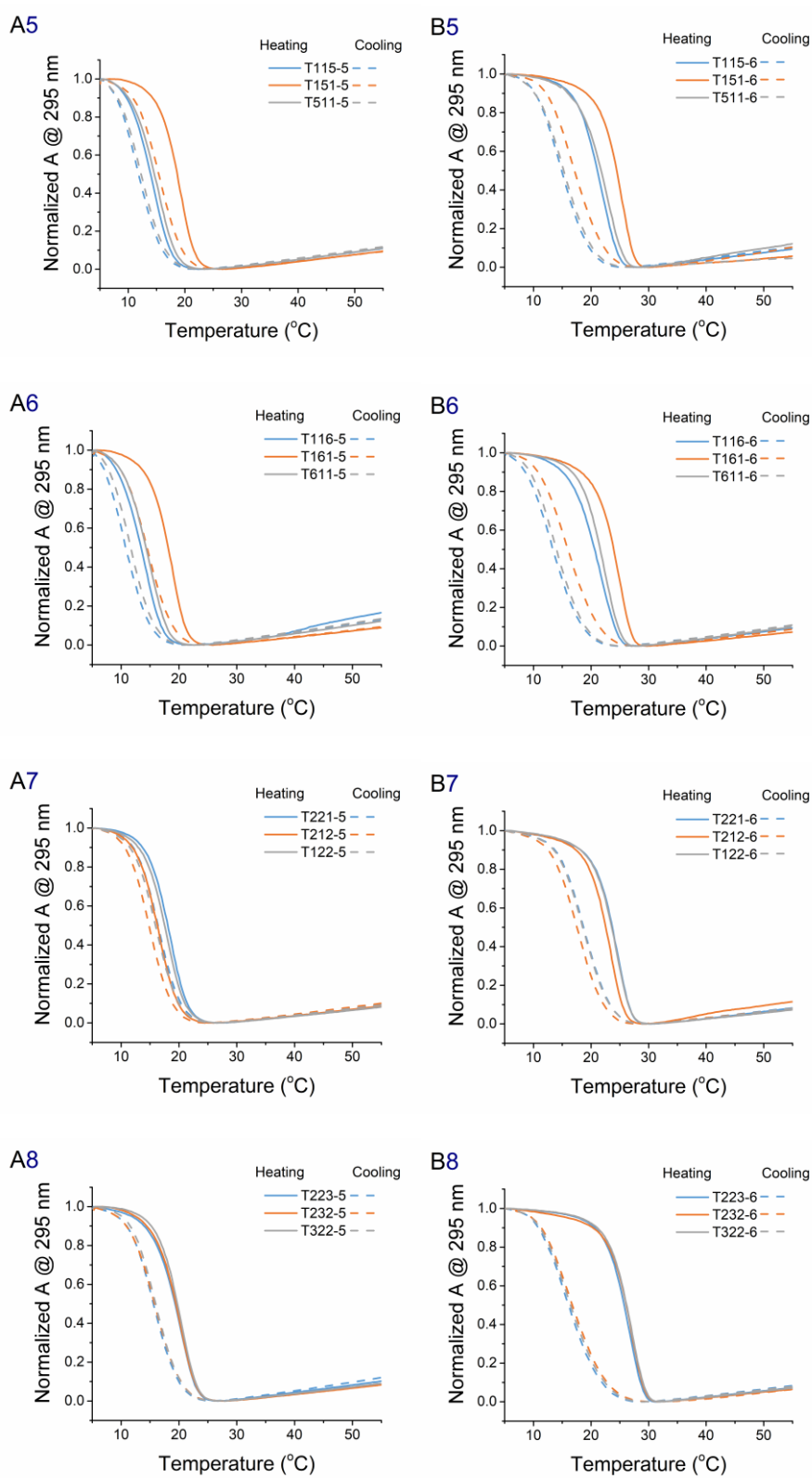
SUPPORTING INFORMATION

Figure S17 UV-melting and annealing curves at pH 7.0.



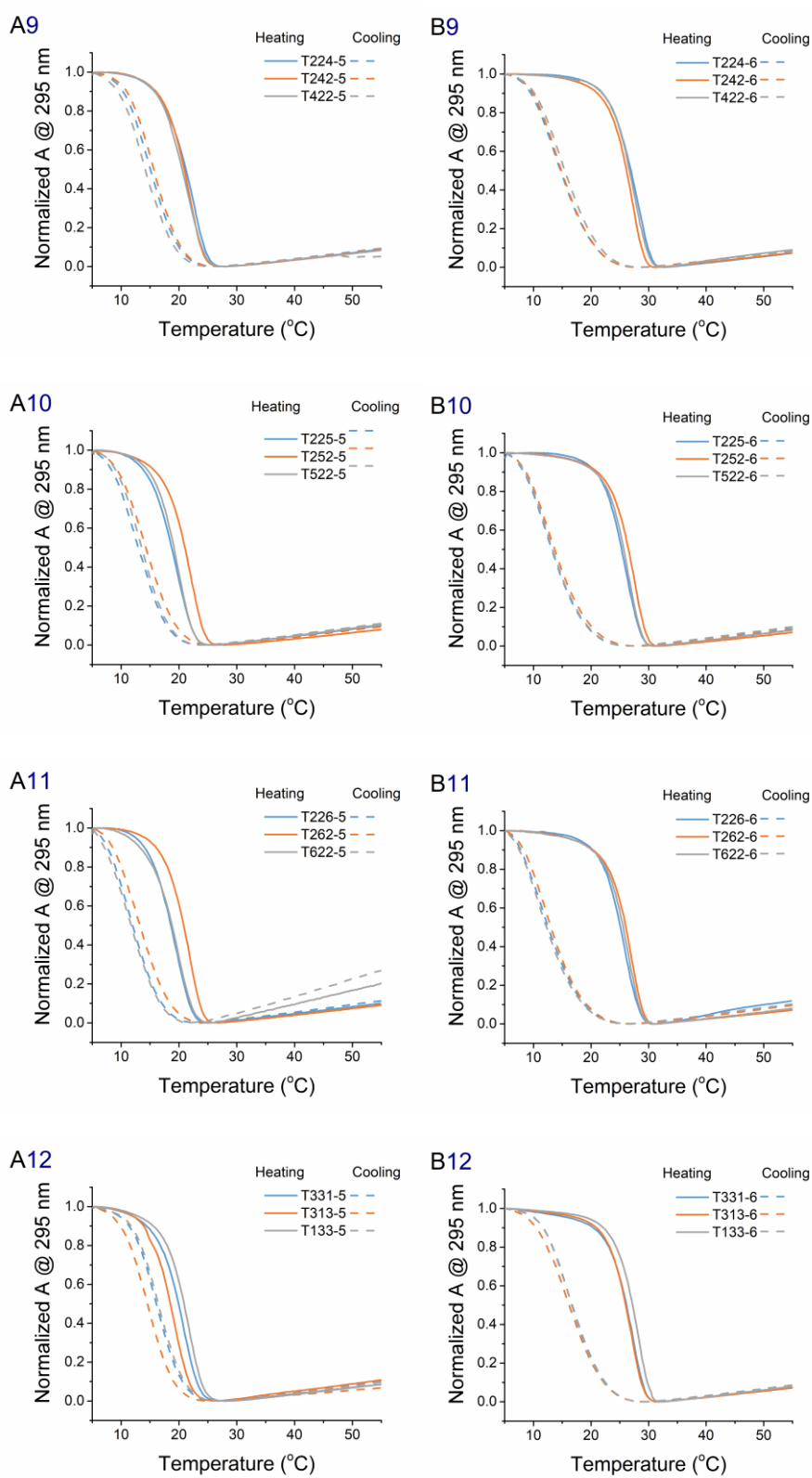
SUPPORTING INFORMATION

Figure S17 UV-melting and annealing curves at pH 7.0. (Continued_01)



SUPPORTING INFORMATION

Figure S17 UV-melting and annealing curves at pH 7.0. (Continued_02)



SUPPORTING INFORMATION

Figure S17 UV-melting and annealing curves at pH 7.0. (Continued_03)

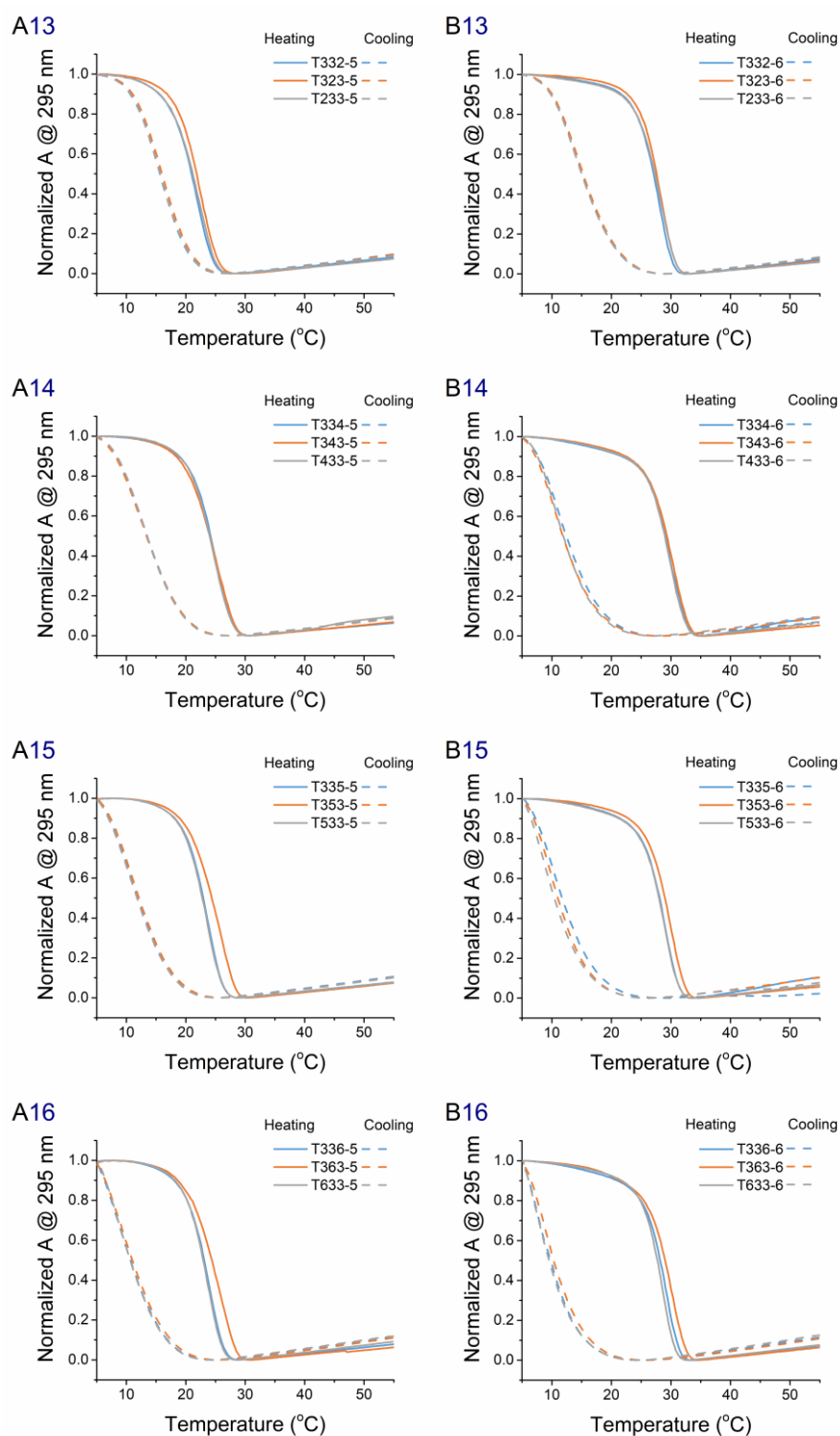


Figure S17 UV-melting (solid line) and annealing (dash line) curves at pH 7.0 of (A) i-DNAs with C_5 tract (first column, A1~A16), (B) i-DNAs with C_6 tract (second column, B1~B16). Temperatures varied between 5 and 55 °C.

SUPPORTING INFORMATION

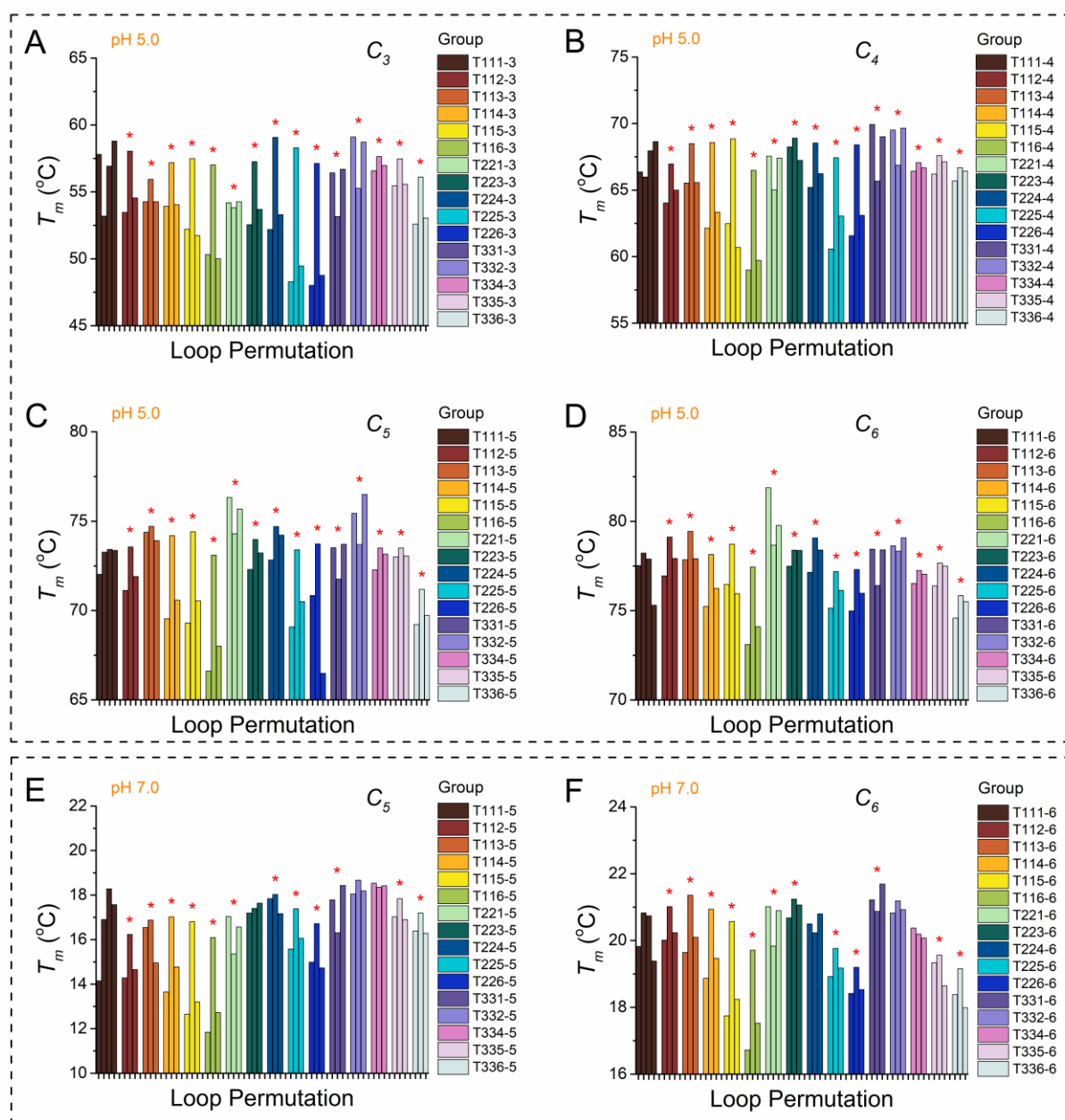
Figure S18 Melting temperature (T_m) at pH 5.0 and 7.0.

Figure S18 Melting temperature: (A) I-DNAs with four C_3 tracts at pH 5.0; (B) I-DNAs with four C_4 tracts at pH 5.0; (C) I-DNAs with four C_5 tracts at pH 5.0; (D) I-DNAs with four C_6 tracts at pH 5.0; (E) I-DNAs with four C_5 tracts at pH 7.0; (F) I-DNAs with four C_6 tracts at pH 7.0. The experiments were carried out in 20 mM Britton-Robinson buffer with 140 mM KCl and 20 mM NaCl. Data in this figure was acquired by UV-melting experiment. The temperatures were recorded from 5 to 95 °C (for sequences in pH 5.0, A-D) at rate of 0.5 °C/min or 5 to 55 °C (for sequence in pH 7.0, E & F) at rate of 0.2 °C/min. Note the differences in Y-axis limits between panels. All oligonucleotide strand concentrations were 5 μ M. Symbol * at top of the bar indicates that in this group the sequence with a longer central loop shows a higher thermal stability.

SUPPORTING INFORMATION

Figure S19 DSC-melting and annealing profiles of selected sequences.

Several results draw from UV-melting/annealing experiments are validated by DSC experiments here.

- In the same group, sequences with longer central loop show higher thermal stability. However, one group is an exception: T112-6 group at pH 7.0
- Melting and annealing processes at pH 5.0 are reversible, but show an obvious hysteresis at pH 7.0.
- Hysteresis is positively correlated to the lengths of total loop length and C-tract.

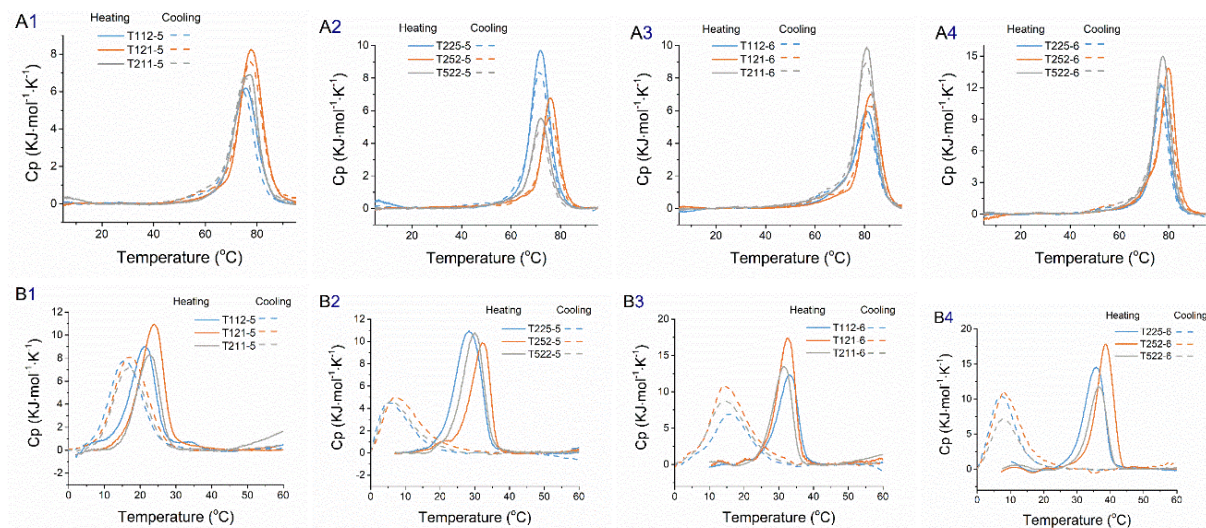
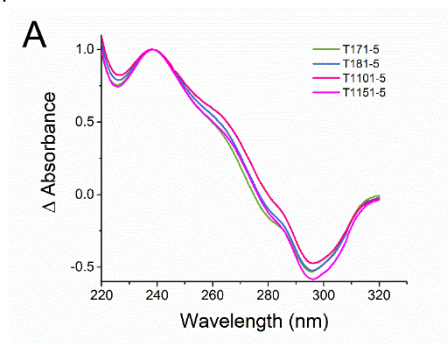
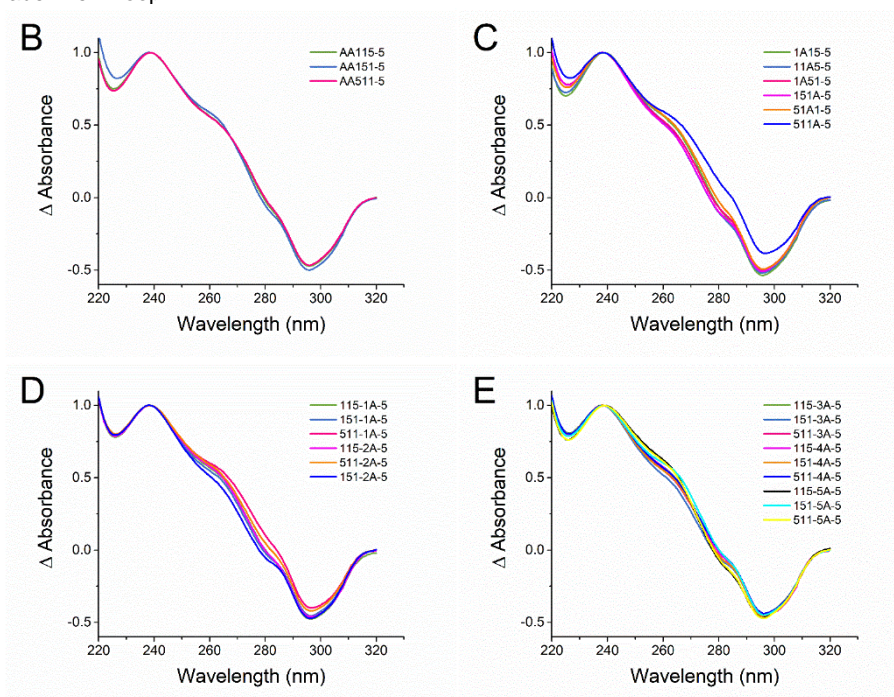
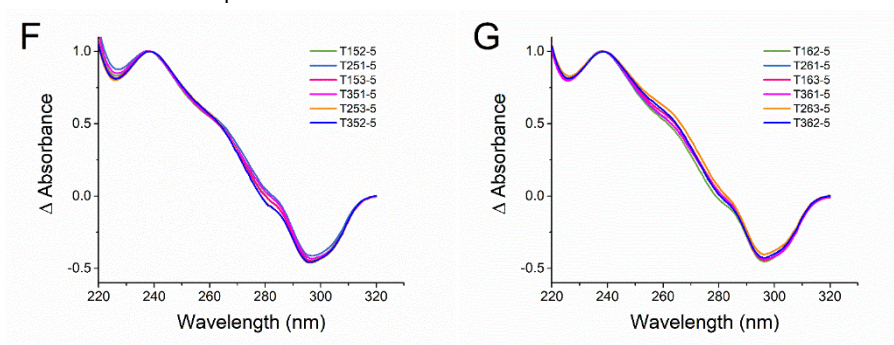
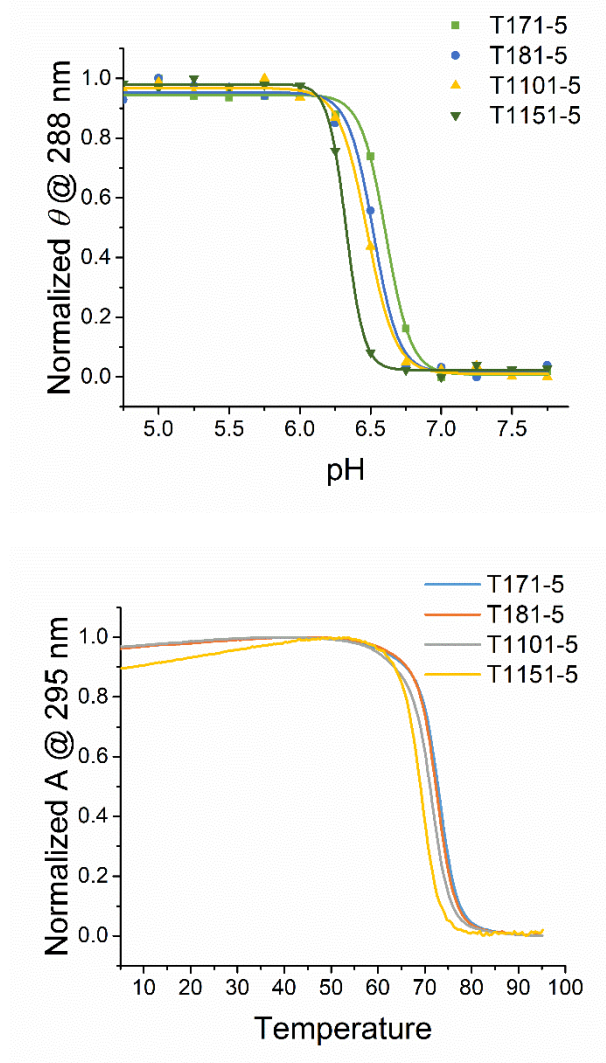


Figure S19 DSC-melting and annealing profiles of 12 selected sequences using a temperature gradient of 1°C/min. (A1-A4) at pH 5.0; (B1-B4) at pH 7.0. Stand concentration is 100 μ M. All scans are performed at 1.0 $^{\circ}$ C/min.

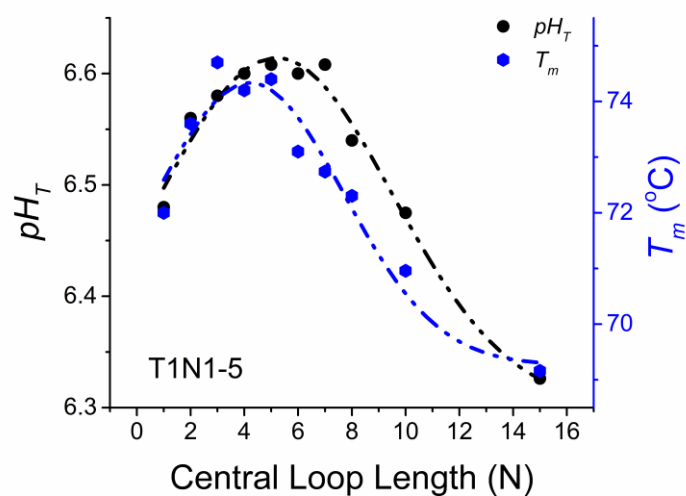
SUPPORTING INFORMATION

Figure S20 Thermal difference spectra (TDS) of 40 extended sequences with C_5 -tract.**A)** Sequences with longer (7-15) central loop.**B-E)** Sequences with adenine in loop.**F-G)** Sequences with two different short loops.**Figure S20** TDS of 40 extended sequences with C_5 -tract at pH 5.0.

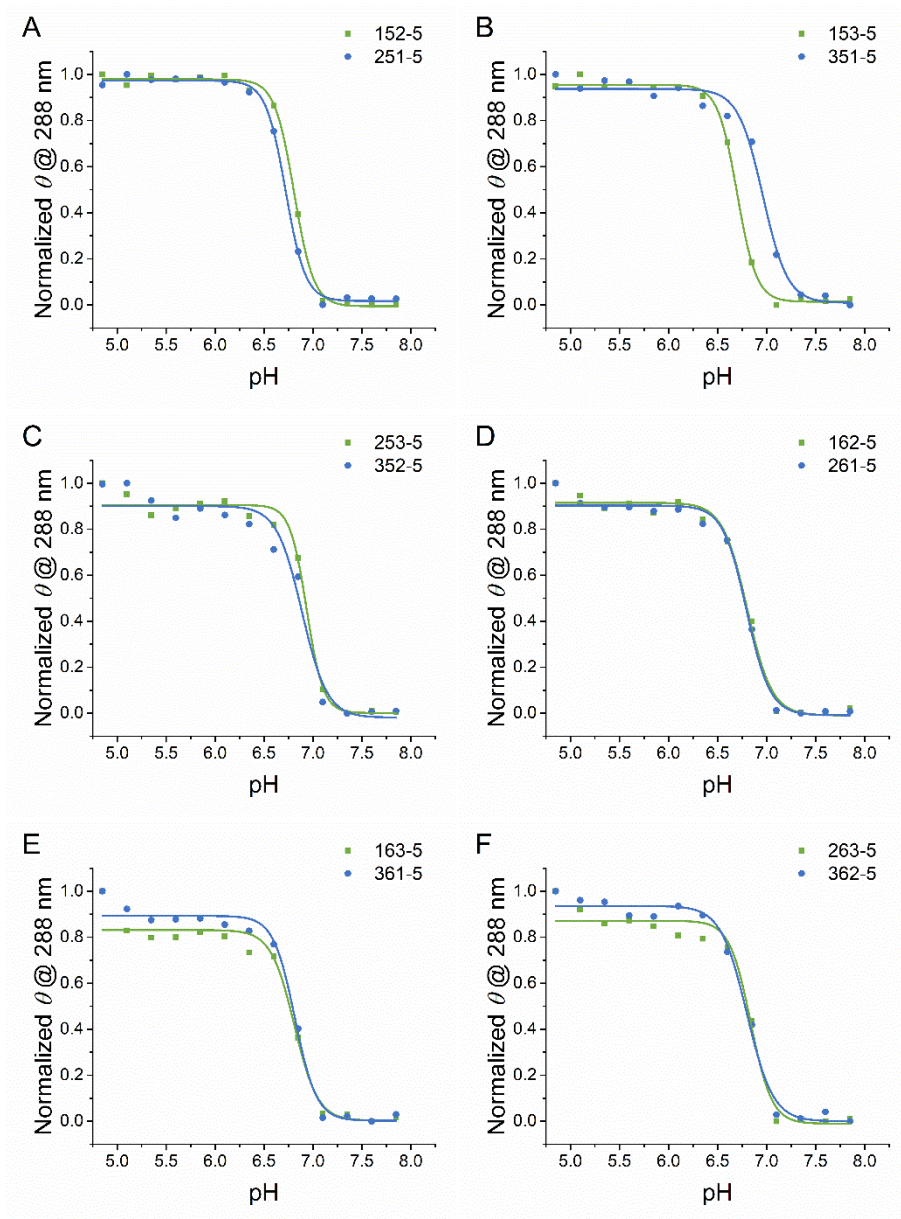
SUPPORTING INFORMATION

Figure S21 pH-dependent ellipticities and UV-melting curves at pH 5.0 of sequences with C_5 -tract and a longer central loop.**Figure S21** pH-dependent CD spectra (upper) and UV-melting curves (lower) at pH 5.0 of sequences with C_5 -tract and a longer (7-15) central loop.

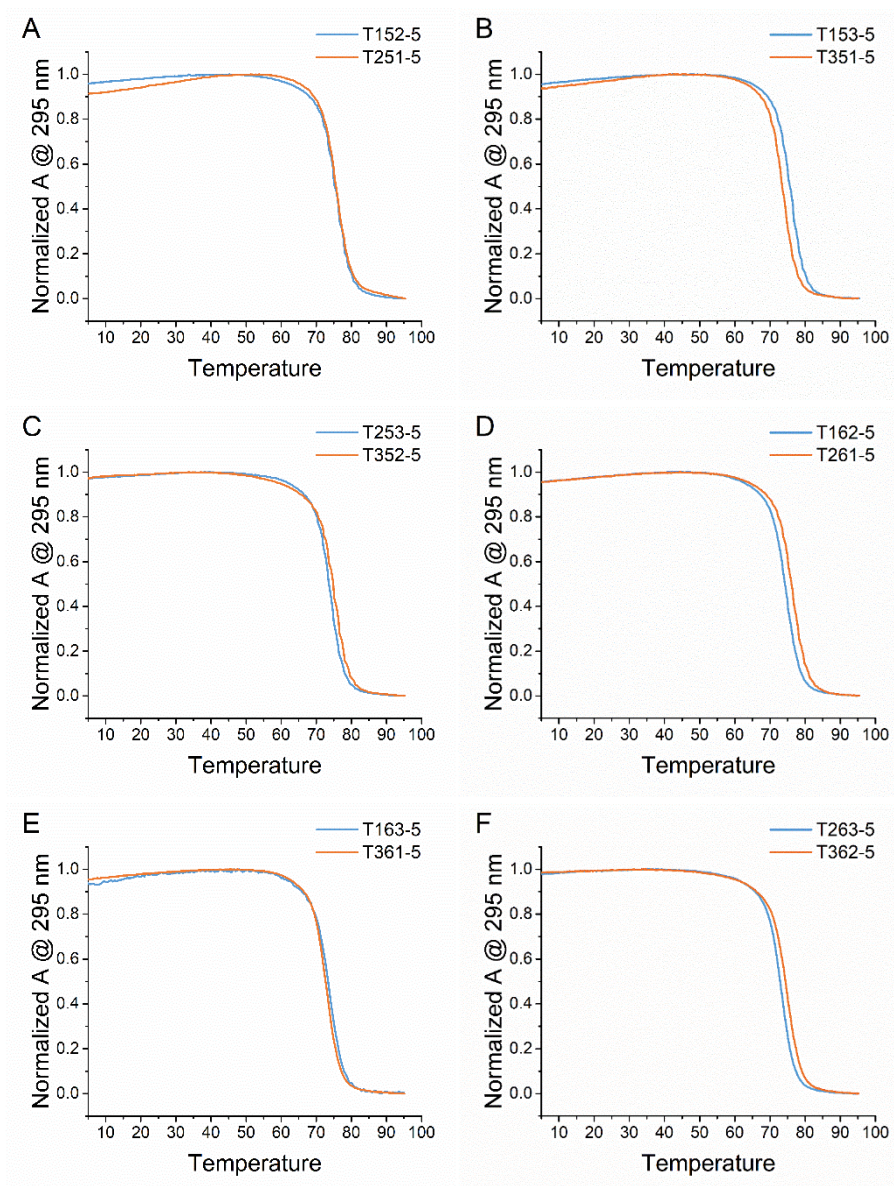
SUPPORTING INFORMATION

Figure S22 Effect of central spacer length on pH_T and T_m of T1N1-5 sequences.**Figure S22** Effect of central spacer length on pH_T and T_m of T1N1-5 sequences. T1N1-5 represents the sequences with C_5 -tract and two single nucleotide spacers, where N is a central spacer of variable length. Sequences are provided in **Tables S1** and **S3**. Gauss functions were used to fit the data.

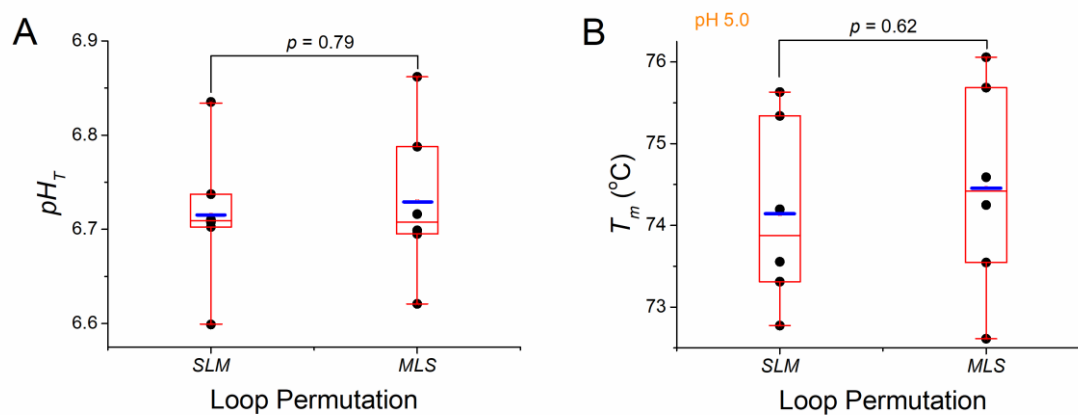
SUPPORTING INFORMATION

Figure S23 pH-dependent CD spectra of sequences with two short loops of different length.**Figure S23** pH-dependent CD spectra of sequences with two short loops of different length. (A) 152-5 group; (B) 153-5 group; (C) 253-5 group; (D) 162-5 group; (E) 163-5 group; (F) 263-5 group.

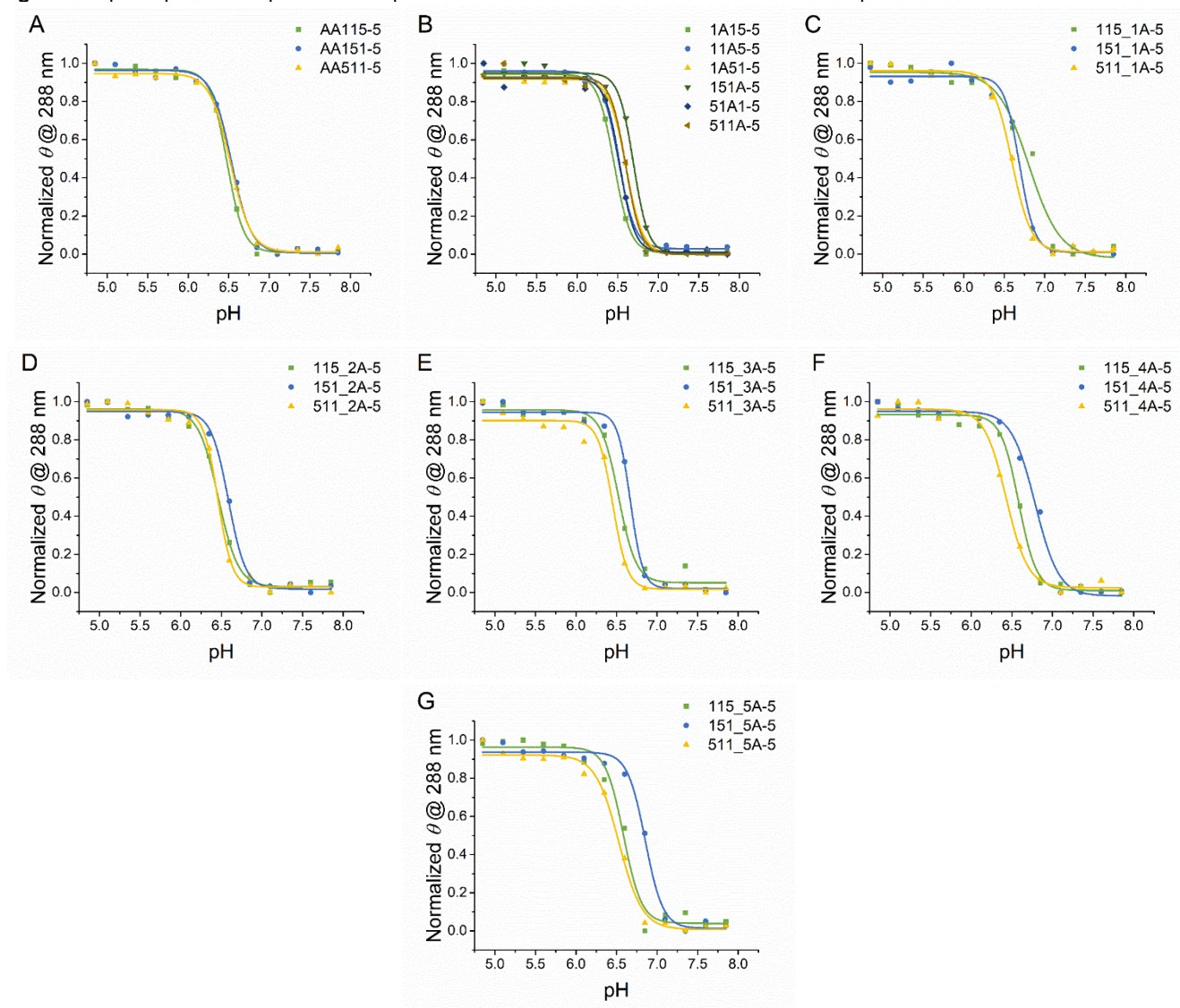
SUPPORTING INFORMATION

Figure S24 UV-melting curves at pH 5.0 of sequences with two short loops of different length.**Figure S24** UV-melting curves at pH 5.0 of sequences with two short loops of different length. (A) 152-5 group; (B) 153-5 group; (C) 253-5 group; (D) 162-5 group; (E) 163-5 group; (F) 263-5 group.

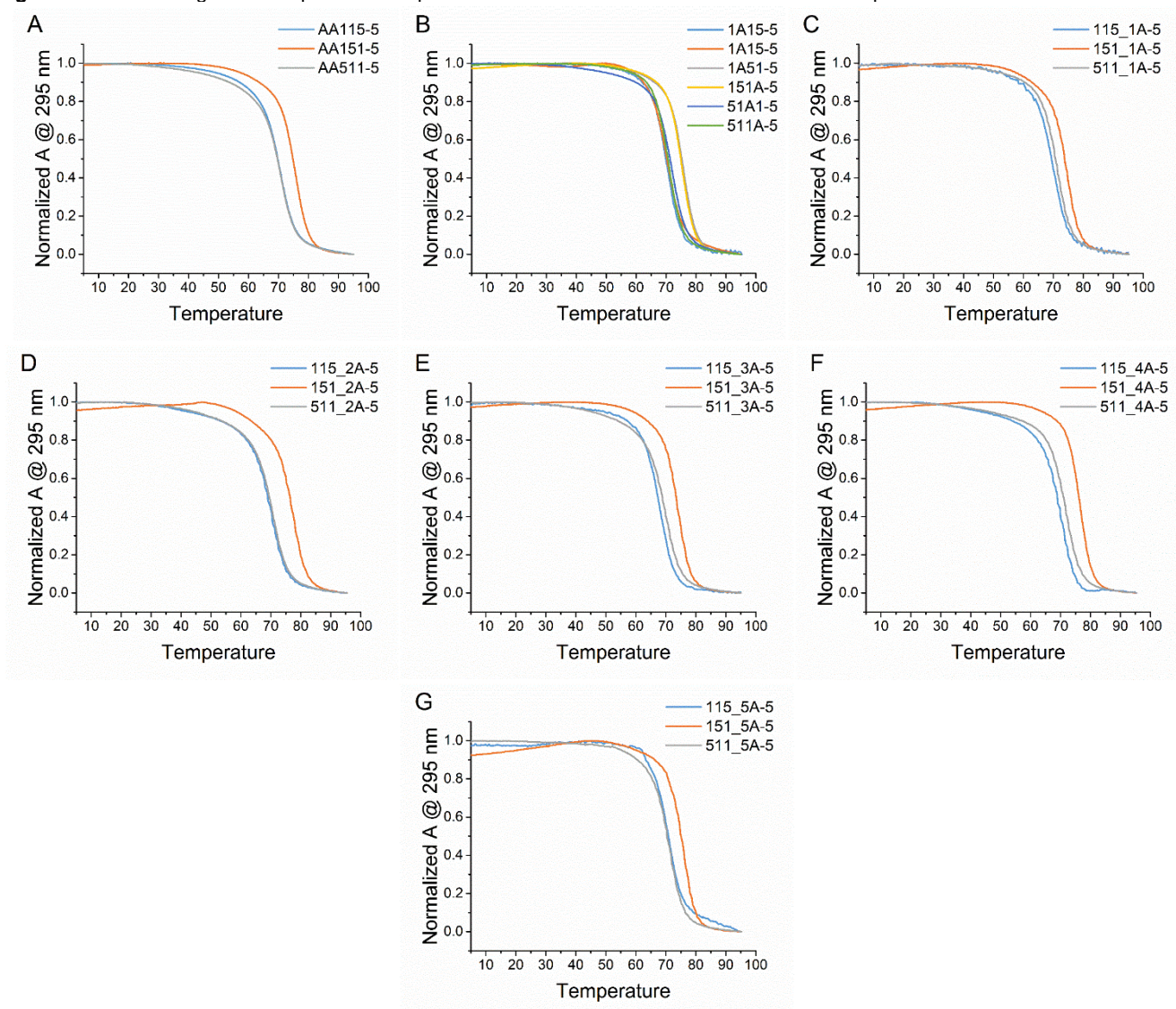
SUPPORTING INFORMATION

Figure S25 Hypothesis of pair-sample *t*-test between *SLM* and *MLS* loop permutations.**Figure S25** Hypothesis of pair-sample *t*-test between *SLM* and *MLS* loop permutations of 12 sequences with C_5 -tract and two different short loops. Two sequences from the same group are paired samples. (A) pH_T and (B) T_m .

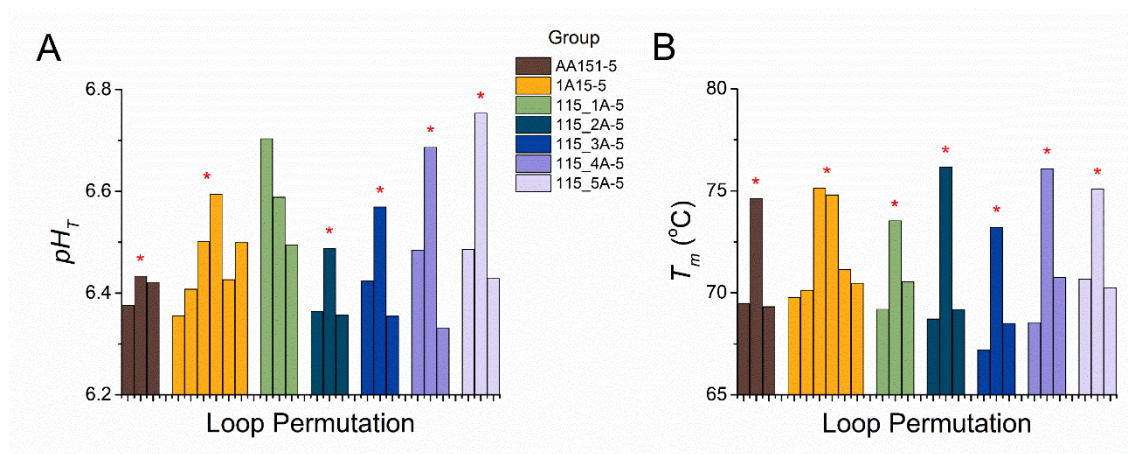
SUPPORTING INFORMATION

Figure S26 pH-dependent ellipticities of sequences with C_5 -tract and one or two adenines in loop.**Figure S26** pH-dependent CD spectra of sequences with C_5 -tract and one or two adenines in loop. (A) AA115-5 group; (B) 1A15-5 group; (C) 115_1A-5 group; (D) 115_2A-5 group; (E) 115_3A-5 group; (F) 115_4A-5 group; (G) 115_5A-5 group.

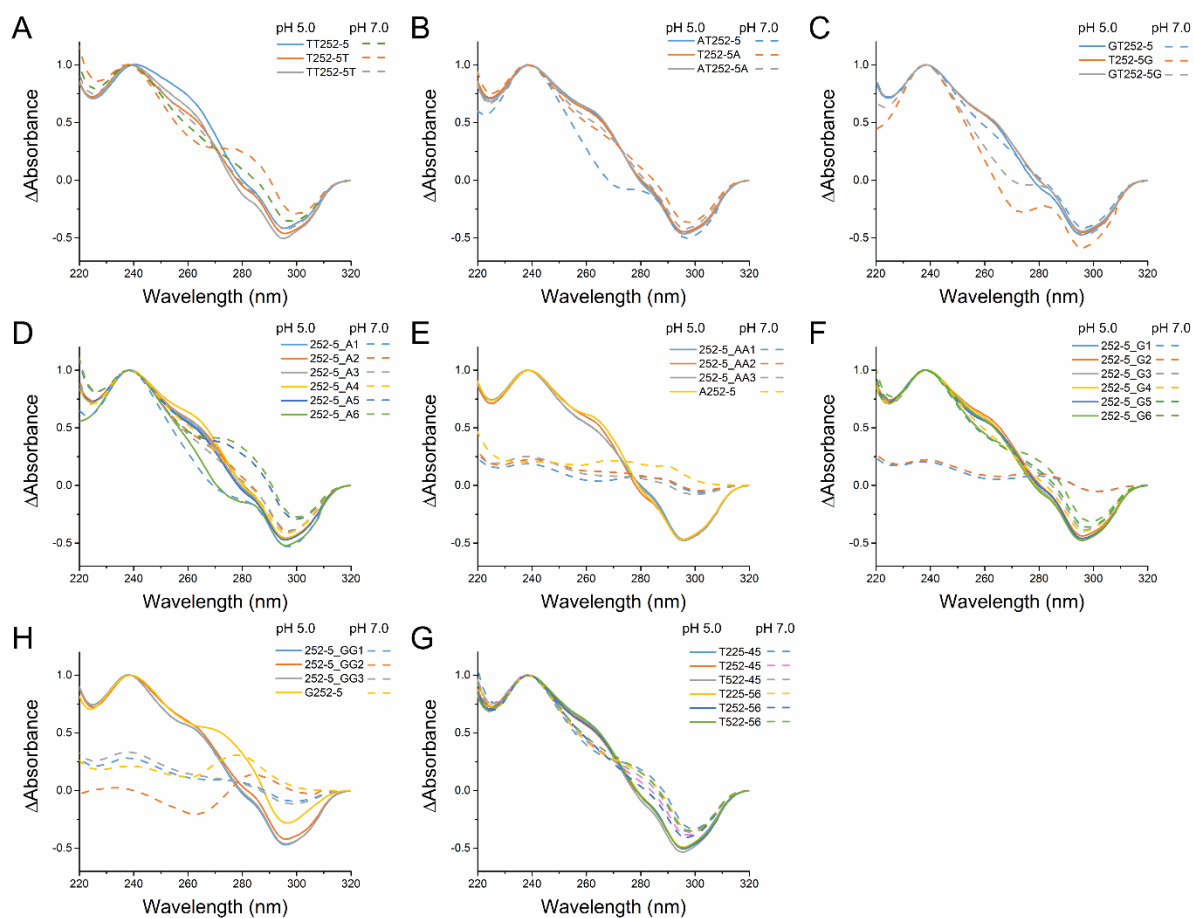
SUPPORTING INFORMATION

Figure S27 UV-melting curves at pH 5.0 of sequences with C_5 -tract and one / two adenines in loop.**Figure S27** UV-melting curves at pH 5.0 of sequences with C_5 -tract and one or two adenines in loop. (A) AA115-5 group; (B) 1A15-5 group; (C) 115_1A-5 group; (D) 115_2A-5 group; (E) 115_3A-5 group; (F) 115_4A-5 group; (G) 115_5A-5 group.

SUPPORTING INFORMATION

Figure S28 Spacer permutation in sequences with different spacer compositions.**Figure S28** Spacer permutation in sequences with different spacer compositions: **(A)** pH_T and **(B)** T_m . Sequences information are given in **Tables S1** and **S3**. Symbol asterisk * at top of the bar indicates that the group obeys the rule that a sequence with a longer central spacer has a higher pH_T transition midpoint **(A)** or thermal stability **(B)**.

SUPPORTING INFORMATION

Figure S29 TDS at pH 5.0 and pH 7.0 of sequences with flanking sequences, different spacer contents and odd number of C-C⁺ base pairs.**Figure S29** TDS at pH 5.0 and pH 7.0 of sequences with flanking sequences (A-C), different spacer contents (D-H) and odd number of C-C⁺ base pairs (G). Sequences are given Table S1.

SUPPORTING INFORMATION

Figure S30 UV-melting/annealing at pH 5.0 of sequences with flanking sequences, different spacer contents and odd number of C-C⁺ base pairs.

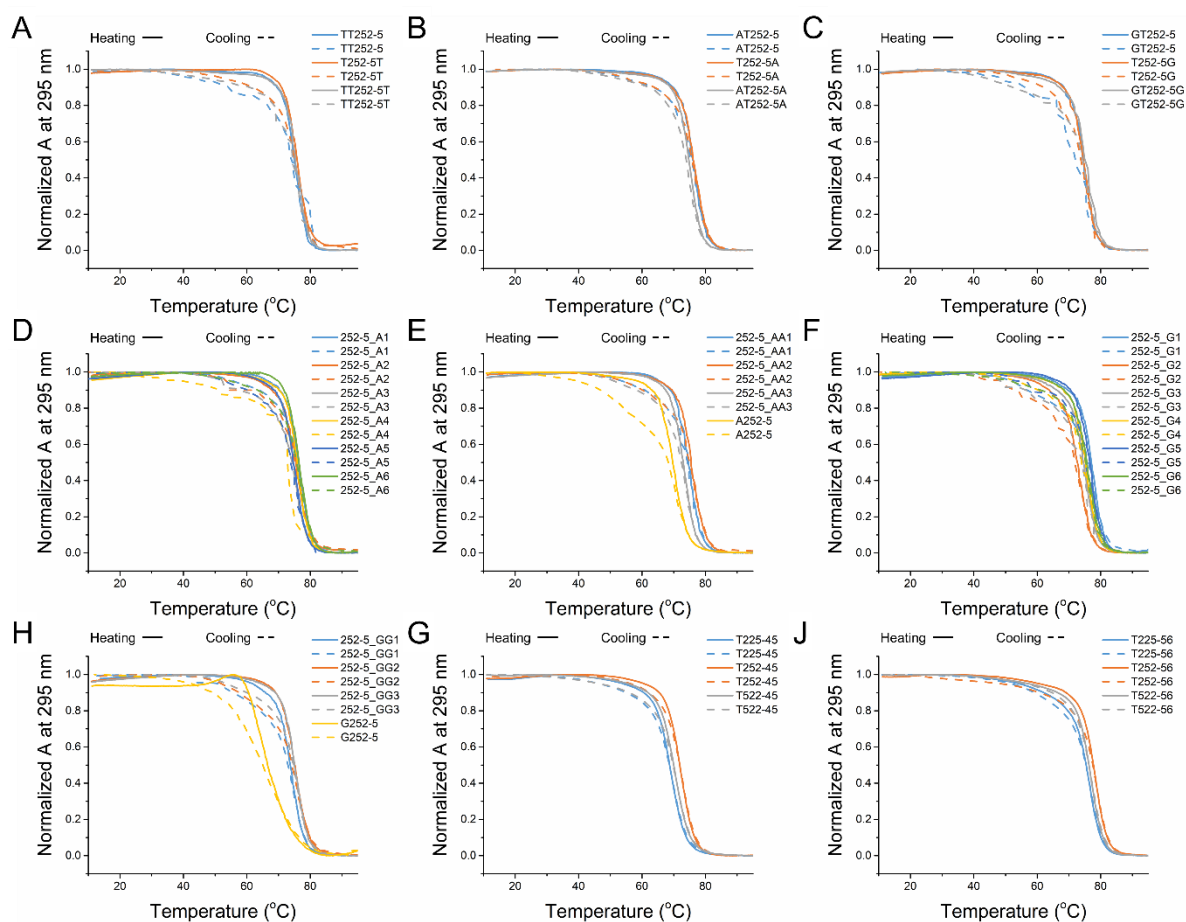
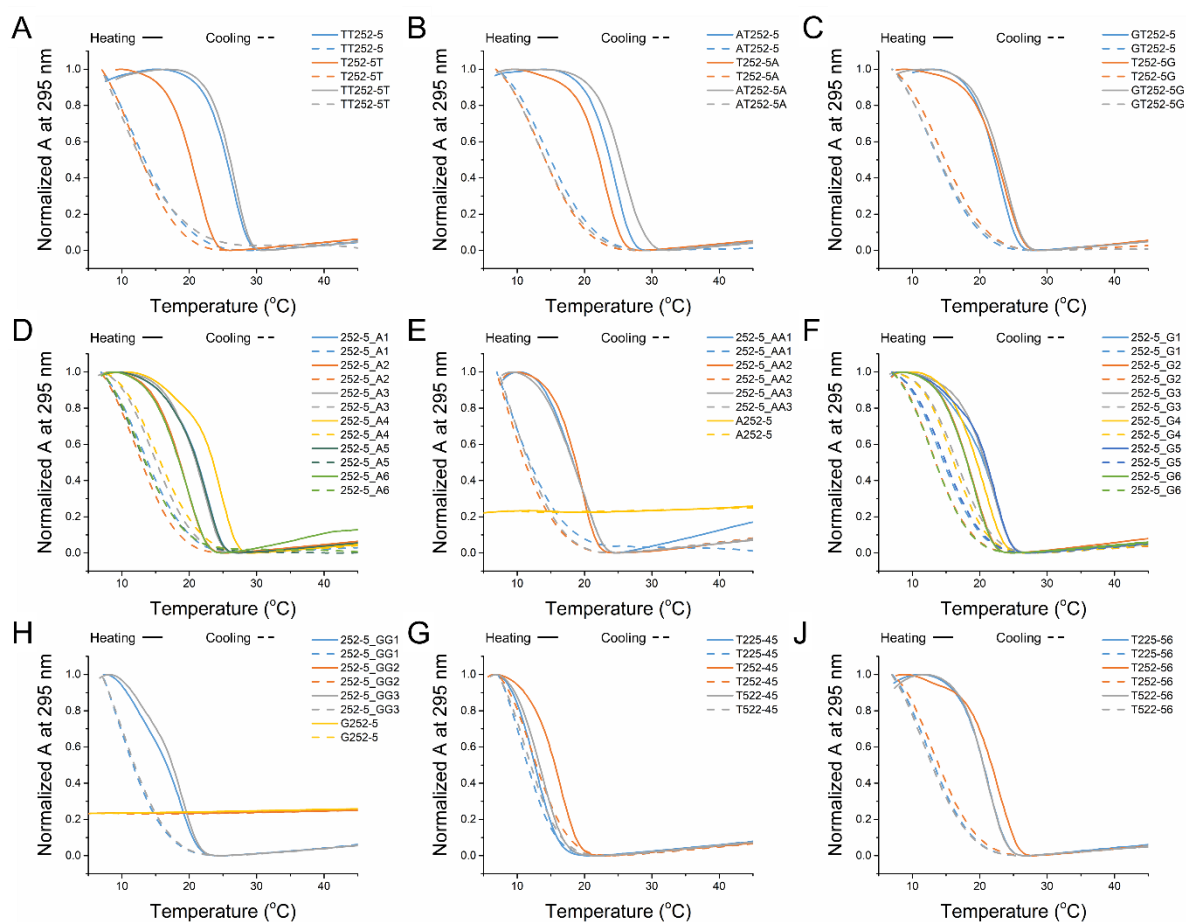


Figure S30 UV-melting/annealing at pH 5.0 of sequences with flanking sequences (A-C), different spacer contents (D-H) and odd number of C-C⁺ base pairs (G-J). Sequences are given **Table S1** and melting temperature are summarized in **Table S5**.

SUPPORTING INFORMATION

Figure S31 UV-melting/annealing at pH 5.0 of sequences with flanking sequences, different spacer contents and odd number of C-C⁺ base pairs.**Figure S31** UV-melting/annealing at pH 5.0 of sequences with flanking sequences (A-C), different spacer contents (D-H) and odd number of C-C⁺ base pairs (G-J). Sequences are given **Table S1** and melting temperature are summarized in **Table S5**.

SUPPORTING INFORMATION

Figures S32-33 Cells viability, level of DNA transfection, and intracellular localization of transfected DNAs for in-cell NMR experiments.

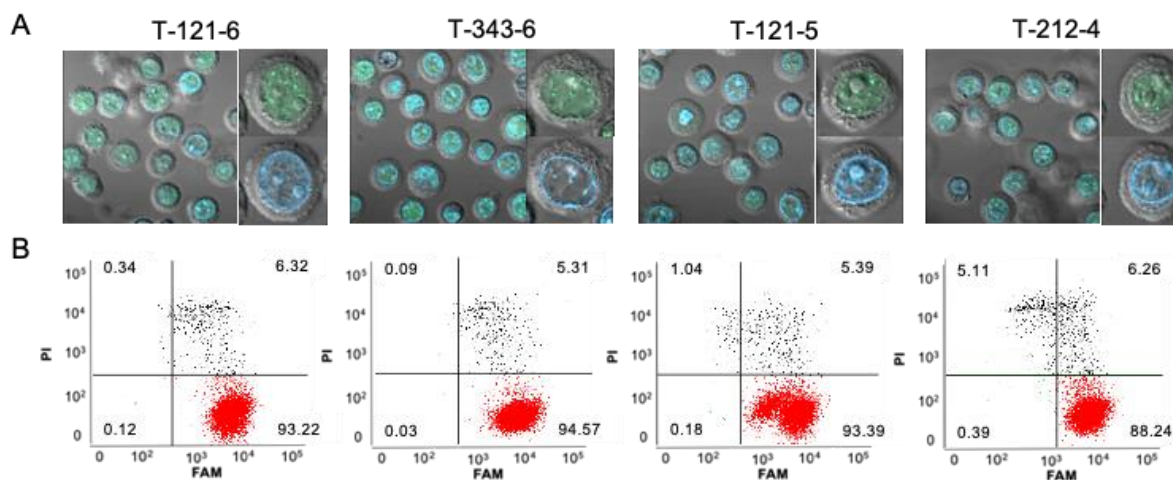


Figure S32 (A) Double-staining (PI/FAM) FCM analysis (post in-cell NMR spectra acquisition) and (B) confocal microscopy images of cells cotransfected with the (FAM)-T121-6, T343-6, T121-5, and T212-4 constructs. In the FCM plots, the percentages of viable nontransfected cells, viable DNA-containing cells, dead/compromised nontransfected cells, and dead/compromised cells transfected with DNA are indicated in the bottom-left, bottom-right, top-left, and top-right quadrants, respectively. In the confocal images, the green color marks the localization of (FAM)-DNA, while the blue color marks cell nuclei stained with Hoechst 33342.

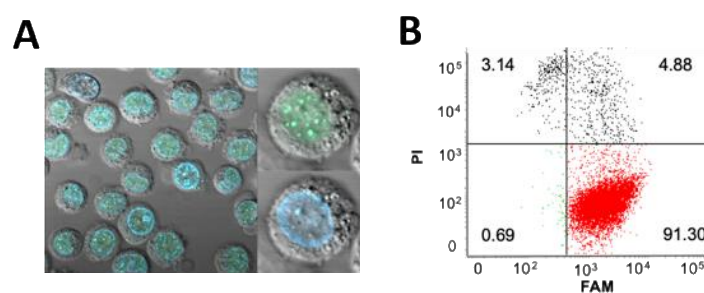


Figure S33 (A) Confocal microscopy image and (B) double-staining (PI/FAM) FCM analysis post temperature resolved in-cell NMR spectra acquisition of cells cotransfected with the (FAM)-T121-6. For meaning of colors and description of quadrants in the confocal image and FCM plot see legend of **Figure S32**.

SUPPORTING INFORMATION

Figure S34 Correlation plots between the experimental stability measures and the i-DNA stability scores obtained via optimized models analogous to G4Hunter.

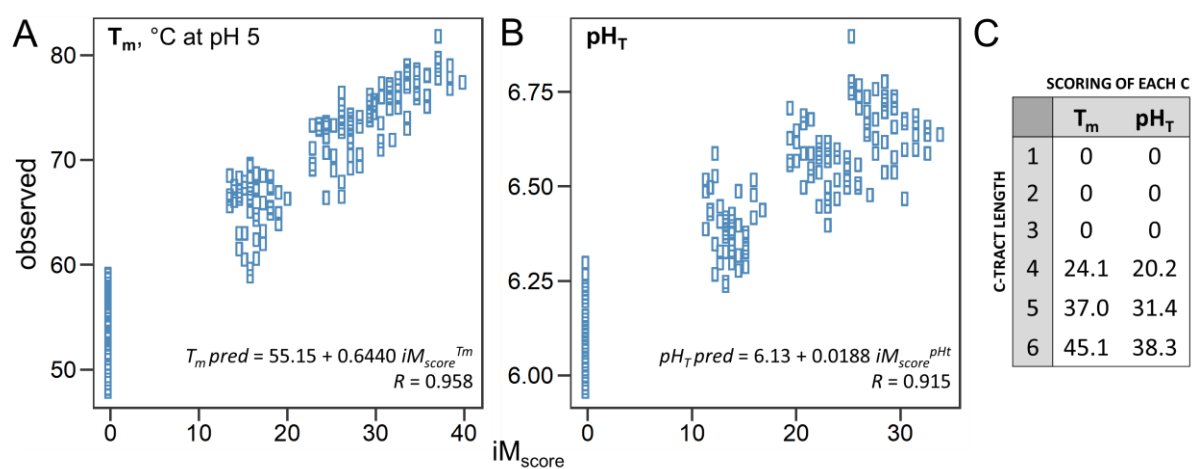


Figure S34 Correlation plots between the experimental stability measures (T_m at pH 5.0 and pH_T) and the i-DNA stability scores (iM_{score}) obtained via optimized models analogous to G4Hunter. Plots are brought for both T_m vs. $iM_{\text{score}}^{T_m}$ (**A**) and pH_T vs. $iM_{\text{score}}^{pH_T}$ (**B**) dependencies. The correlation equations and the Pearson's correlation coefficients (R) are brought on the individual plots (**A**, **B**). The table in (**C**) shows the optimized positive scoring coefficients of each cytosine (counterpart of guanine in the case of G4s) in a C-tract of a given length, brought for both T_m and pH_T .

SUPPORTING INFORMATION

Supplementary References

- [1] M. Cheng, Y. Cheng, J. Hao, G. Jia, J. Zhou, J.-L. Mergny, C. Li, *Nucleic Acids Res.* **2018**, *46*, 9264-9275.
- [2] A. M. Fleming, Y. Ding, R. A. Rogers, J. Zhu, J. Zhu, A. D. Burton, C. B. Carlisle, C. J. Burrows, *J. Am. Chem. Soc.* **2017**, *139*, 4682-4689.
- [3] J.-L. Mergny, J. Li, L. Lacroix, S. Amrane, J. B. Chaires, *Nucleic Acids Res.* **2005**, *33*, e138.
- [4] J.-L. Mergny, L. Lacroix, *Nucleic Acids Res.* **1998**, *26*, 4797-4803.
- [5] P. Viskova, D. Krafcik, L. Trantirek, S. Foldynova-Trantirkova, *Curr. Protoc. Nucleic Acid Chem.* **2019**, *76*, e71.
- [6] V. Sklenář, A. Bax, *J. Magn. Reson. (1969-1992)* **1987**, *74*, 469-479.
- [7] R. Hansel, S. Foldynova-Trantirkova, F. Lohr, J. Buck, E. Bongartz, E. Bamberg, H. Schwalbe, V. Dotsch, L. Trantirek, *J. Am. Chem. Soc.* **2009**, *131*, 15761-15768.
- [8] A. Bedrat, L. Lacroix, J.-L. Mergny, *Nucleic Acids Res.* **2016**, *44*, 1746-1759.
- [9] N. A. G. Johnson, L. Tamon, X. Liu, A. B. Sahakyan. GitHub link to the code: <http://github.com/SahakyanLab/Optimus>, accessed in November 2019.
- [10] T. Chen, C. Guestrin, *arXiv* **2016**, 1-13.
- [11] a) A. Natekin, A. Knoll, *Front. Neurobot.* **2013**, *7*, 21; b) J. H. Friedman, *Computational Statistics & Data Analysis* **2002**, *38*, 367-378; c) J. H. Friedman, *The Annals of Statistics* **2001**, *29*, 1189-1232.
- [12] M. Kuhn, K. Johnson, *Applied predictive modeling*, Springer, New York, USA, **2013**.
- [13] A. B. Sahakyan, V. S. Chambers, G. Marsico, T. Santner, M. Di Antonio, S. Balasubramanian, *Sci. Rep.* **2017**, *7*, 14535.
- [14] M. Schmidt, H. Lipson, *Science* **2009**, *324*, 81-85.
- [15] M. Johnson, I. Zaretskaya, Y. Raytselis, Y. Merezuk, S. McGinnis, T. L. Madden, *Nucleic Acids Res.* **2008**, *36*, W5-9.
- [16] J.-L. Mergny, L. Lacroix, *Oligonucleotides* **2003**, *13*, 515-537.